IN THIS ISSUE




IMAGE: OBSERVATORY WITH STAR TRAILS ON MOUNTAINS FOR CLEAR SKY

London Journals Press

www.journalspress.com

# LONDON JOURNAL OF ENGINEERING RESEARCH

Volume 22 | Issue 1 | Compilation 1.0

Print ISSN: 2631-8474
Online ISSN: 2631-8482
DOI: 10.17472/LJER



COMPILED IN UNITED KINGDOM

ENGLISH


London Journal of Engineering Research

Volume 22 | Issue 1 | Compilation 1.0

## PUBLISHER

London Journals Press
1210th, Waterside Dr,Opposite Arlington Building, Theale, Reading
Phone:+444 0118 965 4033 Pin: RG7-4TY United Kingdom

## SUBSCRIPTION

*Frequency:* Quarterly

Print subscription
$280USD for 1 year
$500USD for 2 year
*(color copies including taxes and international shipping with TSA approved)*

Find more details at https://journalspress.com/journals/subscription

## ENVIRONMENT

London Journals Press is intended about protecting the environment. This journal is printed using led free environmental friendly ink and acid-free papers that are 100% recyclable.



London Journals Press Headquaters

1210th, Waterside Dr,
Opposite Arlington
Building, Theale, Reading
Phone:+444 0118 965 4033
Pin: RG7-4TY
United Kingdom

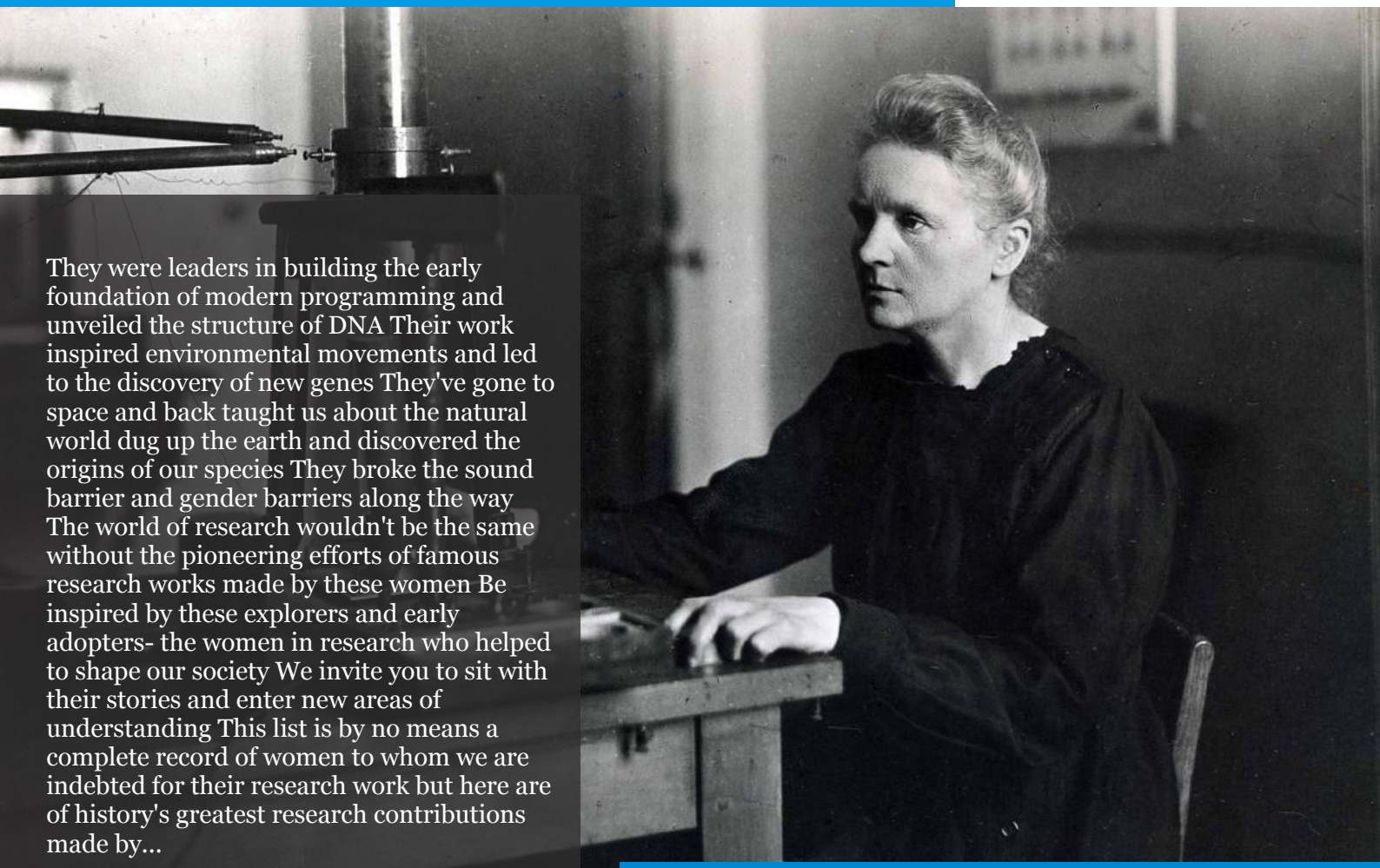

They were leaders in building the early foundation of modern programming and unveiled the structure of DNA Their work inspired environmental movements and led to the discovery of new genes They've gone to space and back taught us about the natural world dug up the earth and discovered the origins of our species They broke the sound barrier and gender barriers along the way The world of research wouldn't be the same without the pioneering efforts of famous research works made by these women Be inspired by these explorers and early adopters- the women in research who helped to shape our society We invite you to sit with their stories and enter new areas of understanding This list is by no means a complete record of women to whom we are indebted for their research work but here are of history's greatest research contributions made by...

Read complete here:
https://goo.gl/1vQ3lS

## Women In Research

## Computing in the cloud!

Cloud Computing is computing as a Service and not just as a Product Under Cloud Computing...

Read complete here:
https://goo.gl/VvHC72

## Writing great research...

Prepare yourself before you start Before you start writing your paper or you start reading other...

Read complete here:
https://goo.gl/np73jP

# Journal Content
## In this Issue

London Journals Press

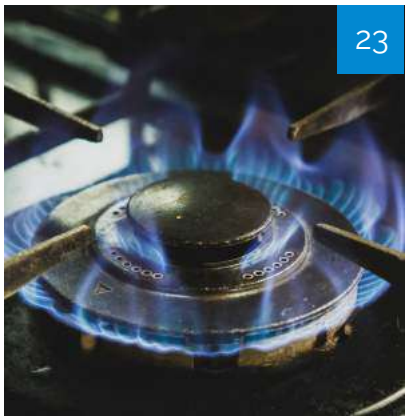



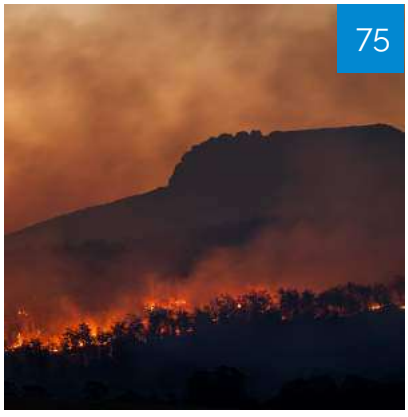

# Editorial Board

## Curated board members

# Optimal ARMAX Model Order Identification of Dynamic Systems

*Quoc-Cuong Nguyen, Viet-Hung Vu & Marc Thomas*

*École de technologie supérieure*

## ABSTRACT

This paper describes an efficient approach for model order determination, which allows identifying the dynamical behavior of the mechanical system by using observation input- output data. The concept based on the minimum means square error of the estimated transfer functions, which can effectively tackle measurement noise and modeling errors to identify appropriate low-order transfer functions of the structures via an Auto-Regressive Moving Average eXogenous (ARMAX) model. The effectiveness of the proposed method is validated exclusively using experimental data obtained from a grinding test of an industrial manipulator SCOMPI robot. Some other criteria, such as the Akaike Information Criterion (AIC), the Bayesian Information Criterion (BIC), and the Noise Order Factor (NOF), are investigated to verify the performance of the proposed methodology. The results demonstrated that the present technique is cost-effective in terms of optimal model order determination, and the ARMAX model turns out to be the most appropriate representation for feature extraction at the low order. Thanks to its flexibility in handling model disturbance, the proposed optimization strategy can capture all the dominant oscillation modes of the structure at the low orders, and system modal properties are efficiently and automatically determined. In contrast, the performance of the ARX model is shown to be less efficient when working at the low orders.

*Keywords:* ARMAX model, ARX model, frequency response functions, optimal orders, modal identification.

*Classification:* DDC Code: 330, LCC Code: HB1

*Language:* English

London Journals Press

LJP Copyright ID: 392971
Print ISSN: 2631-8474
Online ISSN: 2631-8482

London Journal of Engineering Research

Volume 22 | Issue 1 | Compilation 1.0

# Optimal ARMAX Model Order Identification of Dynamic Systems

Quoc-Cuong Nguyen[α] , Viet-Hung Vu[σ] & Marc Thomas[ρ]

## ABSTRACT

*This paper describes an efficient approach for model order determination, which allows identifying the dynamical behavior of the mechanical system by using observation input-output data. The concept based on the minimum means square error of the estimated transfer functions, which can effectively tackle measurement noise and modeling errors to identify appropriate low-order transfer functions of the structures via an Auto-Regressive Moving Average eXogenous (ARMAX) model. The effectiveness of the proposed method is validated exclusively using experimental data obtained from a grinding test of an industrial manipulator SCOMPI robot. Some other criteria, such as the Akaike Information Criterion (AIC), the Bayesian Information Criterion (BIC), and the Noise Order Factor (NOF), are investigated to verify the performance of the proposed methodology. The results demonstrated that the present technique is cost-effective in terms of optimal model order determination, and the ARMAX model turns out to be the most appropriate representation for feature extraction at the low order. Thanks to its flexibility in handling model disturbance, the proposed optimization strategy can capture all the dominant oscillation modes of the structure at the low orders, and system modal properties are efficiently and automatically determined. In contrast, the performance of the ARX model is shown to be less efficient when working at the low orders.*

*Keywords: ARMAX model, ARX model, frequency response functions, optimal orders, modal identification.*

*Author α σ ρ: École de technologie supérieure, 1100 Notre Dame West, Montreal, H3C 1K3, Quebec, Canada.*

## I. INTRODUCTION

Operational Transfer Functions (TFs) or Frequency Response Functions (FRFs) of mechanical structures play a vital role in understanding the dynamic characteristics of the systems and in solving general vibration problems during the operational process. They constitute an effective tool aiding the extraction of modal parameters. Estimating the transfer functions of a mechanical system has thus become an important task in many engineering applications. Different representations of transfer functions are crucial in the description and analysis of system properties. In industrial applications, a measurement of the transfer functions defining the structure properties in the frequency domain can be implemented using vibration instrumentations. Different methodologies are proposed in the literature with the aim of estimating operational transfer functions, with the most common applying the Fourier analysis. The Empirical Transfer Function Estimate (ETFE) is a natural nonparametric method that identifies transfer functions by taking the ratios of the Fourier transform of the outputs to those of the inputs [1]. However, this method requires more data points and raw ETFE estimates are generally not accurate enough. With these estimates, the variance does not decrease as the number of data points increases because they contain no information compression feature. Researchers have conducted various experimental studies on structural dynamics under operational conditions. In [2], the FRFs of a flexible joint industrial manipulator with a serial kinematic were identified based on a non-parametric closed loop. However, due to the nonlinearities of the robot, the method faced a challenge in eliminating disturbances in the estimated FRFs. Operational Modal Analysis (OMA) is another approach for identifying the modal properties of the structure using vibration data obtained under operating

London Journal of Engineering Research

conditions. Yili Peng et al. [3] identified in-process FRFs based on the OMA and Experimental Modal Analysis (EMA), which uses the natural frequencies and damping ratios to build FRFs under operating conditions. A simulation of a three-degree-of-freedom-mass-spring-damper system and experiments on a machine tool are adopted to verify the proposed method. Similarly, Zaghbani et al. [4] used OMA in the identification of the dynamics of a milling machine under a cutting process work. At the same time, another method was presented in [5] to generate FRFs from identified poles and zeros in the low-frequency domain. Recently, Coppotelli et al. [6] proposed an approach for estimating FRFs from operational data by changing different mass and stiffness distributions. This method also allows evaluating the modal parameters of the structure via operational modal testing. Conversely, Özşahin et al. [7] introduced a new technique to calculate the variation in tool point FRFs under different working conditions by using an inverse analysis of self-excited chatter vibration. In their method, chatter frequencies were experimentally determined and applied to estimate tool point FRFs on 5-axis milling machine via the relation between the measured force inputs and acceleration outputs. However, the tool point FRFs are not well estimated at high spindle speeds due to the presence at those speeds of a low signal-to-noise ratio and the bandwidth limitation of the dynamometer. Another in-process FRF identification approach of the spindle structure was presented in [8]. In that case, the tooltip FRFs were identified under operational conditions based on an inverse solution of critical stability limits. The method is helpful for predicting the stability of the tool holders when the direct measurement of the tool point FRFs is uncompromised. Parametric estimation methods constitute another system identification class. In these methods, it is suggested to use time series modeling for the mathematical description of the transfer functions. It combines the advantage and information obtained from both measurements and theoretical modeling. Depending on the availability of the measurement signals, the Auto Regressive model (AR) [9, 10] or the Auto Regressive Moving Average model (ARMA) [11] can be used if only the output is available. In [12, 13], a modal analysis was conducted in different industrial structures based on three Auto-Regressive Moving Average methods, namely, the recursive least-square, output error, and corrected covariance matrix methods to determine the optimal model order. Conversely, in the case of measurable or identifiable excitation forces, the Auto-Regressive eXogenous (ARX) model [14] can exploit, by assuming that the model's errors and disturbances are white noise. However, because of the unavoidable noise contaminated in the measured signals, the quality of estimated FRFs can be adversely affected by noise originating from the test environment. When the system operates in an industrial condition with a lot of disturbance, identifying the transfer functions of a complex structure may become difficult.

In this paper, we present an original method designed for automatically extracting the modal parameters from identified transfer functions based on the concept of the optimal ARMAX model. Particular attention is paid to selecting optimal model orders, which can closely reflect the dynamic system. The work contributes to the determination of a model order based on the estimated transfer functions, by using the framework of the ARMAX model. The proposed method is experimentally applied to a robot during its grinding operation, and the results are compared to those of the original ARX model. The measured grinding forces may be considered the exogenous inputs excitation, and the disturbances of the system are taken into account by adding the Moving Average part into the model. The estimated orders are verified based on the most common selection criteria, such as the Akaike Information Criteria (AIC) [15], the Bayesian Information Criteria (BIC) [16], and the Noise Order Factor (NOF) [17]. In this study, the ARMAX model is expressed in a convenient way for computation at the low orders, which gives a more parsimonious representation and helps improve the modeling performance, with less computational complexity. We have organised the rest of this paper in the following way. The motivation for the research is established in Section 2 through a detailed description of the time series modeling, with a focus on the ARX and ARMAX models. Section 3 proposes an original method to determine an optimal model order of

the mechanical system. Experiments are then conducted on the flexible manipulator, SCOMPI, under grinding operation to validate the proposed methods in Section 4, followed by the identification procedure and the results. We end by drawing several conclusions from this research.

## II. TIME SERIES MODELING

System identification is the art of modeling a dynamical system from raw time series data. We consider the problem of estimating a dynamic system model based on the measurement of an N points input-output data, which will be pre-classified into input $\mathbf{u}(t) \in \mathbb{R}$, $t = 1, \ldots, T$ and output $\mathrm{y}(t) \in \mathbb{R}$, $t = 1, \ldots, T$.:

$$\mathbf{Z}^N = \left(\mathbf{u}(t), \mathbf{y}(t)\right)_{t=1}^{N} \tag{1}$$

Various representations of linear time series such as Auto-Regressive (AR), Auto-Regressive Moving Average (ARMA), Auto-Regressive eXogenous (ARX), and Auto-Regressive Moving Average eXogenous (ARMAX) can be employed to extract dynamic parameters [18]. Since there are various time series data types, we should choose an appropriate model. In general, such models are based on an Auto-Regressive (AR) part or output, an eXogenous (X) part or input, or a Moving Average (MA) part or error term, depending on the situation. The AR model is the simplest time series representation, which linearly depends on output data (the vibration responses). In the availability of both input (the measurable and known excitation force) and output data, the ARX model is usable. It is possible to combine these models with the MA term and produce the ARMA representation for the output-only cases and the ARMAX model for the input-output conditions. Once the most appropriate modal structure is selected, we can apply a model to the measurement by minimizing certain criteria:

$$\hat{\boldsymbol{\theta}}_N = \operatorname{argmin} \mathbf{V}_N\left(\theta, \mathbf{Z}^N\right) \tag{2}$$

where $\theta$ is the unknown parameter vector of the parametric model structure.

In automatic control applications, given the current state and input signal, the model can be applied to predict the output of the system by choosing a cost function in the form.

$$\mathbf{V}_N\left(\theta, \mathbf{Z}^N\right) = \frac{1}{\mathrm{N}} \sum_{t=1}^{N} l\left(\mathbf{L}(q)\ \ (t,\theta)\right) \tag{3}$$

where $\mathbf{L}(q)$ represents a filter that removes unwanted properties in the measurement data, and $l(.)$ is a convex function.

The following quantity is the prediction error. $\hat{y}\left(t|t-1,\theta\right)$ is the one - step - ahead predictor representing the model of the system:

$$\boldsymbol{\varepsilon}(t,\theta) = \mathbf{y}(t) - \hat{\mathbf{y}}\left(t|t-1,\theta\right) \tag{4}$$

A common representation of the Linear Time-Invariant (LTI) system can be expressed in the from of the linear transfer function model:

$$\mathbf{y}(t) = \mathbf{G}(q,\theta)\mathbf{u}(t) + \mathbf{H}(q,\theta)\mathbf{w}(t) \tag{5}$$

where $q$ is the forward shift operator, that is, $q^{-k}.\mathbf{y}(t) = \mathbf{y}(t\text{-}k)$. Here, $\mathbf{y}(t)$ is a $n_y$ dimensional vector of output, $\mathbf{u}(t)$ is a $n_u$ dimensional vector of input, and $\mathbf{w}(t)$ is the disturbance sequence with an appropriate dimension and assumed to be an independent and identically distributed stochastic process, respectively. Furthermore, the transfer functions $\mathbf{G}(q,\theta)$ and $\mathbf{H}(q,\theta)$ are rational functions in the backward shift operator $q$, and the coefficients are given by the elements of the parameter vector $\theta$.

The predictor associated with the output is given by [18]

$$\hat{\mathbf{y}}\left(t|t-1,\theta\right) \triangleq \mathbf{H}^{-1}(q,\theta)\mathbf{G}(q,\theta)\mathbf{u}(t) + \left(1 - \mathbf{H}^{-1}(q,\theta)\right)\mathbf{y}(t) \tag{6}$$

where

$$\mathbf{H}^{-1}(q,\theta) \triangleq 1/\mathbf{H}(q,\theta)\mathbf{u}(t) \tag{7}$$

This model structure is quite general, but we can develop some special cases. A simple case is the ARX model structure, which is:

$$\mathbf{A}(q)\mathbf{y}(t) = \mathbf{B}(q)\mathbf{u}(t) + \mathbf{w}(t) \tag{8}$$

that can be rewritten in a more general polynomial form as:

$$\{\mathbf{y}(t)\}+\sum_{k=1}^{n_a}[\mathbf{A}_k]\{\mathbf{y}[t-k]\}=\sum_{k=1}^{n_b}[\mathbf{B}_k]\{\mathbf{u}[t-n_k-k+1]\}+\{\mathbf{w}(t)\} \quad (9)$$

where

$$\mathbf{A}(q)=I+a_1q^{-1}+a_1q^{-2}\cdots+a_{n_a}q^{-n_a} \quad (10)$$

$$\mathbf{B}(q)=b_0+b_1q^{-1}+b_2q^{-2}\cdots+b_{n_b}q^{-n_k-n_b+1} \quad (11)$$

are autoregressive and exogenous matrix parameters, with $I$ denoting the identity matrix. $n_a$, $n_b$, and $n_k$ are the orders of the ARX model, $n_a$ is equal to the number of poles and $n_b$ is the number of zeros, while $n_k$ is the pure time delay in the system. Since $\mathbf{G}(q,\theta)=\mathbf{B}(q)/\mathbf{A}(q)$ and $\mathbf{H}(q,\theta)=1/\mathbf{A}(q)$,, the predictor of the output can be written as:

$$\hat{\mathbf{y}}(t|t-1\varphi\theta)=\mathbf{B}(q)\mathbf{u}(t)+\left(1-\mathbf{A}(q)\mathbf{y}(t)\right)=\quad (t)^T \quad (12)$$

where

$$\boldsymbol{\varphi}(t)\triangleq\left(-y(t-1)\cdots-y(t-n_a)\;u(t-1)\cdots u(t-n_b)\right)^T \quad (13)$$

$$\boldsymbol{\theta}\triangleq\left(a_1\;\cdots\;a_{na}\;\;b_1\;\cdots\;b_{nb}\right)^T \quad (14)$$

When the noise is assumed to be a white Gaussian process with zero means, which is uncorrelated with the regressors, the model parameters $\theta$ are estimated via the Least-Square (LS) estimator [19]:

$$\hat{\theta}_N^{LS}=\operatorname{argmin}\frac{1}{N}\sum_{t=1}^{N}\left(\mathbf{y}(t)-\boldsymbol{\varphi}(t)^T\boldsymbol{\theta}\right)^2 \quad (15)$$

The variance $\mathbf{y}(t)-\boldsymbol{\varphi}(t)^T\boldsymbol{\theta}$ represents the remaining un-modelled behavior of the data.

The corresponding transfer function is $\mathbf{G}(q,\theta)=\mathbf{B}(q)/\mathbf{A}(q)$.(15-a)

However, in this case, only the deterministic part of equation (1) is estimated by considering no noise $\mathbf{H}(q,\theta)$. If a noise model is sought, additional steps are needed, assuming that the noise is described by a Moving Average process $\mathbf{C}(q)$, which results in an ARMAX structure:

$$\mathbf{A}(q)\mathbf{y}(t)=\mathbf{B}(q)\mathbf{u}(t)+\mathbf{C}(q)\mathbf{w}(t) \quad (16)$$

and its polynomial form

$$\{\mathbf{y}(t)\}+\sum_{k=1}^{n_a}[\mathbf{A}_k]\{\mathbf{y}[t-k]\}=\sum_{k=1}^{n_b}[\mathbf{B}_k]\{\mathbf{u}[t-n_k-k+1]\}+\sum_{k=1}^{n_c}[\mathbf{C}_k]\{\mathbf{e}[t-k]\}+\{\mathbf{w}(t)\} \quad (17)$$

where

$$\mathbf{C}(q)=1+c_1q^{-1}+c_2q^{-2}\cdots+a_{n_c}q^{-n_c} \quad (18)$$

is the polynomial of order $n_c$ which represents for Moving Average term.

In contrast with the simpler ARX model, this presentation form offers a noisy transfer function $\mathbf{H}(q,\theta)=\mathbf{C}(q)/\mathbf{A}(q)$, which allows representing different types of noise characteristics through a proper choice of the MA polynomial term. In engineering applications, it is unavoidable when environmental noise contaminated in measured data. Therefore, a parametric system identification algorithm should be adopted to identify the modal parameters from the noisy data. Under this condition, the ARMAX model with real-time identification proves to be efficient. Figure 1 presents the structures of both ARX and ARMAX models.

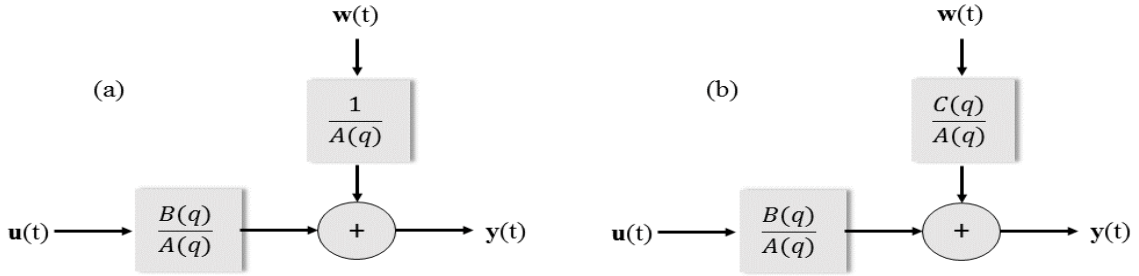


*Fig. 1:* Model structures of ARX (a) and ARMAX (b) [18]

If only the ARX model is use, the noise model is described as $\mathbf{H}(q)=1/\mathbf{A}(q)$ , where $\mathbf{A}(q)$ is also used as the denominator of $\mathbf{G}(q)$ describing the dynamic model. This model implies that the polynomial form must be an average estimate of the poles of $\mathbf{G}(q)$ and $\mathbf{H}(q)$. However, the noise model can be better estimated using the ARMAX model, as described by the numerator polynomial term $\mathbf{C}(q)$. When parametric methods use for model estimation, the transfer functions to be estimated are defined as a function of a parameter vector $\theta_N \triangleq (a_1 \ldots a_{na}\ b_1 \ldots b_{nb}\ c_1 \ldots c_{nc})^T$. For the identification of the value $\hat{\boldsymbol{\theta}}_N$ , $\bar{\mathbf{G}}\left(q,\bar{\theta}_N\right)$ and $\bar{\mathbf{H}}\left(q,\hat{\theta}_N\right)$ are closest to $\mathbf{G}(q,\theta_N)$ , and $\mathbf{H}(q,\theta_N)$. In [20], the authors showed that under reasonable conditions,

$$\hat{\boldsymbol{\theta}}_N \to \boldsymbol{\theta}_N^* \tag{19}$$

where

$$\boldsymbol{\theta}_N^* = \arg\min \frac{1}{\mathrm{N}} \sum_{k=1}^{N} \varepsilon\left\{\varepsilon_k^2(\theta)\right\} \tag{20}$$

and $\boldsymbol{\varepsilon}(t,\theta)$ is prediction error and defined in equation (4). According to [21, 22], with this definition of $\theta_N^*$ , it is possible to split the total estimation error between the true frequency response function $\mathbf{G}(q)$ and the estimated one $\mathbf{G}\left(q,\hat{\theta_N}\right)$ into two parts as follows:

$$\mathbf{G}(q)-\mathbf{G}\left(q,\theta_N\right)=\left[\mathbf{G}(q)-\mathbf{G}\left(q,\theta_N^*\right)\right]+\left[\mathbf{G}\left(q,\theta_N^*\right)-\mathbf{G}\left(q,\theta_N\right)\right] \tag{21}$$

As we can see in equation (21), the errors in the estimated FRF have two components. The first contribution $\left[\mathbf{G}(q)-\mathbf{G}\left(q,\theta_N^*\right)\right]$ is the bias contribution, a deterministic quantity due to the modeling error. If the selected model has a lower or a higher complexity than the true system, this bias error will be present at some frequencies. Choosing the model order should be flexible enough to allow a good fit to the measurement data but adequately constrained so that noise does not invoke unsuitable models. Consequently, selecting an optimal model order respecting this compromise is an important issue in system identification. This concern is analyzed in the following section to select the optimal model orders of an ARMAX model. The second contribution $\left[\mathbf{G}\left(q,\theta_N^*\right)-\mathbf{G}\left(q,\hat{\theta_N}\right)\right]$ represents the noise or variance errors, which are due to noise in the measured input and output data. It is a random variable that will disappear if there is no noise or if the number of data tends to infinity.

## III. A MODEL ORDER DETERMINATION APPROACH

When time series modeling ARX or ARMAX models employed, the performances may be affected by selecting the model order. Choosing a sufficient and correct model order has always been a challenging issue. Once the model orders are properly selected, the models successfully represent the underlying phenomenon with the lowest complexity. This method aims not only to find a model capable of describing a specific set of data but is also helpful for the validation of the inference procedures. Consequently, there is a need to develop a reliable method to identify the orders of AR, MA, and eXogenous polynomials. In general, most of the mechanical structures are operated in the low-frequency range with limited bandwidth. Having a model with orders that are too high may lead to an overfitting problem as it includes too much irrelevant oscillation information and generates high computational costs, and a model with orders that are too low will not be solid enough to capture the underlying physical system dynamics. For its part, a model with an appropriate order can precisely describe the dynamic characteristics of the system. Because of its important role in system identification, model order determination has attracted much attention in the literature, with researchers proposing different criteria for order determination [23]. The final prediction error (FPE) criterion was originally proposed by Akaike [24] for determining the AR order and was extended to the ARMA model by [25]. After adding the inflating effects of estimated coefficients, the optimal order was chosen by minimizin the one-ste-ahead mean square forecast error. A method based on the eigenvalues of a modified covariance matrix, which is robust

to noise levels, was proposed in [12, 13] for determining the model order. Some other concept as information theory like Akaike's Information Criterion (AIC) [15], Bayesian Information Criterion (BIC) [16] or Minimum Description Length (MDL) [26] were developed to produce an estimate model order. Among these techniques, the AIC is a heuristic approach, which has attracted much attention in the literature. His technique penalizes the likelihood of the number of parameters in the model by attempting to choose the most suitable model order.

Considering an N-dimensional time-series data, the AIC is given by equation (22):

$$\mathbf{AIC}(z) = \mathrm{N}\ln\left(\det|\hat{\Sigma}|\right) + 2(z) \tag{22}$$

where N denotes the number of data points, ($z$) is a dimension associated with the vector of unknown parameters to be estimated and

$$\hat{\Sigma} = \frac{1}{\mathrm{N}}\sum_{t=1}^{N}\hat{\mathbf{w}}[t].\hat{\mathbf{w}}^{T}[t] \tag{23}$$

$\hat{\Sigma}$ is the covariance matrix of the innovation sequence associated with the estimated coefficients, the $\boldsymbol{w}$[t] is innovation square, or the model error.

When the AIC value is at a minimum, we obtained the most suitable order. A minimum AIC is theoretically situated at a sufficient value of ($z$) that best represents the dimension of the unknown parameters. For an ARMAX ($n_a$, $n_b$, $n_c$, $n_k$)($p$) model, ($z$) would typically be equal to ($n_a$+$n_b$+$n_c$+$n_k$), with $n_a$, $n_b$, $n_c$ and $n_k$ orders for its AR, MA, eXogenous components and time delay, respectively, while $p$ represents the number of orthonormal functions by which each of these components is multiplied. Here, it should be noted that although there would be many possible combinations of $n_a$, $n_b$, $n_c$ and $n_k$ that can produce the same adequate value of ($z$), only the right combination would yield the smallest AIC value. The $z$ value may be defined as:

$$z = (n_a + n_b + n_c + n_k)(p) \tag{24}$$

The AIC corresponding to an ARMAX ($n_a$, $n_b$, $n_c$, $n_k$)($p$) model is written here as:

$$\mathbf{AIC}(n_a, n_b, n_c, n_k)(p) = \mathrm{N}\ln\left(\det|\hat{\Sigma}|\right) + 2(n_a + n_b + n_c + n_k)(p) \tag{25}$$

where $z$ is the number of scalar parameters in the ARMAX model.

However, in many cases, AIC does not give an optimal order. [27] showed empirical evidence that AIC tends to pick models which are over-parameterized. The BIC overcomes this shortcoming by including an additional term that penalizes the model complexity and enhances the procedure, which are based on the same concepts governing the AIC but are better suited for large data sequences. The BIC criterion has the following general form:

$$\mathbf{BIC}(z) = \ln\left(\det\left|\hat{\Sigma}\right|\right) + (z)\frac{\ln(\mathrm{N})}{\mathrm{N}} \tag{26}$$

In this paper, it is written as:

$$\mathbf{BIC}(n_a, n_b, n_c, n_k)(p) = \ln\left(\det\left|\hat{\Sigma}\right|\right) + (n_a + n_b + n_c + n_k)(p)\frac{\ln(\mathrm{N})}{\mathrm{N}} \tag{27}$$

These criteria rely on the evolution of the error covariance, which monotonically diminishes concerning the model order. It asymptotically chooses the correct order model if the underlying multiple time series has high dimensions but tends to overestimate the model order as the data length increases. Thus, selected model orders can be greater than the optimal model orders.

However, attention has recently shifted to the equally important problem of bias resulting from under-modeling. Wahlberg and Ljung [28] have conducted excessive research on the distribution of bias and variance in the estimated transfer function.

In this paper, we present an improved approach to determining time series model orders based on means square errors of the estimated transfer function. This approach is different from traditional criteria such as AIC and BIC. We transformed an averaged frequency means square

error on the estimated transfer function into a mean square output prediction error criterion.

The proposed method allows extracting the modal residuals with a sufficient order that guarantees the extraction of uncorrelated residual samples and the avoidance of an overfitting problem. The selection of the optimal order is based on a minimal variance of the total mean square error $\varepsilon\left\{\left|\mathbf{G}(q)-\mathbf{G}\left(q,\hat{\theta}_N\right)\right|^2\right\}$ between the true and estimated transfer functions based on N observation data. As we mentioned in the previous section, the means square error between $\mathbf{G}(q)$ and $\mathbf{G}\left(q,\hat{\theta}_N\right)$ is shown to be the sum of two terms, which both depend on the order of the estimated model, namely, a bias term that decreases with the model order and a variance term which increases with this order. We defined $P_{optimal}$ as the optimal order of the structure while assuming that both input and output data are available. The criteria can be formulated as follows:

$$\mathbf{P} \triangleq \frac{1}{2\pi}\int_{-\pi}^{\pi} \hat{\mathbf{E}}_{p_o}(\omega)\mathbf{D}_u(\omega)d\omega \tag{28}$$

where $\hat{\mathbf{E}}_{p_o}(\omega)$ is the estimated Means Square Error (MSE) between the true and estimated transfer functions, $\varepsilon\left\{\left|\mathbf{G}(q)-\mathbf{G}\left(q,\hat{\theta}_N\right)\right|^2\right\}$. The input $\mathbf{u}(t)$ is assumed to be a quasi-stationary sequence with zero time average and $\mathbf{D}_u(\omega)$ denotes the Power Spectrum Density (PSD) of the input.

The optimal order obtained when:

$$\mathbf{P}_{\text{optimal}} = \underset{p_O=1,2,\ldots}{\arg\min}\left(\frac{1}{2\pi}\int_{-\pi}^{\pi} \hat{\mathbf{E}}_{p_o}(\omega)\mathbf{D}_u(\omega)d\omega\right) \tag{29}$$

The aim of this technique is converting the bias error into a random variable by ascribing a prior distribution to it. Consequently, we obtain an estimate for the average characteristics of the total errors. We assume that the transfer function represented by $\mathbf{G}_T(q)$ is a stochastic process indexed by the variable $\omega$, and given some value of $\theta_o$, it can be decomposed as the sum of a parameterized $\mathbf{G}_T(q,\theta_0)$ plus the residual $\mathbf{G}_\Delta(q)$:

$$\mathbf{G}_T(q) = \mathbf{G}_T(q,\theta_0) + \mathbf{G}_\Delta(q) \tag{30}$$

where $\mathbf{G}_\Delta(q)$ is a zero-mean stochastic process:

$$\varepsilon\left\{\mathbf{G}_\Delta(q)\right\} = 0 \tag{31}$$

Each system will provide one realization and analogous to the embedding of the single noise realization in a stochastic process. In the framework of an ARMAX model, for ease of implementation, we restrict our consideration to the linear model structures of the Single Input Single Output (SISO) case. The question of computing asymptotic variance expressions in the presence of under-modeling for transfer function prediction errors in frequency domain identification is addressed in this paper. The discrete linear transfer function of the ARMAX model can be expressed in the following form:

$$\mathbf{G}\left(q,\hat{\theta}_N\right) = \frac{\mathbf{B}(q,\theta)}{\mathbf{A}(q,\theta)} = \frac{b_0 + b_1q^{-1} + b_2q^{-2}\cdots + b_{n_b}q^{-n_k-n_b+1}}{I + a_1q^{-1} + a_1q^{-2}\cdots + a_{n_a}q^{-n_a}} \tag{32}$$

The true transfer function can be expressed by the relationship between the measured input and output of the system:

$$\mathbf{G}_T(q) = \frac{\mathbf{y}(t)}{\mathbf{u}(t)} \tag{33}$$

The $\hat{\mathbf{E}}_{p_o}(\omega)$ means square error between the true and estimated transfer function in (28) is calculated by the following equations:

$$\hat{\mathbf{E}}_{p_o}(\omega) = \varepsilon\left\{\left|\mathbf{G}\left(q,\hat{\theta}_N\right)-\mathbf{G}_T(q)\right|^2\right\} = \text{Trace}\left\{\mathbf{Q}_g\right\} \tag{34}$$

where

$$Q_{\tilde{g}} \triangleq \varepsilon\{\tilde{g}(q)\tilde{g}(q)^T\} \tag{35}$$

$$\tilde{g}(q) \triangleq \begin{bmatrix} \text{Re}\left\{\mathbf{G}_T(q)-\mathbf{G}\left(q,\hat{\theta}_N\right)\right\} \\ \text{Im}\left\{\mathbf{G}_T(q)-\mathbf{G}\left(q,\hat{\theta}_N\right)\right\} \end{bmatrix} \tag{36}$$

This index is an effective criterion since it includes the stochastic participation in the denominator by adding an input power spectral density $\mathbf{D}_u(\omega)$.

We converted a average frequency means square error criterion on the estimated transfer functions into a mean square output prediction error criterion. Due to the presence of measurement errors, the proposed method is adopted to determine the optimal model orders and proved its robustness to parameter uncertainties. This modification bridged the connection between classical variable selection criteria such as AIC and BIC and the non-concave penalized likelihood methodology that allows greater flexibility in choosing the desired models. The goodness of its performance will be assessed in the next section through a comparison with traditional validation methods. The optimal model will be tested by the quality of the residuals, the histogram, and autocorrelation functions.

## IV. INDUSTRIAL APPLICATION ON A SCOMPI ROBOT

### *4.1 Description of the test structure*

Flexible manipulators are employed in the maintenance of large hydro electronic equipment as they represent an effective solution for repair jobs [29]. Despite their attractive properties, controlling lightweight robot manipulators is still a challenging task. Their flexibility induces structure vibration that deteriorates the trajectory tracking accuracy and may lead to instability issues. In this part, the present method is adopted to identify the dynamic behavior of a light, portable, track-based multi-process manipulator named SCOMPI (Super-COMPact Ireq) [30, 31]. The dynamical transfer functions and modal parameters must be monitored during the grinding process to control vibrations. Figure 2 presents the working envelop and the construction of the robot, with its links and joints.

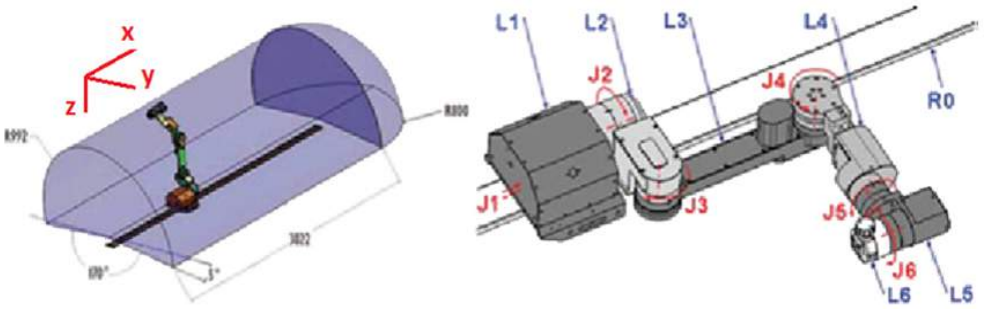


*Fig. 2:* Structure of SCOMPI robot [29-31]

### *4.2 Experimental procedure*

The tool contact point Frequency Response Functions (FRFs) and their modal parameters represent the key for solving the dynamics analysis. In this paper, the actual grinding forces are used as the input excitations in estimating the FRFs. The grinding test is performed at the 3225 rpm rotating speed with an average 0.08 mm axial depth of grinding cut. The grinding work is realized on a hard steel EN31-64HNC workpiece with the dimensions of 150 x 7 x 48 mm. During the cutting operation, cutting forces are measured with a type CH8408 3-axis Kistler dynamometer, which is directly attached under the workpiece to record the normal force direction ($F_x$), the tangential force direction ($F_y$) and the axial force direction ($F_z$). At the same time, three PCB-352C34 piezoelectric sensors with a sensitivity of 5.29 mV/G are used to measure accelerations at the robot's end-effector ($S_1$ - $S_3$) to capture the vibration in three directions. The measurement is conducted through the LMS data acquisition system for 10 s at a 512 Hz sampling frequency. Figure 3 shows the actual experimental setup of the SCOMPI robot under a real grinding operation. An LMS test lab system was used for acquiring the data in real-time during experiments, as well as for calculating averaged FRFs, which were used to validate the estimated results of the proposed approach.

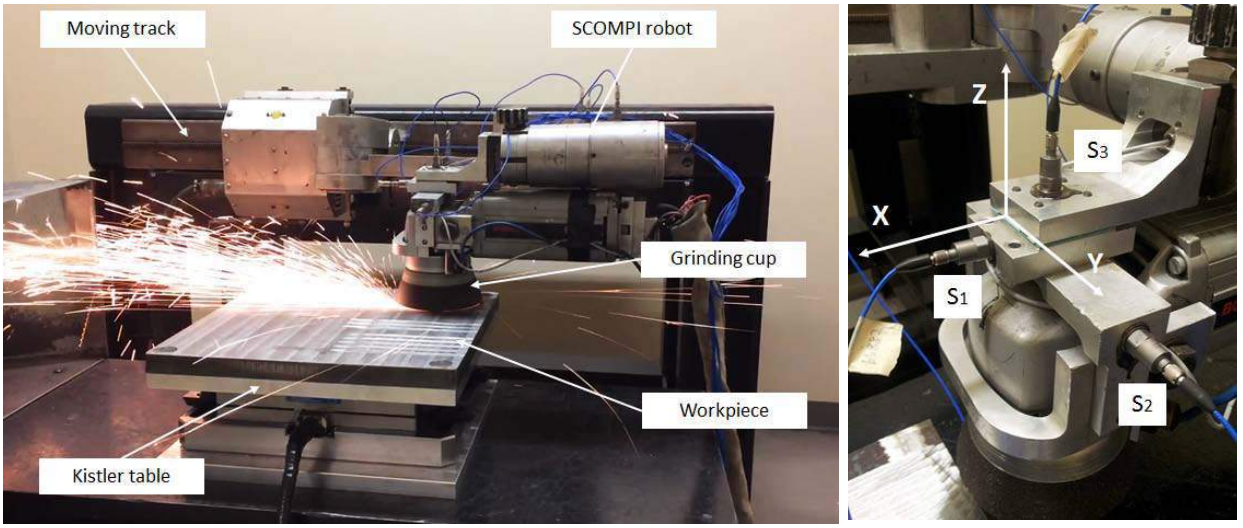


*Fig. 3:* Experimental setup for SCOMPI robot during grinding operation

The structure is excited through a grinding operation, during which all the effects related to the rotating tool or the grinding process are considered. FRFs are obtained during the cutting operation through the relations of the cutting forces and the vibration responses. The measured cutting forces are taken as the excitation sources of the system. In this paper, the operational FRFs are determined from the relation between the cutting forces and responses through the time series ARMAX modeling. The detailed experimental description is provided in Table 1.

*Table 1:* Grinding conditions of the SCOMPI test

| No. | Experimental description | Information | Units |
|---|---|---|---|
| 1 | Grinding cup (Norton BuleFire) diameter | 12.7 | cm |
| 2 | Workpiece material | AISI 1081 | - |
| 3 | Density of AISI 1081 | 7.87 | $g/cm^3$ |
| 4 | Workpiece dimensions | 20.32 x 25.4 x 2.54 | cm |
| 5 | Grinding direction | Normal direction | - |
| 6 | Power | 500 – 3400 | W |
| 7 | Length of cut | 16.2 – 18.5 | cm |
| 8 | Width of cut | 1 – 1.55 | cm |
| 9 | Depth of cut | 0.0158 – 0.00165 | cm |
| 10 | Rotation speed | 3225 | rpm |
| 11 | Angle of grinding cup | 5-10 | degree |

The measured grinding forces and the acceleration responses in each direction are shown in Figure 4.

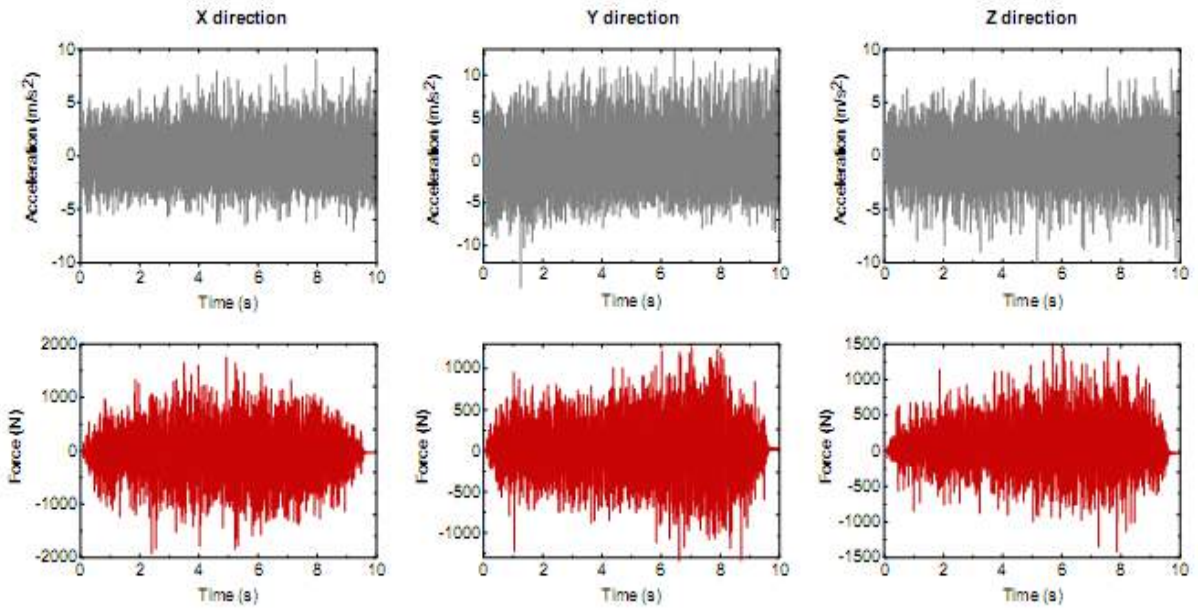


*Fig. 4:* Measured data on SCOMPI robot

## V. IDENTIFICATION PROCEDURE

### 5.1 Model orders estimation

The parametric identification of the structural dynamics is based on force and response signals with a 10s sample length. The modeling strategy consists of the successive fitting of the ARMAX ($n_a$, $n_b$, $n_c$, $n_k$) model. First, the model orders are selected based on the Akaike Information Criterion (AIC) and the Bayesian Information Criterion (BIC). Figure 5 plots result from the AIC and BIC techniques respectively obtained by directly fitting the ARMAX model of increasing orders p = 1– 60 to the different sets of experimental data.

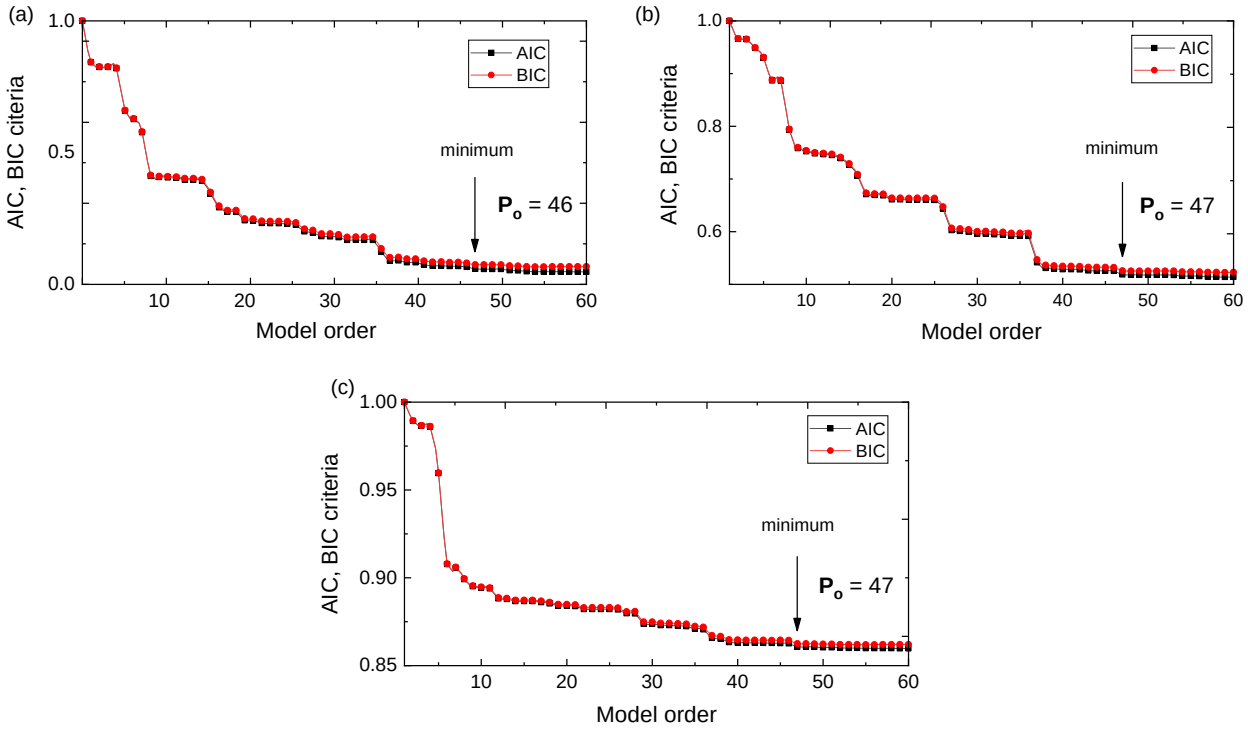


*Fig. 5:* Model order selection based on AIC and BIC criteria for different sets of data: (a) X data, (b) Y data, (c) Z data

By dividing the experiment into different test directions based on the operation of the robot, we can decompose and characterize the dynamical behavior of the system for each direction. From Figure 5, both the AIC and BIC methods decrease with the model order, and a minimum may be assumed close to 47. However, the main limitation of using such techniques is that they may suggest different model orders and not determine the optimal orders. Thus, these values must be judged carefully.

By applying the proposed method in selecting an optimal model order, the orders for which all curves lead to a stable value are identified. Figure 6 illustrates an optimal order, defined as the smallest order value. The point of convergence starts at around order of 10 in all three directions.

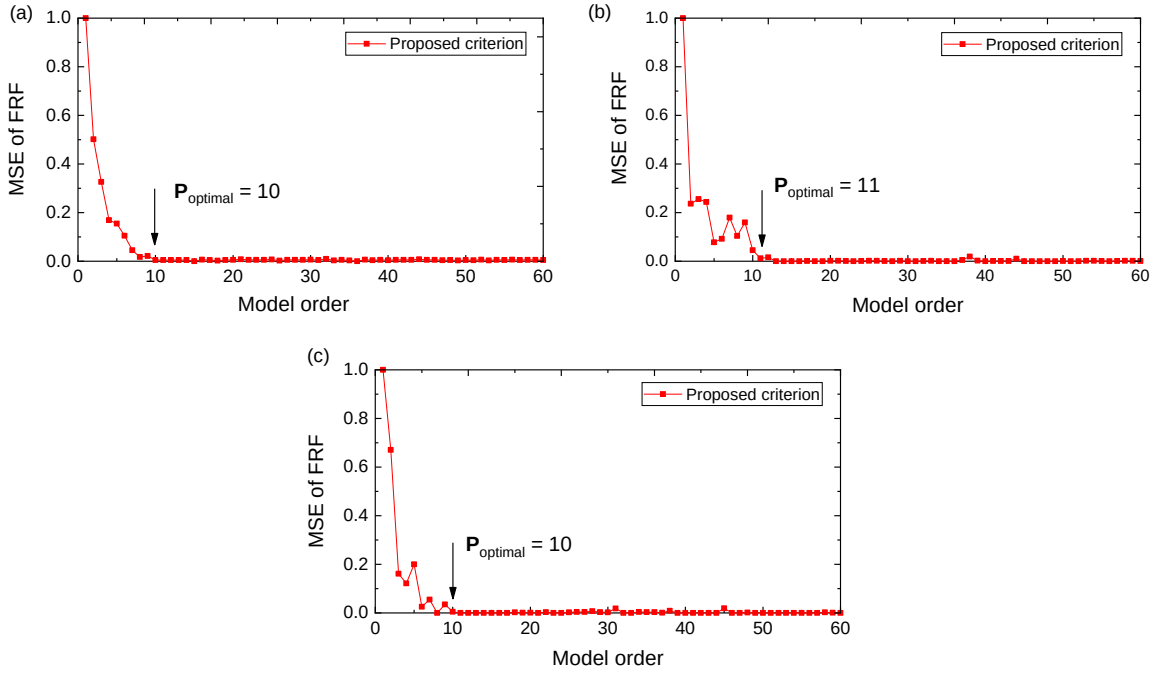


*Fig. 6:* Model orders selection based on the proposed approach for different sets of data: (a) X data, (b) Y data, (c) Z data

To compare the efficiency of the present method, Vu et al. [17] proposed a technique for determining an efficient model order $p_{eff}$ based on the analysis of the Noise-to-Signal Ratio (NSR). The estimated $\hat{\text{NSR}}$ is given in equation (37) based on the trace norm part of the error covariance matrices $\hat{\mathbf{M}}$ and the estimated deterministic $\hat{\mathbf{K}}$.

$$\hat{\text{NSR}} = \frac{\text{Trace}\,(\hat{\mathbf{M}})}{\text{Trace}\,(\hat{\mathbf{K}})}(\%) \quad \text{or} \quad \hat{\text{NSR}} = 10\log_{10}\frac{\text{Trace}\,(\hat{\mathbf{M}})}{\text{Trace}\,(\hat{\mathbf{K}})}(\text{dB}) \tag{37}$$

A Noise-ratio Order Factor (NOF) is calculated as a variation of the NSR between two successive orders:

$$\text{NOF}^{(p)} = \text{NSR}^{(p)} - \text{NSR}^{(p+1)} \tag{38}$$

The NOF is a representative factor for the convergence of the NSR, which changes dramatically at low orders and converges at high orders. Since this criterion is positive and close to zero, the convergence may be assumed close to 10, considered as an efficient model order (Figure 7).

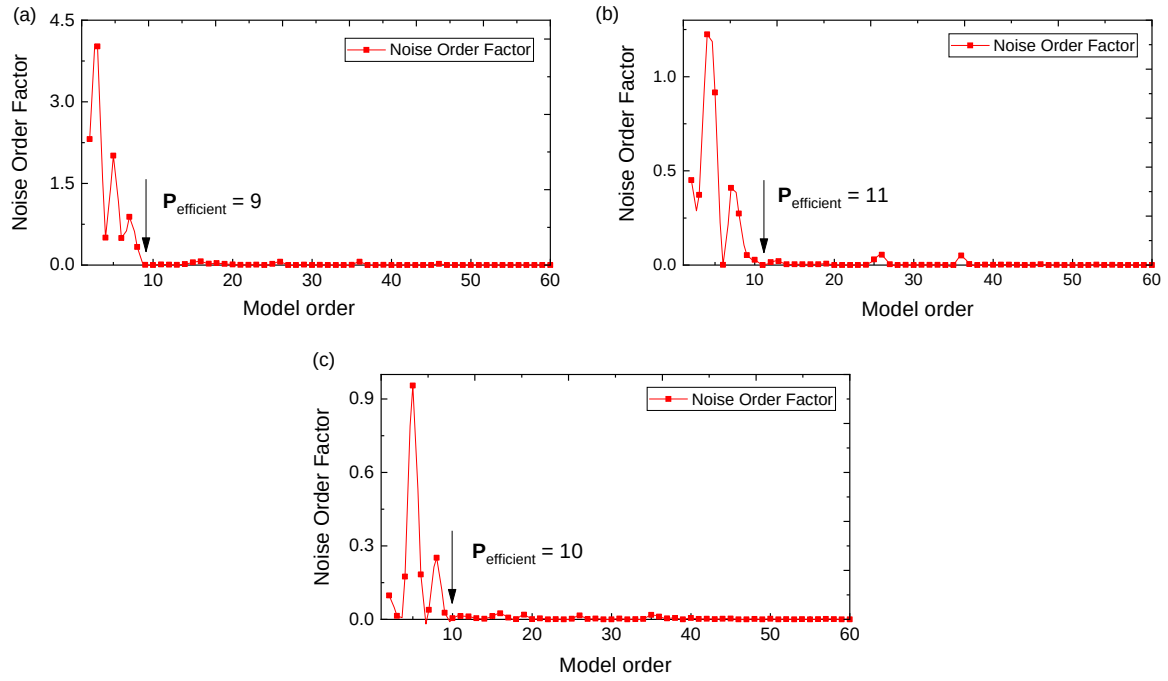


*Fig. 7:* NOF evolution and efficient model orders selection for different sets of data: (a) X data, (b) Y data, (c) Z data

Theoretically, the modeling of a complex structure like the SCOMPI robot should result in a high-order model. Based on the AIC and BIC criteria, a 47-order model should be selected as a suitable choice. However, a lower order could be chosen with all essential characteristics of the real system preserved. By comparison, the Noise-to-Signal Ratio and the proposed method are selected with a model order of around 10.

However, in the case of the complex ARMAX model, it is characterized by three different orders, the model order estimation is not straightforward. In experimental modal analysis, the orders $n_a$, $n_b$, and $n_c$ depend on the model parameterization. According to [32, 33], the choice of $n_b$ is a function of the type of response measurements used and the inter-sample behavior of the data. Moore et al. [34] suggest an ARMAX ($p$,$p$,$p$) model in which $p = n_a = n_b = n_c$, for the case of a vibration acceleration measurement, or ARMAX($p$, $p$ - 1, $p$), for the case of a vibration displacement or velocity measurement with an appropriate time delay. As can be noted, since structural vibrations are usually measured in terms of acceleration rather than displacement and velocity in actual experiments, we would choose $p_{optimal} = n_a = n_b = 10$.

The Moving Average order is initially set equal to the Auto Regressive part since the resulting noise model has the flexibility of representing several stochastic processes, including white noise. There is some experimental evidence in the structural systems [34, 35], which indicates that for low noise levels, the required MA order is often smaller or equal to the AR one. The order $n_c$ of the MA matrix and time delay order $n_k$ are dependent on the noise present in the system, and generally, no information on the nature of this disturbance is available. Therefore, the extracted required value of the MA order, as well as an appropriate time delay order, will be carefully examined in this study. This can be done by initially setting $n_a = n_b = 10$, and then selecting the best model by using a proposed criterion to test the effectiveness of changing $n_c$ and $n_k$ from the set of {1, 2, ..., 20}, resulting in the estimated results presented in Figure 8.

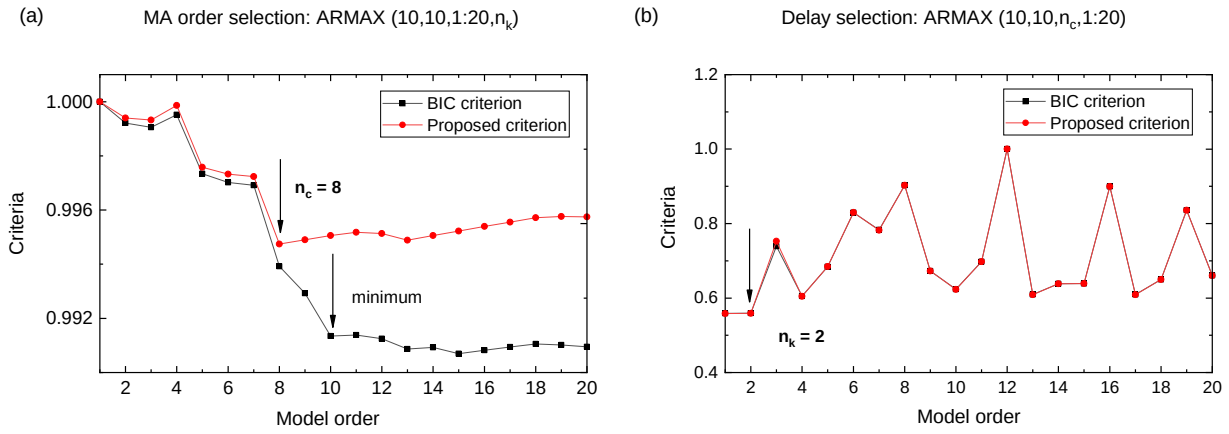


*Fig. 8:* Moving average order (a) and time delay order (b) selection

Based on these results, the set of orders (10,10,8,2) is chosen as consisting of the smallest order values, which can be applied to fit the data with a negligible discrepancy and can be effectively utilized for modal analysis. However, a further step needs to be validated to assess the adequacy of the estimated model. Several diagnostic checks can be used to decide whether the ARMAX model is adequate based on the residuals, which characterized by an uncorrelated sequence. Figures 9 and 10 display the histogram, Quantile-Quantile (QQ) plot, Autocorrelation Function (ACF), and Partial Autocorrelation Function (PACF) of the residuals of the ARMAX model. The histogram is unit-modal and symmetric around zero. From the QQ-plot, the residual approximately fit a straight line, and this can be assumed normal. The values of both ACF and PACF are located roughly between the upper and lower bounds of a confidence interval. Therefore, the residual can be assumed independent, and the selected orders can be used.

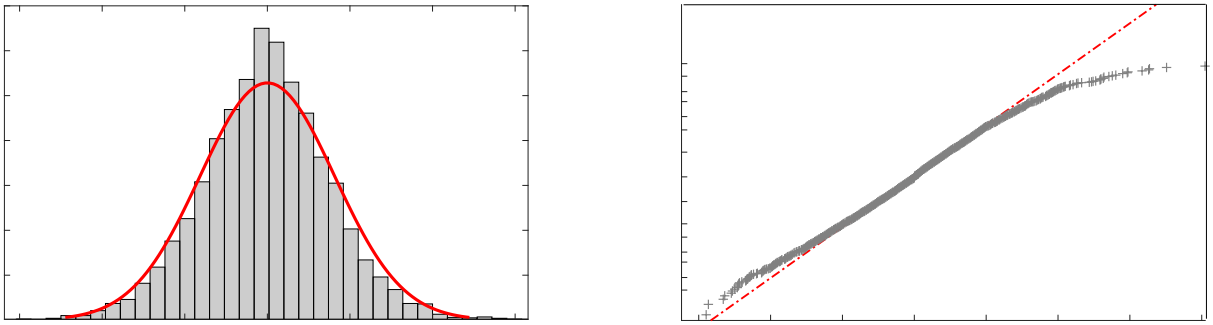

*Fig. 9:* Residual errors histogram and normal probability plot of an estimated ARMAX (10,10,8,2) model

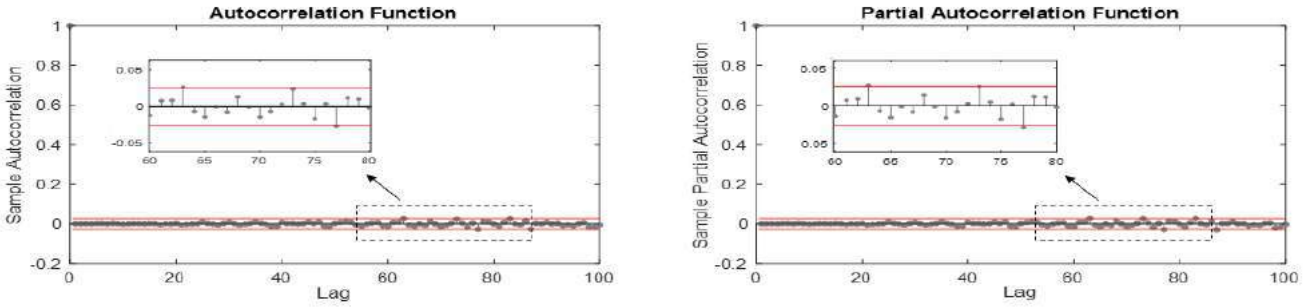


*Fig. 10:* Autocorrelation function (ACF) and Partial Autocorrelation Function (PACF) of the residual ARMAX (10,10,8,2)

The above identification procedure leads to an optimal ARMAX (10,10,8,2) model, which is selected as an adequate model for structural analysis, and for the extraction of modal parameters. The next section evaluates the performance and effectiveness of this dominant reduced model, in which all the essential characteristics of the real system can be retained.

### 5.2 Frequency Response Functions identification

Based on the discussion above, once the excitation and vibration measurement data have been selected with the appropriate orders, an ARMAX model needs to be estimated within the model structure. In this section, the two parametric transfer function estimators for assessing the dynamic flexible manipulator are analyzed. The FRFs estimation is performed using two parametric models, ARX ($n_a$, $n_b$, $n_k$) and ARMAX ($n_a$, $n_b$, $n_c$, $n_k$), based on data records from the structure. A scalar Single Input – Single Output (SISO), ARX and ARMAX models are used at a time. The input signals to each model are the force signals, and the output signals are measured accelerations, respectively. The assessments of an ARX model, and an ARMAX model, are undertaken based on an experimental SCOMPI structure during the grinding operation. Figures 11-19 demonstrate the estimated Frequency Response Functions obtained by the ARX and ARMAX models, which are compared to those measured by the LMS system.

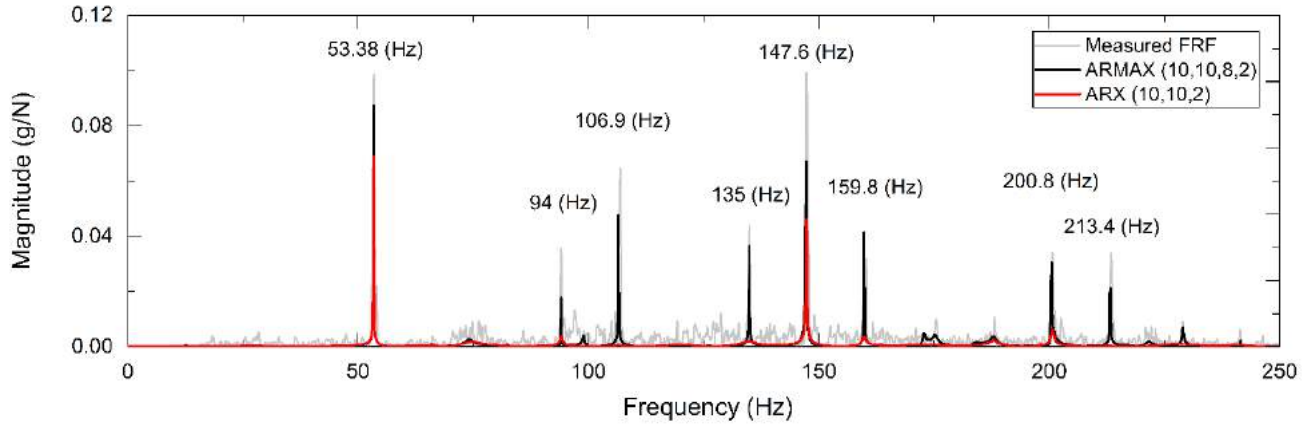


*Fig. 11:* Estimated Frequency Response Function $FRF_{xx}$

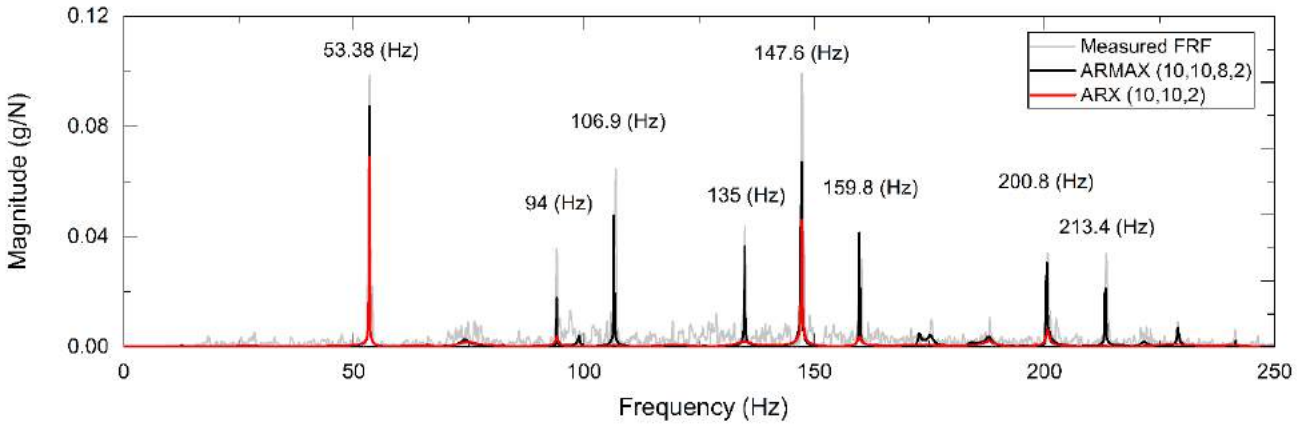


*Fig. 12:* Estimated Frequency Response Function $FRF_{xy}$

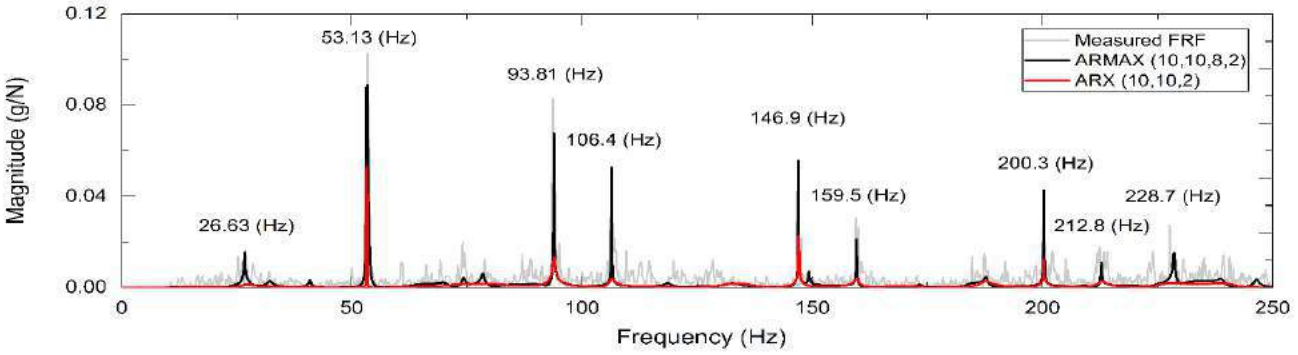


*Fig. 13:* Estimated Frequency Response Function $FRF_{xz}$

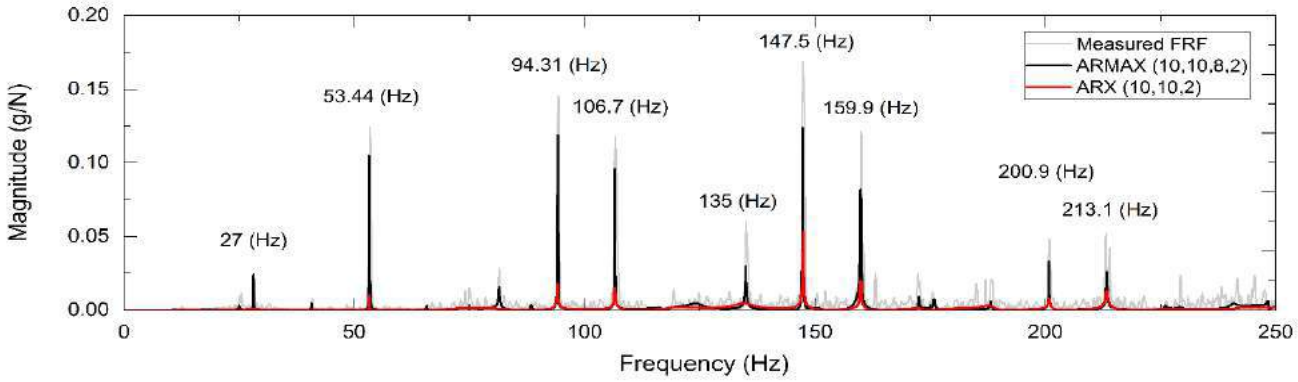


*Fig. 14:* Estimated Frequency Response Function $FRF_{yx}$

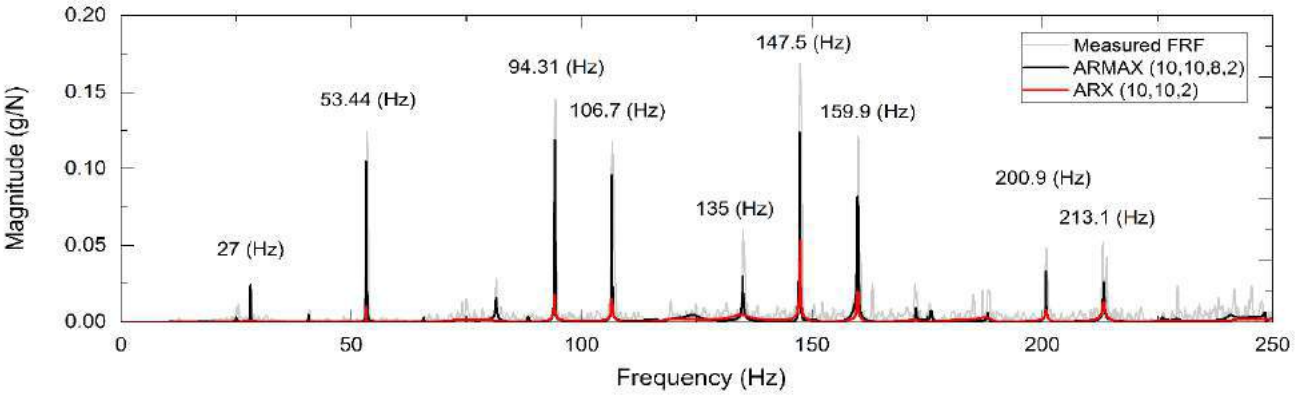


*Fig. 15:* Estimated Frequency Response Function $FRF_{yy}$

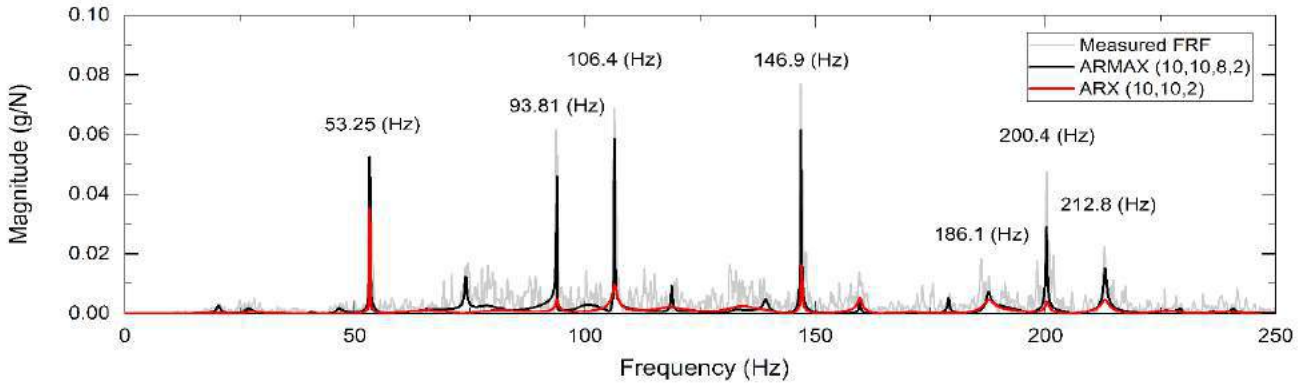


*Fig. 16:* Estimated Frequency Response Function $FRF_{yz}$

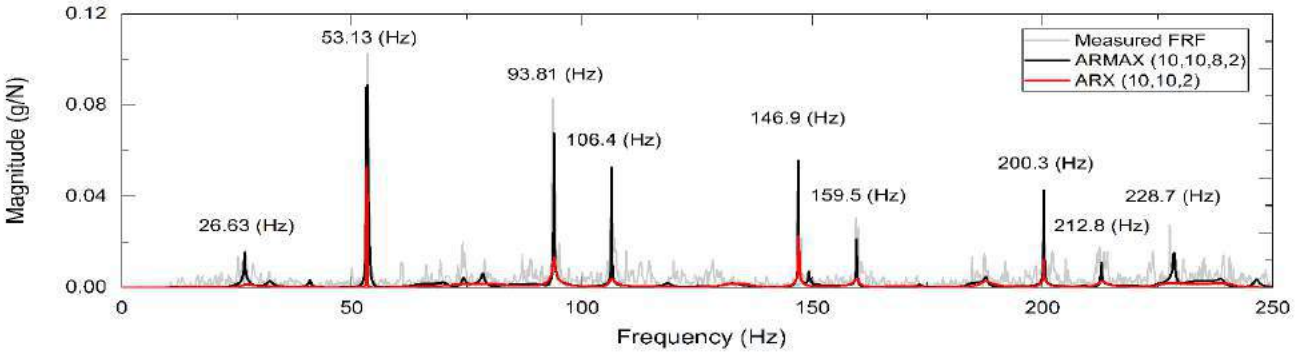


*Fig. 17:* Estimated Frequency Response Function $FRF_{zx}$

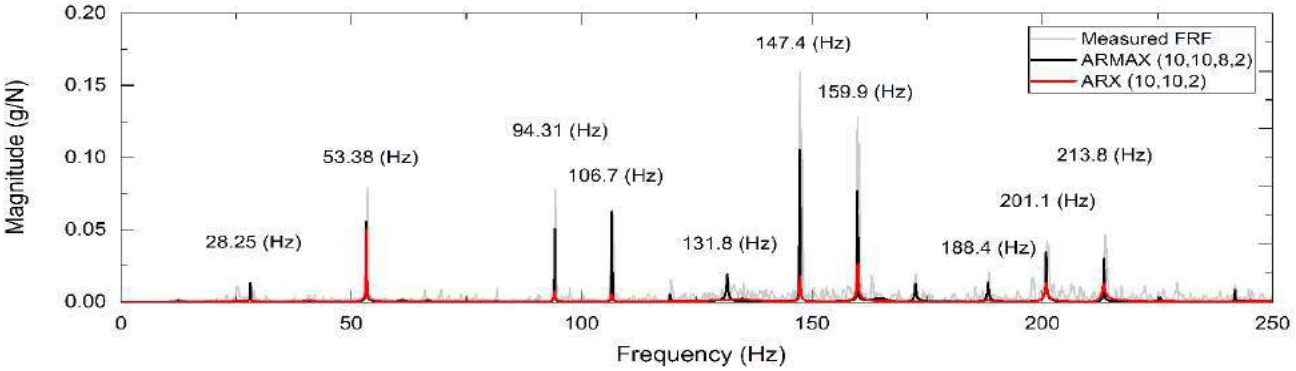


*Fig. 18:* Estimated Frequency Response Function $FRF_{zy}$

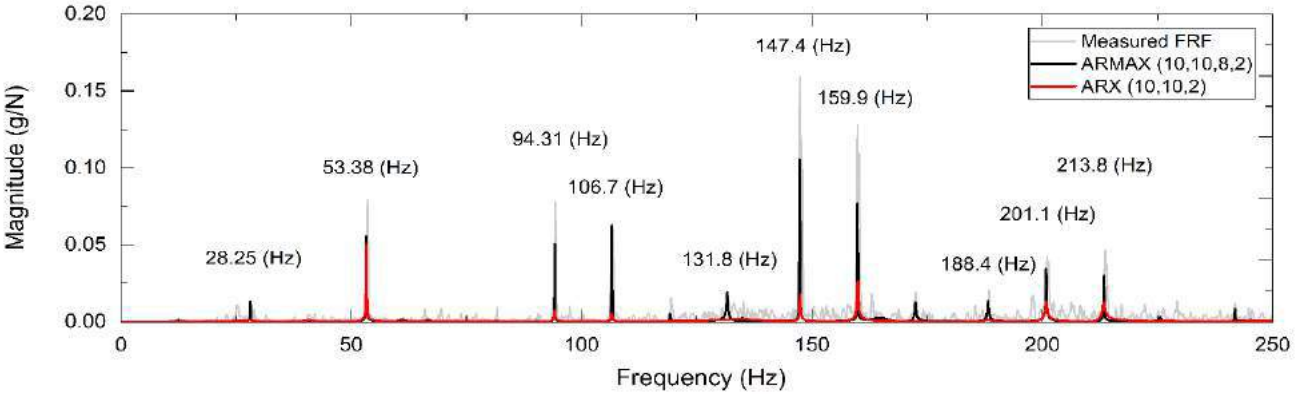


*Fig. 19:* Estimated Frequency Response Function $FRF_{zz}$

In comparing the ARX and ARMAX models' performance with different measurement data, it can be observed that the ARMAX model achieves much better fit than the ARX counterpart at low orders, where all frequencies of the system are clearly revealed. Conversely, at the same model orders, the ARX model proves inadequate in providing accurate estimated FRFs compared to the measured one. The ARMAX method was both economic and effective in accurately identifying the frequency response functions of the structure based on input-output experimental data corrupted by noise. This model also gives a more parsimonious representation and precision. These results matching those of [35]. The model orders of the ARMAX model are related to the number of structural modes in a given frequency range.

Meanwhile, in the ARX model, the number of degrees of freedom devoted to the description of the system dynamics is limited due to the fact that the system dynamics and the noise are partially described by the same polynomial $\mathbf{A}(q)$. For this reason, larger complexities are needed to achieve good adherence to the true system. Consequently, the orders of the ARX model tend to be chosen

greater than those of the ARMAX model when considering the noise present in the measurements.

### 5.3 Extraction of modal parameters

The estimated Frequency Response Functions (FRFs) representing the structural dynamic $\left[\mathbf{B}(q,\bar{\theta})/\mathbf{A}(q,\bar{\theta})\right]$ will be applied to distinguish the actual structural modes from the extraneous modes, based on the construction of the stabilization diagram, and will be used for the extraction of the modal parameters. Each transfer function representing a scalar excitation and response pair is evaluated directly from the estimated discrete ARMAX model. Complete model information such as natural frequencies, damping factors, and mode shapes can be obtained. Their global parameters can be extracted as follows:

$$f_{nl} = \frac{1}{\mathrm{T}2\pi}\sqrt{\left(\frac{\ln\left(\lambda_l.\lambda_l^*\right)}{2}\right)^2 + \left(\cos^{-1}\left(\frac{\lambda_l+\lambda_l^*}{2\sqrt{\lambda_l.\lambda_l^*}}\right)\right)^2} \qquad (39)$$

$$\zeta_l = \frac{1}{\mathrm{T}}\sqrt{\frac{\left[\ln\left(\lambda_l.\lambda_l^*\right)\right]^2}{\left[\ln\left(\lambda_l.\lambda_l^*\right)\right]^2 + 4.\left(\cos^{-1}\left(\frac{\lambda_l+\lambda_l^*}{2\sqrt{\lambda_l.\lambda_l^*}}\right)\right)^2}} \qquad (40)$$

In the above expression, $f_{nl}$ denotes the $l^{\text{th}}$ natural frequency in (hz) unit, $\zeta_l$ represents the corresponding damping ratio, $\left(\lambda_l,\lambda_l^*\right)$ is the $l^{\text{th}}$ discrete complex conjugate eigenvalue pair, and T is the sampling period.

To determine the extraction mode, a particular discrete-to-continuous transformation must be performed for determining continuous-time residues. The $l^{\text{th}}$ mode shape $\phi_l$ is then obtained as:

$$\phi_l = \left[1\frac{\mathbf{R}_{i2l}}{\mathbf{R}_{i1l}}\ldots\frac{\mathbf{R}_{iml}}{\mathbf{R}_{i1l}}\right]^T \qquad (l=1, 2,\ldots, m) \qquad (41)$$

where $m$ represents the estimated number of structural degrees of freedom and $\mathbf{R}_{ijl}$ is the $ij^{th}$ element of the $l^{th}$ ($l$=1, 2, ..., $m$) residue matrix $\mathbf{R}_l$ of the continuous-time receptance transfer matrix.

In modal analysis, knowledge of the model order is necessary but insufficient. It is important to understand that with noisy data, the optimal model order is typically smaller than the existing order. When evaluating the parameters with the minimum order model, it is hard to obtain all the modes if the measurements are corrupted by experimental noise. Previous studies [12, 13, 17] have shown that it is more difficult to identify the damping rates than the natural frequency from ambient vibration data due to a higher sensitivity to measurement noise. Therefore, to obtain all the modes and construct a stabilization diagram, a value higher than the minimum required order to establish the convergence must be set. However, the advantage of the ARMAX modeling is that it includes the Moving Average part, which is already accounted for the noise present in the system. Consequently, there is no need to go up to a very high order, as in the case of AR or ARX models. To prevent the contamination of more numerical modes and avoid the overfitting problem, a computational model order should not be too much higher than the optimal one. In this paper, order 50 was selected for visually establishing stabilization diagrams and distinguishing between the structural and the spurious modes, and the identified low-order FRFs in the previous section were applied to extract the modal properties. The results computed by both the ARX and ARMAX models are illustrated in Figures 20-23.

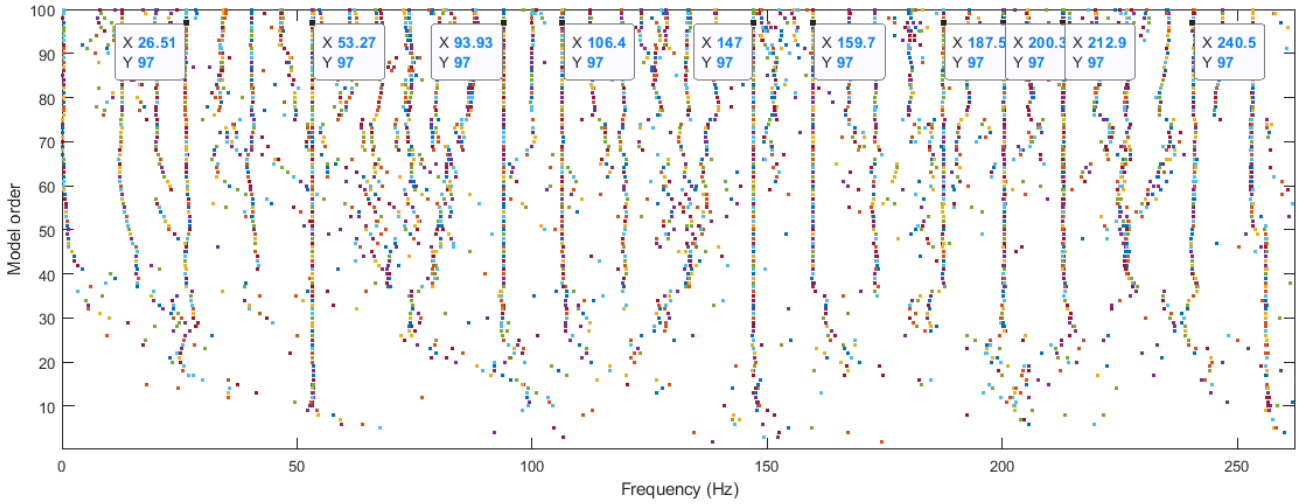


*Fig. 20:* Stabilization diagram by the ARX model

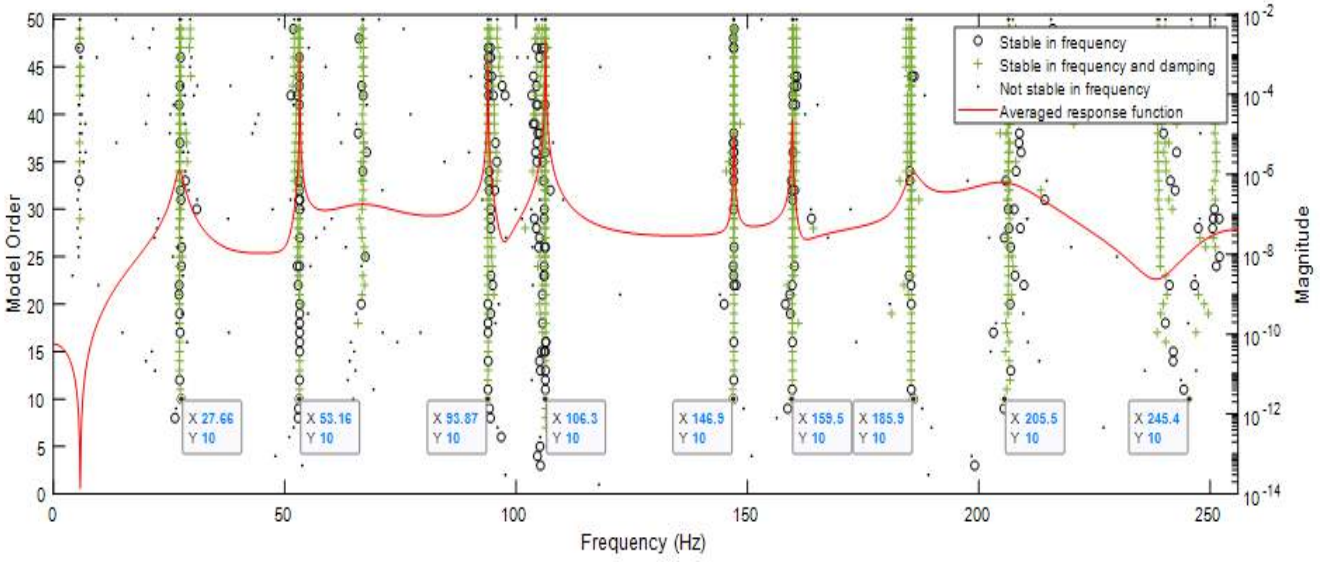


*Fig. 21:* Stabilization diagram based on average estimated FRFs in X direction by the ARMAX model

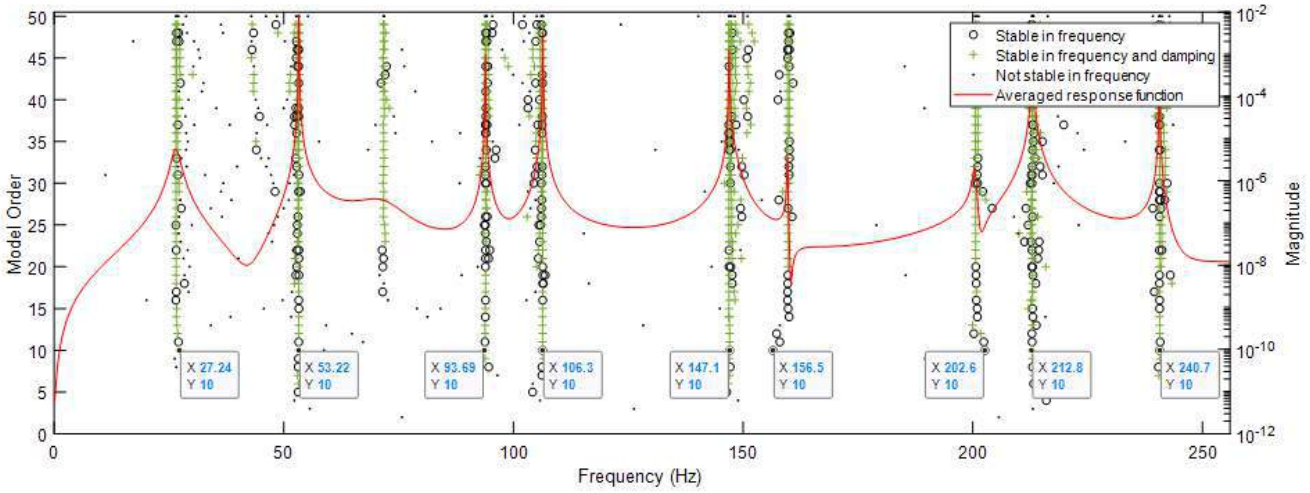


*Fig. 22:* Stabilization diagram based on average estimated FRFs in Y direction by the ARMAX model

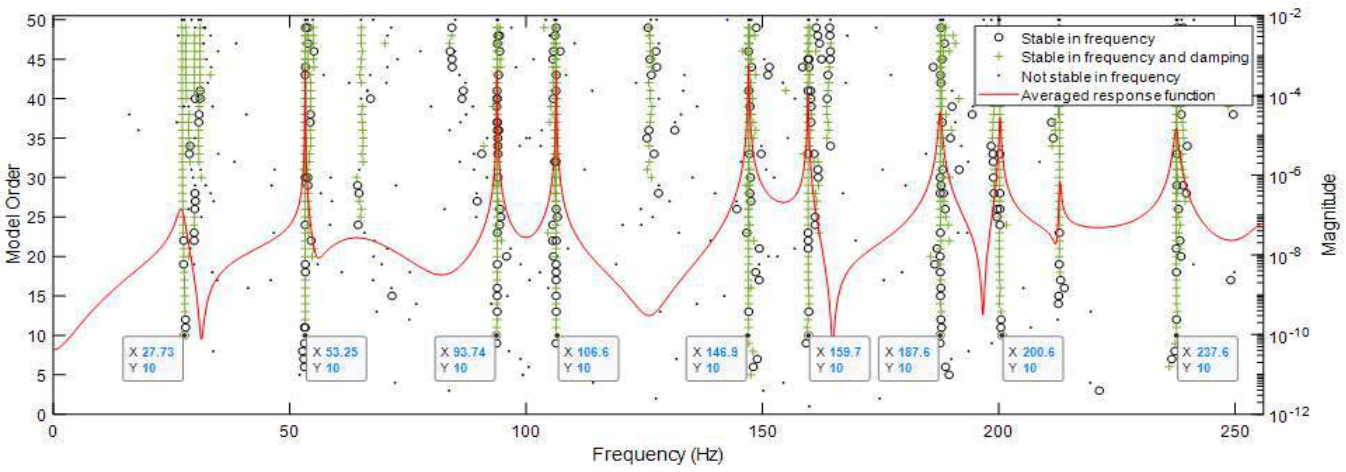


*Fig. 23:* Stabilization diagram based on average estimated FRFs in the Z direction by the ARMAX model

As can be seen from Table 2, all modal parameters obtained by two different methods are identified.

*Table 2:* Comparison of estimated modal parameters between ARMAX and ARX models

| Modes | ARMAX model | | ARX model (Least Squares) | |
|---|---|---|---|---|
| | Frequency (Hz) | Damping ratio (%) | Frequency (Hz) | Damping ratio (%) |
| 1 | 27.54 | 1.28 | 26.51 | 2.55 |
| 2 | 53.21 | 0 | 53.27 | 0 |
| 3 | 93.76 | 0.15 | 93.93 | 0.14 |
| 4 | 106.40 | 0 | 106.4 | 0 |
| 5 | 146.96 | 0.13 | 147.0 | 0.07 |
| 6 | 158.56 | 0 | 159.7 | 0 |
| 7 | 186.75 | 0.27 | 187.5 | 0.59 |
| 8 | 202.90 | 0.31 | 200.3 | 0.22 |
| 9 | 212.80 | 0 | 212.9 | 0 |
| 10 | 239.13 | 0.23 | 240.5 | 0.28 |

The stabilization diagrams help to distinguish between spurious modes and vibration ones. Since the frequency response function is considered converging to the optimal order $p_{optimal}$ = 10, all the natural frequencies in the measured range start to show up on the stabilization diagrams, meaning that the optimal order $p_{optimal}$ is the minimum value from which all available physical modal properties are revealed. The assessments of both the ARX model and of the ARMAX model are undertaken based on an experimental SCOMPI structure. As the results indicate in Table 2, both models are effective for modal identification, but using different approaches. In the case of the ARMAX model, the harmonic frequencies, the natural frequencies, and damping ratios are extracted directly from the estimated low-order frequency response functions. In contrast, the ARX model is based on the minimum Least Square method [19] at the higher orders. The ARMAX model exhibits the lowest complexity, while the ARX method requires many model parameters to extract the modal properties. As can be seen in Figure 20, due to an applied higher order up to 100 in the case of the ARX model, the stabilization diagram exhibits a lot of irrelevant oscillation information, which results in an overfitting problem and heavy computation. Meanwhile, the stabilization diagrams of an ARMAX model with different measurement data sets revealed all the frequencies, without overfitting problems and with less computational time. In general, the ARMAX model is better at capturing the significance of the mismatches introduced and provides satisfactory results in terms of frequencies and damping coefficients estimation.

The model offers easy computation, with sufficient low-order performance despite the noise contamination in the experimentally measured data. However, in the case of the ARX

model, there is a need for higher orders. Under such conditions, the time delay problem can also be neglected, which results in a time-consuming and higher computational burden.

## VI. CONCLUSION

To summarize, this paper presents an effective identification technique for computing optimal ARMAX model orders based on experimental measurement data. The present method allows selecting of a minimum order of the mechanical system in a given frequency range, which correctly incorporates the effect of modeling error and measurement noise under the expression of a minimum error variance of the identified transfer functions. The estimated results were validated with other common criteria, such as AIC, BIC, and NOF, to ensure that the selected model extracted uncorrelated residuals and simultaneously prevented overfitting. The search for the best time delays is also addressed in this paper. The proposed optimization strategy was successfully applied on an industrial application, namely, the flexible SCOMPI manipulator robot under grinding operation. The relationship between the actual structural and disturbance dynamic is formulated in the discrete form of an ARMAX representation, which helps to improve the modeling performance and to gain flexibility in handling the residual error caused by environmental noises. Further validation was carried out by comparing model predictions with actual measurements of transfer functions from the LMS Test Lab system and the original ARX technique. Comparative results show that the identified ARMAX model is economic and appropriate for structural identification and achieves better results. The low-order transfer functions estimated by the present technique were scientifically closer to the measured values, and are proposed for use in automatic modal extraction. Results show that the approach is successful and superior to a state-of-the-art order determination technique in obtaining a sufficient order and can accurately capture all the dominant oscillation modes with fewer discrepancies. The proposed method is expected to be a useful tool for capturing the transfer functions of difficult-to-measure structures such as rotating grinding systems. The determined low-order FRFs may eventually be used in the feedback controller design of the manipulator or in constructing a Stability Lobe Diagram (SLD) for determining operating and natural frequencies.

*Declaration of Competing Interest*

The authors declare that they have no known competing financial interests or personal relationships that could influenced the work reported in this paper.

## ACKNOWLEDGMENTS

The support of NSERC (Natural Sciences and Engineering Research Council of Canada) through Discovery Research RGPIN-2016-05859 grants and of the Vietnam International Education Development (VIED) – Ministry of Education and Training of Vietnam is gratefully acknowledged. The authors would like to thank Hydro-Quebec's Research Institute for its substantial collaboration.

## REFERENCES

1. L. Ljung, On the estimation of transfer functions, Automatica, 21 (1985) 677-696.
2. F. Saupe and A. Knoblach, Experimental determination of frequency response function estimate for flexible joint industrial manipulators with serial kinematics, Mechanical Systems and Signal Processing, 52-53 (2015) 60-72.
3. Y. Peng, B. Li, X. Mao, H. Liu, C. Qin and H. He, A method to obtain the in-process FRF of a machine tool based on operational modal analysis and experiment modal analysis, The International Journal of Advanced Manufacturing Technology, 95 (2018) 3599-3607.
4. I. Zaghbani and V. Songmene, Estimation of machine-tool dynamic parameters during machining operation through operational modal analysis, International Journal of Machine Tools and Manufacture, 49 (2009) 947-957.
5. W.A. Smith and R.B. Randall, Cepstrum-based operational modal analysis revisited: A discussion on pole-zero models and the

regeneration of frequency response functions, Mechanical Systems and Signal Processing, 79 (2016) 30-46.
6. G. Coppotelli, On the estimate of the FRFs from operational data, Mechanical Systems and Signal Processing, 23 (2009) 288-299.
7. O. Özşahin, E. Budak and H.N. Özgüven, In-process tool point FRF identification under operational conditions using inverse stability solution, International Journal of Machine Tools and Manufacture, 89 (2015) 64-73.
8. M. Postel, O. Özsahin and Y. Altintas, High-speed tooltip FRF predictions of arbitrary tool-holder combinations based on operational spindle identification, International Journal of Machine Tools and Manufacture, 129 (2018) 48-60.
9. V.H. Vu, M. Thomas, A.A. Lakis and L. Marcouiller, Operational modal analysis by updating autoregressive model, Mechanical Systems and Signal Processing, 25 (2011) 1028-1044.
10. V.-H. Vu, Z. Liu, M. Thomas, W. Li and B. Hazel, Output-only identification of modal shape coupling in a flexible robot by vector autoregressive modeling, Mechanism and Machine Theory, 97 (2016) 141-154.
11. H.C. Chen, E.K. Lee and Y.G. Tsuei, Method for Determining System Eigenvalues From FRF for Noise Contaminated Subsystems, 1993, pp. 21-26.
12. M. Smail, M. Thomas, and A. Lakis, ARMA models for modal analysis: Effect of model orders and sampling frequency, Mechanical Systems and Signal Processing, 13 (1999) 925-941.
13. M. Smail, M. Thomas and A.A. Lakis, Assessment of optimal ARMA model orders for modal analysis, Mechanical Systems and Signal Processing, 13 (1999) 803-819.
14. V.H. Vu, L. Zhaoheng, M. Thomas, A.M. Tahvilian and B. Hazel, Identification of frequency response functions of a flexible robot as tool-holder for robotic grinding process, 2016.
15. H. Akaike, A new look at the statistical model identification, IEEE Transactions on Automatic Control, 19 (1974) 716-723.
16. S. Gideon, Estimating the Dimension of a Model, The Annals of Statistics, 6 (1978) 461-464.
17. V.H. Vu, M. Thomas, F. Lafleur, and L. Marcouiller, Towards an automatic spectral and modal identification from operational modal analysis, Journal of Sound and Vibration, 332 (2013) 213-227.
18. L. Lennart, System identification: theory for the user, PTR Prentice Hall, Upper Saddle River, NJ, 28 (1999).
19. T. Soderstrom, H. Fan, B. Carlsson, and S. Bigi, Least-squares parameter estimation of continuous-time ARX models from discrete-time data, IEEE Transactions on Automatic Control, 42 (1997) 659-673.
20. L. Ljung and T. Söderström, Theory and Practice of Recursive Identification, MIT Press, Cambridge, 1983.
21. G.C. Goodwin, M. Gevers and B. Ninness, Quantifying the error in estimated transfer functions with application to model order selection, IEEE Transactions on Automatic Control, 37 (1992) 913-928.
22. J. Schoukens and R. Pintelon, Quantifying model errors of identified transfer functions, IEEE Transactions on Automatic Control, 39 (1994) 1733-1737.
23. P. Stoica and Y. Selen, Model-order selection: a review of information criterion rules, IEEE Signal Processing Magazine, 21 (2004) 36-47.
24. H. Akaike, Fitting autoregressive models for prediction, Annals of the Institute of Statistical Mathematics, 21 (1969) 243-247.
25. S. Beveridge and C. Oickle, A Comparison of Box—Jenkins and objective methods for determining the order of a nonseasonal ARMA Model, Journal of Forecasting, 13 (1994) 419-434.
26. A. Barron, J. Rissanen, and Y. Bin, The minimum description length principle in coding and modeling, IEEE Transactions on Information Theory, 44 (1998) 2743-2760.
27. H. Bozdogan, Model Selection and Akaike's Information Criterion (AIC): The General Theory and Its Analytical Extensions, Psychometrika, 52 (1987) 345-370.

28. B. Wahlberg and L. Ljung, Design variables for bias distribution in transfer function estimation, IEEE Transactions on Automatic Control, 31 (1986) 134-144.
29. D. Zhu, X. Feng, X. Xu, Z. Yang, W. Li, S. Yan, and H. Ding, Robotic grinding of complex components: A step towards efficient and intelligent machining – challenges, solutions, and applications, Robotics and Computer - Integrated Manufacturing, 65 2020 101 08.

# Advances and Challenges of Anaerobic Biodigestion Technology

*Minister Obonukut & Uwem Inyang*

*University of Uyo*

## ABSTRACT

This paper reviewed the advances and challenges of anaerobic biodigestion technology. The technology is an attractive waste to wealth strategy exploited to proffer solutions to the environmental, energy and agricultural needs. As reviewed, the process is generally considered to be slow and unstable due to strict nature of the anaerobes and difficult to operate. The advances in anaerobic digestion technology considered in this study are attributed to the diversity in bio-sourced feedstock, digester design and variability of process conditions. These highly researchable areas were extensively reviewed. It was found that pretreatment of feedstock, substrate interaction with the novel inoculum and substrate combo which involves mixture of different classes of feedstock that ferment better together than separately due to their enriched microbial load as well as their nutritional requirements, are recent strategies exploited to improve anaerobic biodigestion process. In addition, research on thermal effect, alternating thermophilic, mesophilic and psychrophilic stages while evaluating the impacts of temperature, pH and pressure have been adequately investigated as reviewed. However, the process is challenged by poor biodigester design/configurations, the inhibitory episodes from antagonistic substrate combo and the offensive odor of the effluent on fertilizer application.

*Keywords:* advances, challenges, anaerobic biodigestion, bio-sourced feedstock.

*Classification:* DDC Code: 628.35, LCC Code: TD755

*Language:* English

London Journals Press

LJP Copyright ID: 392972
Print ISSN: 2631-8474
Online ISSN: 2631-8482

London Journal of Engineering Research

Volume 22 | Issue 1 | Compilation 1.0

# Advances and Challenges of Anaerobic Biodigestion Technology

Minister Obonukut[α] & Uwem Inyang[α]

## ABSTRACT

*This paper reviewed the advances and challenges of anaerobic biodigestion technology. The technology is an attractive waste to wealth strategy exploited to proffer solutions to the environmental, energy and agricultural needs. As reviewed, the process is generally considered to be slow and unstable due to strict nature of the anaerobes and difficult to operate. The advances in anaerobic digestion technology considered in this study are attributed to the diversity in bio-sourced feedstock, digester design and variability of process conditions. These highly researchable areas were extensively reviewed. It was found that pretreatment of feedstock, substrate interaction with the novel inoculum and substrate combo which involves mixture of different classes of feedstock that ferment better together than separately due to their enriched microbial load as well as their nutritional requirements, are recent strategies exploited to improve anaerobic biodigestion process. In addition, research on thermal effect, alternating thermophilic, mesophilic and psychrophilic stages while evaluating the impacts of temperature, pH and pressure have been adequately investigated as reviewed. However, the process is challenged by poor biodigester design/configurations, the inhibitory episodes from antagonistic substrate combo and the offensive odor of the effluent on fertilizer application. The review on these challenges is necessary towards improving the process. On the whole, for improved biodigestion of substrates, these strategies such as pretreatment, co-digestion, etc. should be exploited. Specifically, pretreatment of feedstock facilitates biodigestion and improves the accessibility of the source carbon utilizable by the microbial community, and mixing sources (co-digestion), working together as substrates, provides several advantages that improves biogas yields, methane production, and various other benefits.*

*Keywords:* advances, challenges, anaerobic biodigestion, bio-sourced feedstock.

*Author:* Department of Chemical and Petroleum Engineering, University of Uyo, Nigeria.

## I. INTRODUCTION

Anaerobic digestion process is an attractive waste to wealth strategy in which a consortium of microorganisms (anaerobes) produces biogas and bio-fertilizer from biomass in an oxygen-free environment. However, the process was originally developed for waste disposal/treatment several centuries ago. As expected, based on exponential increase in population witnessed globally, huge wastes are generated daily from domestic, industrial and commercial activities (Bamgboye and Ojolo, 2004; Cheng et al., 2010). These wastes are seen to litter the street claiming more lands as number of dumping sites keeps increasing. Waste treatment/disposal is one of the environmental challenges confronting the modern societies globally. Bio-waste (organic waste) constitutes over 60% of these wastes in the advanced nation and even more in the developing nations (Arvanitoyannis et al., 2007; Cheng et al., 2010; Mata-Alvarez et al., 2014). However, these biological material (biomass) includes not only bio-waste but all materials from natural processes which in most cases are nuisance to our environment constituting waste (Babatola and Ojo, 2020; Edenseting et al., 2020).

The technology is not obsolete despite centuries of existence as it is presently an interesting subject in the research community. It proffers solution not only to the environmental issue but also found its applications in both the energy and the agricultural sectors of the economy (Figure 1).

Research shows that the conditions of the process (temperature, pH, and pressure), digester design and substrate characteristics contributed immensely towards the success/failure of the process (Ofoefule and Onukwuli, 2010; Hoefnagels and Germer, 2018; Kalyanasundaram et al., 2020). Specifically, the variability of process conditions, digester design and diversity of bio-sourced feedstock are the key areas exploited to take the anaerobic digestion process this far.

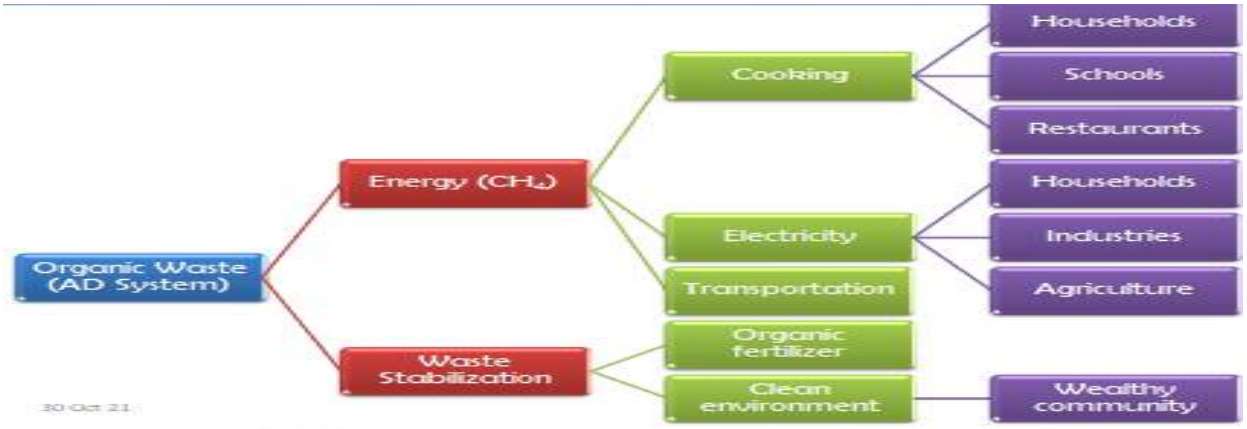


*Figure 1:* Anaerobic Biodigestion Technology: A waste to wealth strategy

Despite these advances, several researchers have reported that the process is strict and difficult to operate (Kozo et al., 1996; Zuru et al., 1998, Uzodinma et al., 2007; Ofoefule and Uzodinma, 2009). One of the challenges is the difficulty associated with substrate digestion making the process slow and unstable. Specifically, most of the substrates combo exploited has antagonistic /inhibitory effects resulting in low/delayed or termination of biogas production when exploited (Uzodinma et al., 2007; Ofoefule and Uzodinma, 2009). The strict nature of the anaerobes is another challenge as they can be inactive (lethargic) if there is a deviation in process condition. The sensitivity of these anaerobes leads to early termination of the process. Moreover, scum builds up due to poor digester design which eventually becomes strongly bonded to the wall and bottom of the biodigester resulting in a reduced digesting capacity is equally a challenge to this technology. A review of these advances as well as the challenges confronting the technology is necessary. Specifically, the current study presents these advances in terms of diversity of feedstock, biodigester design and and variability in process conditions. However, the challenges encountered are presented with the aim of achieving more from the process while addressing the challenges.

### *1.1 Advances in Anaerobic Biodigestion Technology: Diversity in Bio-sourced Feedstock*

Digestion is a biology term relating to eating of food and biodigestion connotes a special type of eating by microbes. In view of this, digestion is a biological process in which a consortium of micro-organisms converst biological material (organic matter) into volatile components (biogas) and water resulting to mass loss and perhaps destruction of pathogens. Biodigestion technology was originally formulated for waste treatment/disposal to address one of the global issues posed by its counterparts: pyrolysis, gasification and thermal incineration (combustion) with respect to greenhouse effect (Arvanitoyannis et al., 2007; Cheng et al., 2010). Hence, it is also known as sludge digestion.

Biomass (biological material) constitutes the feedstock exploited for anaerobic biodigestion operation. The diversity of bio-sourced feedstock (Edenseting et al., 2020) cheaply sourced domestically and industrially has drawn the interest of several researchers to the technology. The organic substrate varies in degradable effluents and complex solids waste and it is generally made up of complex chemical substances which vary in proportion (Steffen et al., 1998). These include: as carbohydrates,

proteins, lignin, water and traces of inorganic matter. These bio-Sourced feedstocks are classified based on residues and as well by the products they produce, etc. (Ben-Iwo et al., 2016; Hoefnagels and Germer, 2018; Edenseting et al., 2020).

### 1.1.1 Bio-Sourced Feedstocks Based on Residue

In this category, there are primary, secondary and tertiary residues (Hoefnagels and Germer, 2018). Figure 2 indicates the sources and the products derived from this class of bio-sourced feedstocks and its application.

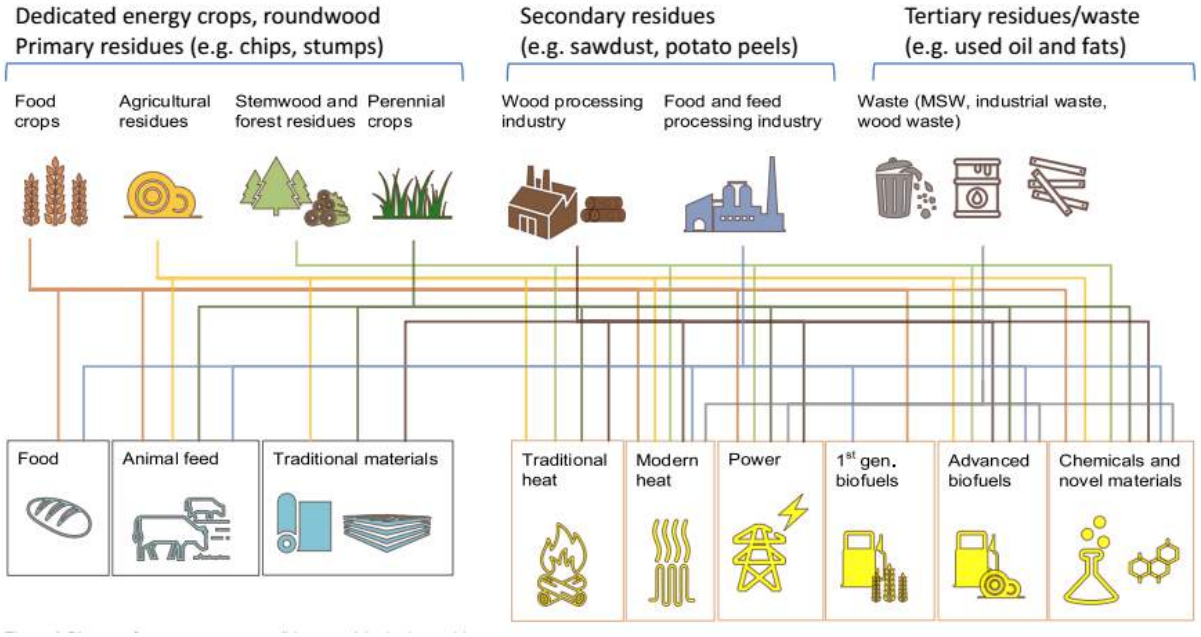


*Figure 2:* Bio-sourced feedstocks and application

*Sourced: Hoefnagels and Germer (2018)*

#### 1.1.1.1 Primary Residues

Biomass from this category can be exploited mainly for animal feed and other traditional materials. They include: chips, stumps and other residues from food crops, agricultural wastes and forest tree residues (Zhu et al., 2010).

#### 1.1.1.2 Secondary Residues

This category of bio-sourced feedstock constitutes industrial wastes from wood, feed and food processing industries. They are: sawdust, potato peels and others exploited for animal feed, heating and power generation (Bamgboye, 2012; Bruni et al., 2010; Pisutpaisal et al., 2014; Patel, 2017).

#### 1.1.1.3 Tertiary Residues

These bio-sourced materials are mainly wastes from sewage and industries such as: used oil and fats that are converted to biofuels and bio-chemicals (Gelegenis et al., 2007).

In terms of the products, biological materials are classified into four generations: first generation, second generation, third generation and fourth generation. More on these class of bio-sourced feedstock can be found in Dutta et al. (2014); Edenseting et al. (2020).

### 1.2 Advances in Anaerobic Biodigestion Technology: Variability in Process Conditions

The impact of anaerobic biodigestion technology in several sectors of the economy is attributed to the variability of the process conditions in which the anaerobic biodigestion can be operated. In this section, the essential parameters that influence anaerobic digestion are discussed. These include the pre-treatment of bio-sourced feedstock (section 2.2.1), activators/innocula

(section 2.2.2), temperature (section 2.2.3), pH (section 2.2.4), and pressure (section 2.2.5).

### 1.2.1 Pre-treatment Bio-Sourced Feedstock

These are mainly the biomaterial in which the anaerobes digest as substrates. Generally, any biodegradable material can be used as bio-sourced feedstock for energy production. In view of this, several biological materials (bio-sourced feedstock) have been exploited for biogas production via anaerobic digestion. There are myriads of biologically digestible materials (substrates) exploited for anaerobic digestion classified as first generation (food mostly energy crop), second generation (residue, grasses mostly lignocelluloses and wastes), third generation (sea weed algae) and genetically modified biomass constituting fourth generation substrates (Demirel et al., 2009; Wall et al., 2014; Edenseting et al., 2020).

About a decade ago, Germany has over 6000 digesters exploiting mainly energy crops anaerobically (Allen, 2015). Similar developments were reported in Brazil, China, USA, Ireland etc., where energy crops like sugar cane, cassava, maize (first generation) were utilized as bio-sourced feedstock (Mitchell, 2008; Edenseting et al., 2020). However, with the hike in food prices globally, there is much concern over the use of energy crops for biogas production. This has shifted the onus for exploitation of second, third and fourth generation substrates eliminating competition between food and agricultural land. Akinbami et al. (2001) reported feasible substrates for anaerobic process to include: water lettuce, water hyacinth, cattle dung, cassava leaves, urban refuse, agricultural residue, sewage and industrial waste. Table 1 shows some of these feedstocks as well as their yield.

*Table 1:* Bio-sourced Feedstock and Potential

| Materials and their main components | Yield of Biogas $m^3$/kg TS | Methane content (%) |
|---|---|---|
| Animal barnyard manure | 0.260 ~ 0.280 | 50 ~ 60 |
| Pig manure | 0.561 | |
| Horse droppings | 0.200 ~ 0.300 | |
| Green grass | 0.630 | 70 |
| Flax straw | 0.359 | |
| Wheat straw | 0.432 | 59 |
| Leaves | 0.210 ~ 0.294 | 58 |
| Sludge | 0.640 | 50 |
| Brewery liquid waste | 0.300 ~ 0.600 | 58 |
| Carbohydrate | 0.750 | 49 |
| Liquid | 1.440 | 72 |
| Protein | 0.980 | 50 |

*Source: Ampomah-Benefo (2018)*

Potentially, all biological material can be exploited by anaerobes for production of biogas and organic fertilizer. This is attributed to the presence of essential nutrient in these materials to support growth and metabolic activities of anaerobic bacteria for biogas production (Duku et al., 2011). Research has shown that chemical composition and biological availability of the nutrients in these materials differ with species as well as factors affecting growth and the age of the biological material (Ofoefule and Onukwuli, 2010). The energy stored in these materials can be extracted when digested. The choice of conversion method is usually influenced by the physical properties (moisture content, calorific value, and particle size) and chemical content (alkali metal content Na, K, Mg, P and Ca,) of the feedstock.

Biomaterials with low moisture content (< 15 %) are considered dry and are suitable for direct combustion, gasification, or pyrolysis, while those with high moisture content is suitable for anaerobic digestion. If wet digestion is desired, water has to form the highest proportion (> 70 %). Consequently, when feedstock with low moisture content has to be used in an anaerobic digestion, large quantities of water have to be added for optimum biogas yield, especially if wet digestion is being considered. The bio-sourced feedstock is mixed with a proportional amount of water and seeded with a consortium of microbes to form slurry.

Recently, various studies have been conducted with co-digestion and the results have seen improvement over single feedstock digestion (Gashaw, 2014; Li et al., 2015; Jena et al., 2017; Tasnim et al., 2017; Dahunsi et al., 2017). Specifically, simultaneous digestion of a mixture (blending) of two or more substrates is referred to as co-digestion. In co-digestion, the feedstock is mixed with other biomaterial that contains relevant microbes. The co-existence of different types of substrates in the same geographical area promotes integrated management offering considerable environmental benefit such as energy saving, recycling of nutrients back to the land and reduction of greenhouse gas GHG emission (Kacprzak et al., 2010). Co-digestion is expected to enhance the performance of the anaerobic digestion process as different properties of the constituent substrates are exploited due to positive synergism established in the digestion medium by providing a balanced nutrient supply and sometimes by suitably increasing the moisture content required in the digester (Darwin et al., 2014).

However, a successful co-digestion involves more than simultaneous digestion of multi-feedstock/substrates for biogas production. In essence, the composition of these substrates, the process conditions and the activity of microbial community in the system are equally important as they are linked to biogas production and stability of the process. In addition, there are other locally found lignocellulosic materials and organic wastes that have received considerable research attention recently (Okoroigwe and Agbo, 2007; Ofoefule and Onukwuli, 2010; Eze and Agbo 2010; Fang, 2010; Ezekoye et al., 2011; Eze and Ojike, 2012). Meanwhile, plant materials mostly lignocellulosic materials such as crop residues are more difficult to digest than animal waste as special bacteria found in the stomach of these ruminant animals had initiated biomaterial fermentation (i.e., hydrolysis) prior to anaerobic digestion (Itodo et al., 1992; Eze, 2003).

The organic substrate varies in degradable effluents and complex solids waste (Steffen et al., 1998). During AD process, the raw material decomposition occurs at different kinetics. AD may occur more rapidly, if the substrates are short-chain hydrocarbons or simpler sugars. On the other hand, process could be slow if substrates are quite complex such as cellulose and hemicellulose (Bhatia 2014). Alkaline pretreatment of the feedstocks, nutrient addition, and co-digestion have increased biogas yield and productivities, eventually affecting the overall process performance (Ivo Achu 2012). Figure 3 shows the role of feedstock on the rate of AD.

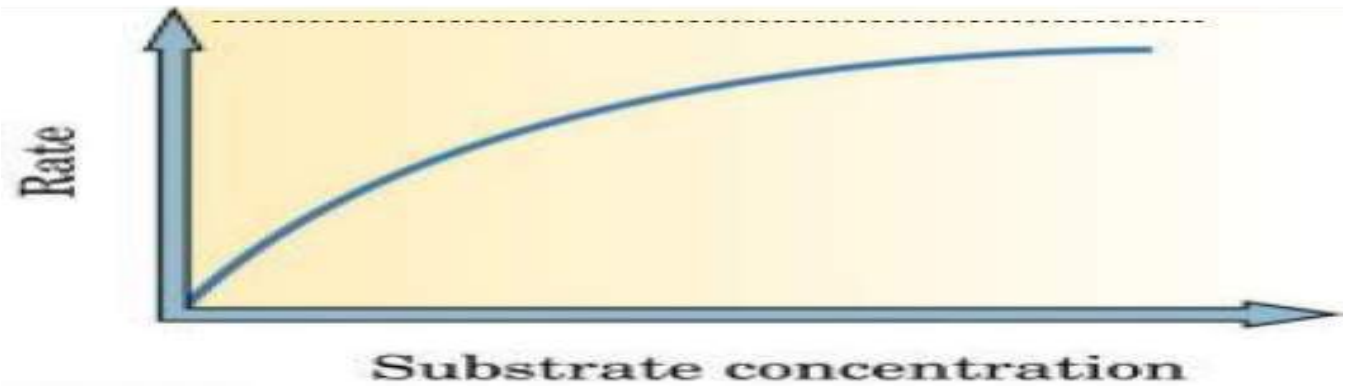


*Figure 3:* Impact of substrate concentration on rate of AD

However, the challenge for the use of this type of feedstock is its structure. Hydrolysis of insoluble complex organic material in soluble monomers and oligomers is the first step in biogas generation from lignocellulosic material. For this, it is necessary that the responsible enzymes be produced by the microorganisms and that there is direct interaction amongst the enzymes as well as the substrate (Chandel et al., 2019). However, pretreatment of lignocellulosic biomass is necessary for using them further in biogas production via AD. Pretreatment removes or breaks the lignin as well as hemicellulosic portion of the biomass, thereby enabling the cellulosic material accessible to the microorganisms during the AD process (Karp et al., 2013; Fan et al., 2016).

### 1.2.2 Activator/Inoculum

It is the seed of microbes added to the feedstocks to initiate anaerobic digestion process. It is also called inoculum or starter. It can be sourced from an existing active digester or from animal dung (droppings) which contain large quantities of consortium of microbes. The inoculum can also be extracted in the laboratory from a pure culture of microbes. The role of enzyme in anaerobic digestion process is critical especially initiating the hydrolysis and as well catalyze other stages.

Microbe is needed to secrete enzymes to initiate the process. Immediate production of biogas within a short period is a function of the quantity of inoculum and how quickly they can adjust and populate. Research showed that they are sensitive environmental conditions such as temperature, pH and nutrients/substrates (Ezeonu et al., 2005; Filmax, 2009; Zhang, 2017; Vivekanandan, 2017). The medium (slurry) in which the inoculum is introduced must be maintained with the optimal conditions to achieve optimal microbial activities (Figure 4).

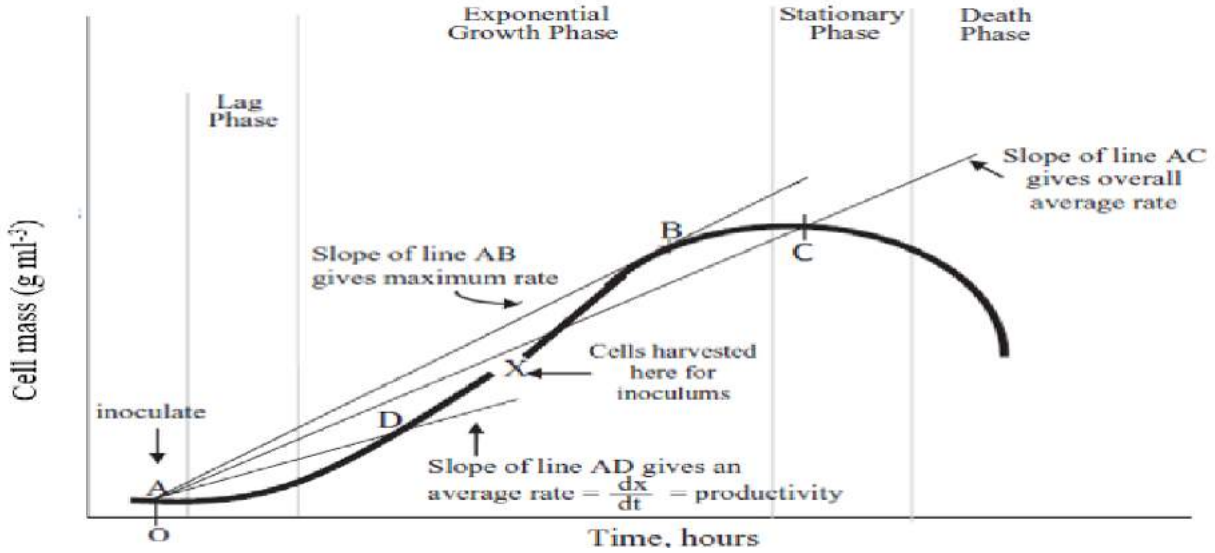


*Figure 4:* Growth phases of typical microbes in an anaerobic system

*Source: Ampomah-Benefo (2018)*

The microbial activities of the inoculum in the slurry as well as growth rate are summarized in four growth phases (Ampomah-Benefo, 2018). These include: lag phase, exponential growth phase, stationary phase and the death phase (Mosier and Ladisch, 2009). The lag phase is the time it takes the inoculated microbe to adapt to the new environment. This phase is also known as the incubation period. The duration of the lag phase is greatly influenced by the source of the inoculum and how quickly it can adjust to its new environment. Inoculum taken from an active digester with the same kind of slurry as the new digester usually have minimal lag phase period as it adjust easily with negligible adaptation period. After the lag phase, then exponential growth phase sets in.

This is the period of highest microbial activity as the microbe begins to populate at an exponential rate. At this period, substrate is consumed rapidly because of the population growth of microbes. Substrate consumption rate remains constant at maximum microbial growth. As substrate gets depleted, the microbial activity remains constant as the substrate is depleting (Stationary growth phase). As the substrate gets exhausted, the microbe has nothing to feed on and goes to extinction (death phase).

However, during anaerobic digestion processes various microbes play specific roles in a sequential manner. The anaerobes which are generally fermentative bacteria comprise: acidogens, acetogens and methanogens. Each of them has different regeneration time as acidogenic anaerobes spent less than an hour to about 36 hours to regenerate. Acetogenic anaerobes spend about twice as much of time (3.3 days to 3.75 days) used by acidogenesis to regenerate.

Methanogenic anaerobes, which are the final microbes to convert substrate to biogas, spend between 5 days and 16 days to regenerate (Deublein and Steinhauser, 2008). A correct balance of time for regeneration of all these anaerobes is necessary for optimization of biogas generation. It therefore suggests that in an anaerobic digestion system biogas production can be expected between 5 days to 16 days. In the case where lag time is minimized, biogas can be realized within a day (Ampomah-Benefo, 2018). This work will exploit inoculum from different sources and the varieties in the feedstocks offered by co-digestion for improved biogas production.

### *1.2.3 pH of the Slurry*

It is a measure of performance and stability of chemical reaction taking place in the digester. Each stage in anaerobic digestion processes requires a particular pH range for optimal microbial activities (Figure 5) Several researchers reported that acidogenesis stage occurs around a pH of 5.0, whereas methanogenesis occurs at pH of 7.0 (Ann et al., 1996; Lin et al., 2013).

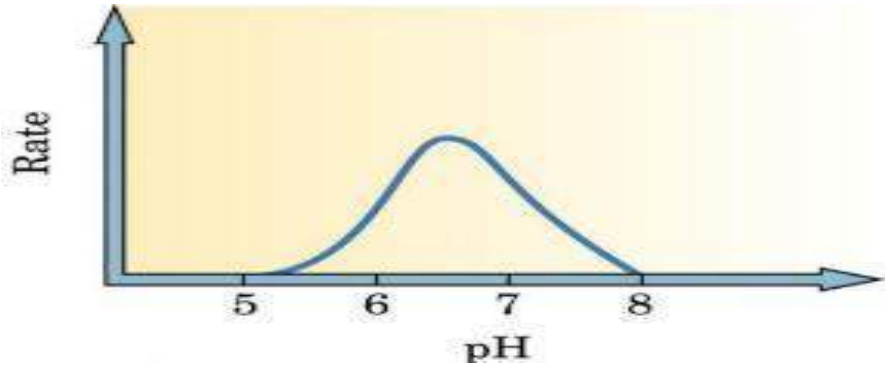


*Figure 5:* pH and Rate of biodigestion dependency

In a single stage anaerobic digester, where all the various digestion stages take place in a single tank, the system acts like a combined culture with pH range of 6.8 – 7.4, with neutral pH being the optimum (Boone and Luying, 1987). The rate of $CH_4$ production may decrease if the measured pH is either lower than 6.3 or higher than 7.8 (Kim et al., 2004). For low pH, acidogens populate and increase the production of volatile fatty acids and $H_2$ (Ann et al., 1996; Chen et al., 2008). If the process is not corrected it could lead to failure of the anaerobic processes to produce biogas. This can be corrected by first reducing the organic loading rate and then the introduction of chemicals such as $NaHCO_3$, NaOH, or $Na_2CO_3$ to adjust the pH to neutral.

The process condition in a single stage may promote a particular reaction at the expense of the other and the overall process efficiency is relatively low. To optimize biogas production, it is necessary to create favorable environmental condition by dividing the reactions into stages such that effluent of the previous reactor becomes

a substrate in the next reactor and ensuring that the process condition in each of the stages is favorable for optimal yield.

### 1.2.4 Pressure

High biogas pressure above the slurry (gas cavity) in a biodigester causes CO2 to dissolve in the slurry. This dissolved CO2 increases the acidity of the digestate (Lemmer et al., 2017). As a result of increasing pressure, the rate of biogas formation is consequently reduced (Hamad et al., 1983; Mateescu, 2016). Mateescu (2016) presented the result of the study on the variation of hydrostatic pressure with percentage yield of biogas conducted. The maximum biogas yield was achieved at 0 kPa (gauge pressure), which was above 60 % of CH4. At 600 kPa, CH4 production was generally less than 20 %. To reduce the effects related with CO2 solubility, large increase of pressure is avoided by regularly withdrawing and combusting the gas yield or by venting the accumulated gas regularly as will be exploited in this study.

### 1.2.5 Temperature

Anaerobic digestion can occur at three different ranges of temperature: (i) psychrophilic < 20 oC, (ii) mesophilic 20 - 40 oC, and (iii) thermophilic 45 - 60 oC. These temperature ranges are suitable for specific microbes. Beyond these ranges the respective microbes are not able to withstand the temperature changes, hence are destroyed, or become inactive (Ryckebosh, 2011; Evans and Furlong, 2003). Generally, an increase in temperature increases the activities of the microbes, hence an increase in the rate of conversion of slurry to biogas. Studies show that the growth rate of the microbes (in each temperature range) increases exponentially with temperature. This growth continues until an optimum temperature is attained. Beyond this optimum temperature, further increase in temperature will impede the growth and result in the death of microbes (Diamantis, 2010).

Generally, advances in anaerobic digestion technology as presented (Table 2) is attributed to the diversity in feedstock, digester design and variability of process conditions. Specifically, studies have been carried out on pretreatment of bio-sourced feedstock, novel inocula and their interaction with bio-sourced feedstock as well as their nutritional requirements (Tchobanoglous et al., 2003; Fekadu, 2014; Cestonaro et al., 2015; Fu et al., 2015). In addition, research on thermal effect on the AD process, alternating thermophilic, mesophilic and psychrophilic stages while evaluating the productivity, kinetics, and net energy balance have been adequately investigated (Ampomah-Benefo, 2018; Velazquez-Marti et al., 2019). For best degradation of substrates, methods such as pretreatment and co-digestion are used. Pretreatment facilitates the digestion and improves the accessibility of the source carbon utilizable by the microbial community, and mixing sources (co-digestion), working together as substrates, provides several advantages that improves biogas yields, methane production, and various other benefits.

*Table 2:* Advances in Anaerobic Digestion Process

| Researcher | Bio-Sourced Feedstock | Process Condition | Gas Potential ($m^3$/kgSV) |
|---|---|---|---|
| Bayrakdar *et al.*2018 | Chicken manure | Mesophilic | 0.272 |
| Franco *et al.*2018 | Wheat straw + inoculum | Mesophilic | 0.229 |
| Franco *et al.*2018 | Wheat straw + glucose + ac. Formic + inoculum | Mesophilic | 0.276 |
| Guo *et al.*2018 | Excessively withered corn straw + glucose | Mesophilic | 0.282 |
| Li *et al.*2018 | Parton + sheep manure | Mesophilic | 0.152 |
| Li *et al.*2018 | Paper + sheep manure | Mesophilic | 0.199 |
| Mancini *et al.*2018 | Lignocellulose in general | N-methylmorpholine N-oxide | 0.304 |
| Martín *et al.*2018 | Microalgae + pig manure | Alkaline pretreatment with NAOH | 0.377 |

| | | | |
|---|---|---|---|
| Mustafa *et al.*2018 | Bagasse of sugarcane + inoculum* | Hydrothermal pretreatment | 0.318 |
| Vazifehkhoran*et al.*2018 | Wheat straw + sewage | Mesophilic | 0.314 |
| Xu *et al.*2018 | Corn straw + Bacillus Subtilis | Microaerobic mesolithic | 0.270 |
| Zahan *et al.*2018 | Gallinaza (sawdust, wood shavings, and rice or straw husk) with yogurt serum | Mesophilic | 0.670 |
| Aboudi *et al.*2016 | Dry sediment of sugar beet tails + pig manure | Mesophilic | 0.260 |
| Dennehy *et al.*2016 | Food waste and pig manure | Mesophilic | 0.521 |
| Glanpracha and Annachhatre, 2016 | Cassava pulp with pig manure | Mesophilic | 0.380 |
| Marin *et al.*2015 | Vinasse and chicken manure (chicken dung) | Mesophilic | 0.650 |
| Aboudi *et al.*2015 | Dry beet granules of sugar beet + cow dung | Mesophilic | 0.280 |
| Belle *et al.*2015 | Fodder radish with cow dung | Mesophilic | 0.200 |
| Cestonaro *et al.*2015 | Sheep litter (mixture of rice husk with feces and urine) + cattle manure | Mesophilic | 0.171 |
| Di Maria *et al.*2015 | Sludge from wastewater with fruit and vegetable waste | Mesophilic | 0.216 |
| Fu *et al.*2015a | Corn straw + inoculum | Thermophilic microaerobic | 0.326 |
| Fu *et al.*2015b | Corn straw + inoculum | Secondary thermophilic microaerobic | 0.381 |
| Agyeman and Tao, 2014 | Food waste + livestock manure | Mesophilic | 0.467 |

*Source: Velazquez-Marti et al. (2019)*

## II. CHALLENGES CONFRONTING ANAEROBIC BIODIGESTION PROCESS

Anaerobic biodigestion process, though an age-long process, is unattractive, difficult and highly unstable process due low methane yield. In addition, its effluents are not suitable for direct discharge to the environment due to offensive odor. In this section, these challenges are discussed. The challenges are generally based on biodigester design/configurations (section 3.1), the inhibitory episodes from antagonistic substrate combo (section 3.2) and the offensive odor of the effluent on fertilizer application (section 3.3). The review on these challenges is necessary towards improving the process. However, in each of these challenges, the author proffers the way out towards addressing them.

### *2.1 Challenges Attributed to Biodigester Design and Configuration*

The bioreactor's design and configurations is one of the keys to successful anaerobic digestion operation. It is the chamber in which the anaerobes digest the substrates and as a result produce biogas and the nutrient-rich biol for plant growth. As stated earlier, maintaining an air-tight chamber is difficult in practice and failure to maintain this condition leads to oxidization of most of the methane forming compounds as more ammonia gas, $CO_2$ are produced at the expense of methane as methanogens (methane-forming anaerobes) are very sensitive to oxygen and die when they are exposed to oxygen. This is aerobic digestion which as reviewed is more thermo-dynamic feasible with stable products than anaerobic digestion. The effect is low methane yield as the process has deviated to aerobic digestion.

Furthermore, it is reported that anaerobic digestion comprises of four stages (hydrolysis, acidogenesis, acetogenesis and methanogenesis) requiring a synchronized action of four groups of microbes. In each of these stages, individual group of anaerobes require different process conditions for optimum microbial activity as acidogens thrive in acidic medium while acetogen and methanogens need relatively high pH (7-7.4) to explore effectively (Ampomah- Benefo et al.,2013). Most digesters are operated as a single stage where all the anaerobes are lumped together in one chamber (stage), regardless of their disparities; it would be a case of 'survival of the

fittest'. Sadly, the most important pathway in methanogenesis, acetoclastic methanogenesis, where acetoclastic methanogens (methanosarcina and methoanosaeta) formed more than 60% of the methane, the most valuable constituent of biogas is not thermodynamically favorable as its Gibb's free energy is comparatively near positive (-31.0kJ/mol) than the other methanogenesis pathways, hydrogenotrophic methanogenesis and homoacetogenesis, with - 135.0kJ/mol and -104. 00kJ/mol respectively (Ampomah - Benefo, 2018). The outcome is better imagined as production of methane would be suppressed.

However, the challenge of primary concern to this study is the problem of scum. It is attributed to solid accumulation when biodigester's design is inadequate (Anonymous, 2020). Scum originated from the substrate as suspended solids like straw, grass, stalk, dried dung, feather, etc., tend to be floating to the surface. These eventually may become a problem when they are not digested as they form a thick scum layer which blocks the surface. This posed a danger of blocking the gas by the rising scum. The trapped gas may cause CO2 to dissolve which reduces the pH of the slurry to acidic which inhibits methanogens resulting low methane yield. The surface scum has to be removed and that leads to shutting down of the digester for cleaning translating to economic loss and down time.

Solid and mineral materials like sand and earthed material may be picked up by animal during feeding and egested undigested by animals. Such particles are usually seen in poultry birds, cow or pig dung. Based on their weight, gravitational pull on these heavy undigested particles settle/sink to the bottom and eventually pile up to scum which block the outlet pipe or reduce the active digester capacity. Scum is not brittle but very filthy and tough. It can become so strong within a short time that needs heavy equipment to break it (Wang et al., 2009). To destroy it, it is either the scum must be watered from the top or pushed down into the liquid. Both operations demands costly apparatus and the plant have to be shutdown accounting to huge economic loss and downtime.

However, when scum is fully developed, stirring is not a viable solution for breaking scum (Budiastuti and Rahayu, 2016). The only solution is to avoid scum formation by ensuring that the digester content is sufficiently/perfectly or by carefully selecting suitable substrates. However, as far as the substrate involve animal manure, the presence of sand, stone and other debris in the animal dung is inevitable as such sufficient mixing operation is the only way forward. As reviewed, the challenge of sufficient mixing irrespective of types is an issue currently investigated as the mechanical, hydraulic and pneumatic approaches to mixing have peculiar challenges. Therefore, the low methane yield, poor effluent quality, instability and early termination of gas production are related to digester's design and configuration. Designing a multi-stage with improved mixing efficiency will address these issues.

### *2.2 Challenges Attributed to Substrates*

Researchers have exploited several biomaterials for biogas production. These materials include among others animal wastes (Zuru et al., 1998), industrial waste (Uzodinma et al., 2007), plant waste (Bori et al., 2007; Ofoefule et al., 2009), food processing wastes (Arvanitoyannis et al., 2007). However, animal wastes (manure) are readily digested than plant materials. The difficulty posed by digesting plant materials especially crop residues is associated with its high cellulosic and ligninic content which is difficult to be broken during hydrolysis (Itodo et al., 1992; Garba and Uba, 2002; Kozo et al., 1996; Dioha et al., 2006; Eze, 2003; Okoroigwe, 2005) coupled with attendant acidity in the biogas system leading to reduction if not termination of biogas production (Uzodinma et al., 2007; Ofoefule and Uzodinma, 2009). Meanwhile, all organic materials contain enough nutrients essential to support the growth and metabolism of anaerobic bacteria in biogas production (Ofoefule and Onukwuli, 2010). The choice of substrates for biogas production is critical as it can mar or promote the process.

Several optimization techniques for enhancing biogas production has been reported to including blending (co-digestion), size reduction, inoculation, chemical treatment, addition of metals and others (Batstone et al., 2007; Ofoefule and

Uzodinma, 2006; Ofoefule and Uzodinma, 2009). Co-digestion involves the digester with a blend of substrates combo to exploit its synergistic effects by provision of balanced micro and macro nutrients for optimum microbial activity. It involves enhancement of digestion of biomass (mostly plants) due to the addition of easily degradable substrates (mostly animal waste).

However, impact of co-digestion can be adverse as several inhibitory episodes have been reported of co-digestion involving a mixture of two or more substrates resulting in low methane yield, instability and even poor effluent quality (Oparaku et al., 2013; Teng 2014; Forgacs et al., 2019). The inhibitory episode from antagonistic substrate combo is one of the challenges and many researchers seek to unmask (Agyeman et al., 2014; Fu et al., 2015; Di Maria et al., 2015; Belle et al., 2015; Aboudi et al., 2015; Glanpracha and Annachhatre ,2016; Dennehy et al., 2016; Aboudi et al., 2016; Li et al., 2017; Zahan et al., 2017; Mancini et al., 2018; Franco et al., 2018; Guo et al., 2018; Martín et al., 2018; Mustafa et al., 2018; Vazifehkhoran et al., 2018; Xu et al., 2018). The task is finding two or more substrates with complementary characteristics so that methane yield, effluent quality and process stability are enhanced through their joint treatment. This portrays co-digestion process as a trial and error technique whose impact can be positive or negative.

However, organic materials harnessed for biogas production is limited and new substrates should be sought to meet the ever-increasing energy demand. Further research on many locally available wastes especially plant residues as potential feedstock for biogas production is still ongoing. In view of this, several researchers have reported that biogas production as well as the stability of the process is dependent on several factors such as pH of the digesting medium, total solids, volatile solids, ambience and slurry temperature, nature (especially composition) of waste, organic loading rate, retention (residence) in the biodigester and mixing ratio of substrates, and others (Garba and Sambo, 1992; Carl and Lamb, 2002; Dioha et al., 2005; Ezeonu et al., 2005; Anonymous, 2020).

### *2.3 Challenge Attributed to Effluent as Bio-Fertilizer*

In the course of conducting anaerobic digestion process especially using second generation constituting crop residue and organic waste, it is of concern that the process too would not generate waste to the community especially as the effluents from anaerobic digestion are of poor quality than that of aerobic digestion (Babatola and Ojo, 2020). Generally, oxidizing agents such as O2, NO3, SO4, and CO2, destroy cells by oxidizing various cell components. The reaction releases energy in the form of heat. This is why air should be avoided as the slurry in the presence of O2 undergoes oxidation referred to as aerobic digestion, in which the reaction releases energy. Table 3 shows the oxidization of glucose where free energy of ΔGo =-2840 kJ mol-1 is released with the production of CO2 and H2O. In this reaction no CH4 is formed. This is because methanogens, which forms CH4, are very sensitive to oxygen and die when they are exposed to O2 (Ampomah-Benefo, 2018).

*Table 3:* Aerobic reaction of biomass

| Component | Aerobic reaction |
|---|---|
| Reaction | $C_6H_{12}O_6 + 6O_2 \rightarrow 6CO_2 + 6H_2O$ |
| Energy released | $\Delta G^0$ = -2840kJ/mol |
| Energy balance | 60% biomass, 40% heat released |

*Source: Ampomah-Benefo (2018)*

Moreover, odorous substances include high concentration of ammonia, light metal ions (Na, K, Mg, Ca, and Al) and heavy metals (Cr, Fe, Co, Cu, Zn, Cd, and Ni) in the digester (Cheng, 2008). Ammonia is produced from urea and proteins biodegradation and causes microorganisms to cease growth. The light and heavy metals may form salts, which may dehydrate microbial cells







London Journal of Engineering Research

due to osmotic pressure. The digester effluent when used as fertilizer on land often creates serious environmental problem as the odor bothers neighboring residents (Filmax, 2009).

The most important problem in substrate management is that associated with the scum (sludge) while in the digester and when disposed.

A protocol to exploit the scum anaerobic treatment gives the same high effluent quality as aerobic treatment. Studies are currently conducted to evaluate the effluent sludge in order to assess not only its fertilizing effect but also environmental impact (Anonymous, 2020). In view of this, the author suggests the effluent can be filtered and its residue pyrolysed to create biochar and it absorption property can be investigated. The biochar can be soaked with the effluent filtrate while evaluating its fertilizing effect as well as odor emission.

## III. CONCLUSION

Anaerobic biodigestion process is generally considered to be slow and unstable due to strict nature of the anaerobes and difficult to operate. However, the process is promising as it applications cut across several sectors of the economy including the energy, agricultural and environmental sectors. The advances and challenges confronting the anaerobic digestion technology have been extensively reviewed. The advances are attributed to technological innovations with regards to the diversity in bio-sourced feedstock, digester design and variability of process conditions. A variety of bio-sourced feedstock such as: animal manure, agro-residues, lignocellulosic biomaterials, food waste and municipal refuse/sewage exploited in a closed reactor/tank or bioreactor so-called anaerobic biodigester of various classes. Typically, the AD process may be categorized into four phases, i.e., hydrolysis, acidogenesis, and acetogenesis followed by methanogenesis. Pretreatment of feedstock is an unavoidable process to make the lignocellulosic substrate amenable for consortium of microorganisms (anaerobes).

It was found that pretreatment of these feedstocks, substrate interaction with the novel inoculum and substrate combo, mixture of different classes of feedstock that ferment better together than separately due to their enriched microbial load as well as their nutritional requirements, are recent strategies exploited to improve anaerobic biodigestion process. In addition, research on thermal effect, alternating thermophilic, mesophilic and psychrophilic stages while evaluating the productivity, kinetics, and net energy balance have been adequately investigated as reviewed. However, the process is challenged by poor biodigester design/ configurations, the inhibitory episodes from antagonistic substrate combo and the offensive odor of the effluent on fertilizer application. The review on these challenges is necessary towards improving the process.

On the whole, for improved degradation of substrates, several strategies such as pretreatment and co-digestion, etc. have been exploited. Specifically, pretreatment of feedstock facilitates biodigestion and improves the accessibility of the source carbon utilizable by the microbial community, and mixing sources (co-digestion), working together as substrates, provides several advantages that improves biogas yields, methane production, and various other benefits.

## REFERENCES


1. Aboudi, K., Álvarez-Gallego C. J. and Romero -García, L. I. (2015). Semi-continuous anaerobic co-digestion of sugar beet byproduct and pig manure: Effect of the organic loading rate (OLR) on process performance. Bioresource Technology, 194:283-290.
2. Aboudi, K., Álvarez-Gallego C. J. and Romero-García, L. I. (2016). Evaluation of methane generation and process stability from anaerobic co-digestion of sugar beet by-product and cow manure. Journal of Bio-science and Bioengineering. 121(5): 566-572.
3. Agyeman, F. O. and Tao, W. (2014). Anaerobic co-digestion of food waste and dairy manure: Effects of food waste particle size and organic loading rate. Journal of Environmental Management; 133: 268-274.

4. Akinbami, J. F. K, Ilori, M. O., Oyebisi, T. O., Akinwumi, I. O, Adeoti, O. (2001) Biogas energy use in Nigeria: Current status, future prospects and policy implications. Renewable and Sustainable Energy Review, 5: 97-112.
5. Allen, E. (2015) Biogas Production from Novel Substrates. PhD Thesis, University College, Cork.
6. Ampomah-Benefo, K., Boafo-Mensah, G., Animpong, M. A., Oduro, W. O., Kotey, E. N., Akufo-Kumi, K. and Laryea, G. N. (2013). Thermal Efficiency of Charcoal Fired Cook stoves in Ghana.Global Advanced Research Journal of Engineering, Technology and Innovation, 2(3):102-110.
7. Ampomah-Benefo, Kofi (2018) A Prototype of an Adaptive, Multi-Feedstock, Anaerobic Biomass Digester for Biogas Production, PhD Thesis, University of Ghana, Legon.
8. Ann, J., Kessel, V. and Russel, J. B. (1996).The Effect of pH on Ruminal Methanogenesis. FEMS Microbiology Ecology, 20, 205-210.
9. Anonymous (2020). Asian-Pacific Regional Biogas Training Manual. Cheugdu Center, China.
10. Arvanitoyannis, I. S., Kassaveti, A and Stefanatos, S. (2007) Int. J. Food Sci. Tech. 42 (7): 852 – 867.
11. Babatola, J. O. and Ojo, O. M. (2020) Dung-Aided Water Hyacinth Digestion Mixes: Association between Biogas Quality and Digester Temperature for Selected Animal J. Appl. Sci. Environ. Manage. 24 (6) 955-959.
12. Bamgboye, A. I. and Ojolo, S. J. (2004). Characterization of municipal solid wastes being generated in Lagos State, Nigeria. LAUTECH J. Eng. Tech. 2(1):36-38.
13. Bamgboye, I. A. (2012). The potential of producing fuel from biomass in Nigeria In: Jekayinfa S. O. (Ed). Building a non-oil export based economy for Nigeria: the potential of value-added products from agricultural residues. CuvillierVerlag Gottingen. pp. 35-41.
14. Bayrakdar, A., Sürmeli, R. Ö.and Çalli, B. (2018). Anaerobic digestion of chicken manure by a leach-bed process coupled with side-stream membrane ammonia separation. Bioresource Technology, 258:41-47.
15. Belle, A. .J, Lansing, S., Mulbry, W. and Weil, R. R. (2015). Anaerobic co-digestion of forage radish and dairy manure in complete mix digesters. Bioresource Technology.178: 230-237.
16. Ben-Iwo, Juliet, VasilijeManovic, and Philip Longhurst (2016) Biomass resources and biofuels potential for the production of transportation fuels in Nigeria. Renewable and Sustainable Energy Reviews63: 172–192.
17. Bhatia, L., Garlapati, V. K., Chandel, A. K. (2019). Scalable Technologies for Ligno-cellulosic Biomass Processing into Cellulosic Ethanol. In: Pogaku R (ed) Horizons in Bioprocess Engineering. Springer Nature, Switzerland AG, Pp. 73–90.
18. Boone, D. R. and Luying, X. (1987). Effects of pH, Temperature, and Nutrients on Propionate Degradation by a Methanogenic Enrichment Culture. Applied and Environmental Micro-biology, 7: 1589-1592.
19. Bori, M.O., Adebusoye, S.A., Lawal, A.K. and Awotiwon, A. (2007). Advances in Environ. Biol. 1(1): 33-38.
20. Bruni, E., Jensen, A. P., Pedersen, E. S. and Angelidaki, I. (2010).Anaerobic Digestion of Maize Focusing on Variety, Harvest Time and Pretreatment Applied Energy, 87: 2212–2217.
21. Budiastuti H and Rahayu E S (2016) Hydraulic Loads towards Methane Gas Production and Anaerobic bacteria in Anaerobic Fixed Bed Reactor. Proc. IRWNS Bandung Indonesia.
22. Carl, N. and J. Lamb (2002). Final Report: Haubenschild Farms Anaerobic Digester, Updated. The Minnesota Project.
23. Cestonaro, T., Costa MSS de M, C., Rozatti, M. T., Pereira, D. C., Francisconi, H. E. (2015) The anaerobic co-digestion of sheep bedding and ⩾50% cattle manure increases biogas production and improves biofertilizer quality. Waste Management, 46:612-618.
24. Chandel, A. K., Albarelli, J. Q., dos Santos, D. T., Chundawat, S. P. S., Puri, M. and Meireles, M. A. A. (2019). Comparative analysis of key Technologies for Cellulosic Ethanol Production from Brazilian sugarcane bagasse at the commercial-scale. Biofuels Bioprod Biorefin 13(4): 4–1014.

25. Chen, Y., Cheng, J. J., & Creamer, K. S. (2008). Inhibition of Anaerobic Digestion Process: A review. Bioresource Technology, 99: 4044-4064.
26. Cheng, S., Li, Z., Mang, H.P., Huba, E.M., Gao, R., Wang, X. (2008). Development and application of prefabricated biogas digesters in developing countries. Renew. Sust. Energy Rev. 34: 387-400.
27. Cheng, L. L., Lee, Y. H., Lin, J. H., Chou, M. S. (2010). Treatment of mixture of sewage and partially treated swine wastewater by a combination of UASB and constructed wetlands. Practice Periodical of Hazardous, Toxic, and Radioactive Waste Management, 14 (4), 234-239.
28. Cherubini, F. (2010). The biorefinery concept: Using biomass instead of oil for producing energy and chemicals. Energy Convers Manag 51:1412–21.
29. Dahunsi, S. O., Oranusi, S. and Efeovbokhan, V. E. (2017). Cleaner Energy for Cleaner Production: Modeling and Optimization of Biogas Geneaton from Carica Papayas (Pawpaw) Fruit Peels. Journal of Cleaner Energy Production., 156:19-29.
30. Darwin, C., Liu, Z., Gontupil, J. and Kwon, O. (2014) Anaerobic co-digestion of rice straw and digested swine manure with different total solid concentration for methane production. Int J Agr Biol Eng 7:79–90
31. Demirel, B. and Scherer, P. (2008). Production of methane from sugar beet silage without manure addition by a single-stage anaerobic digestion process. Biomass and Bioenergy, 32: 203-209.
32. Dennehy, C., Lawlor, P. G., Croize, T., Jiang, Y., Morrison, L., Gardiner, G. E, (2016). Synergism and effect of high initial volatile fatty acid concentrations during food waste and pig manure anaerobic co-digestion. Waste Management. 56:173-180.
33. Deublein, D. and Steinhauser, A. (2008). Biogas from Waste and Renewable Resources: An Introduction. Weinheim: WILEY-VCH Verlag GmbH & Co.
34. Di Maria, F., Sordi, A., Cirulli, G. and Micale C. (2015). Amount of energy recoverable from an existing sludge digester with the co-digestion with fruit and vegetable waste at reduced retention time. Applied Energy. 150:9-14.
35. Diamantis, A. and Aivasidis, V. (2010).Kinetic Analysis and Simulation of UASB Anaerobic Treatment of a Synthic Fruit Waste water. Global NEST Journal,, 175-180.
36. Dioha. I. J., Eboatu. A. N., Arinze R. U., Onuegbu. T. U. and Okoy P.A.C (2006). Biogas production from mixture of poultry Droppings and cow dung. Nigerian Journal of Solar Energy 16: 1- 4.
37. Dioha, I. J., Eboatu .A. N., Akpuaka M.U., Abdullahi .D. Arinze R.U. and Okoye P.A.C. (2005). Comparative studies of the Effects of Brands of cow dung and NPK fertilizers on the growth of okra plants. Nigerian Journal of Solar Energy 16: 15 – 18.
38. Duku, M., Gu, H., Hagan, S. and Ben, E. (2011) A comprehensive review of biomass resources and biofuels potential in Ghana. Renew Sustain Energy Rev; 15: 404–15.
39. Dutta, K., Daverey, A.and Lin, J. G. (2014) Evolution retrospective for alternative fuels: First to fourth generation. Renew Energy; 69:114–22.
40. Edenseting, B. O., Obonukut, M. E. and Oboh, I. O. (2020) Bio-Sourced Feedstocks for Biofuel Production: Nigeria as a Case Study. bJournal of Scientific and Engineering Research. 7 (12): 1-18.
41. Evans, G. M. and Furlong, J. C. (2003). Environmental Biotechnology: Theory and Application. Chichester: Johy Wiley & Sons.
42. Eze, J. I. (2003) Maximizing the potentials of biogas through upgrading. Am. J. Sci. Ind. Res., 1(3): 604-609.
43. Eze, J. I. and Agbo, K. E. (2010). Studies on the microbial spectrum in anaerobic bio-methanization of cow dung in 10m3 fixed dome biogas. Int. J. Phy. Sci., 5(8): 1331-1337.
44. Eze, J. I. and Ojike, O.1. (2012). Anaerobic production of biogas from maize wastes. International Journal of the Physical Sciences 7(6):982 – 987.
45. Ezekoye, V. A., Ezekoye, B. A. and Offor, P. O. (2011) Effect of Retention Time on Biogas Production from Poultry Droppings and Cassava Peels. Nig J. Biotech. 22: 53-59.

46. Ezeonu, S. O., Dioha, I. .J. and Eboatu, A.N. (2005). Daily Biogas production from different wastes and identification of methanogenic bacteria involved. Nigerian Journal of Solar Energy 15: 80 – 85.
47. Fan, X., He, S., Katukuri, N. R., Yuan, X., Wang, F. and Guo, R. .B (2016). Enhanced methane production from microalgal biomass by anaerobic bio-pretreatment. Bioresour Technol 204:145–151
48. Fang, C. (2010) Biogas production from food-processing industrial wastes by anaerobic digestion. PhD Thesis, Technical University of Denmark.
49. Fekadu, M. (2014). Biogas production from Water Hyacinth (eichhorniacrassipes) Co-digestion with cow-dung. M.Sc thesis, Haramaya University
50. Filmax P. (2009). The Biogas Digester Expert Pages. Http/www.rosneath.com.au Date accessed: 17/9/2021.
51. Forgacs G., Smyth M. and Arnot T. (2019) Co-Digestion and Food Waste Ad: Biowin Modelling to Optimise OLR and HRT on the Avonmouth Food Waste Digesters, Water Innovation and Research Centre, UK.
52. Franco, R. T., Buffière, P. and Bayard, R. (2018).. Coensiling of cattle manure before biogas production: Effects of fermentation stimulants and inhibitors on biomass and methane preservation. Renewable Energy, 121:315-323.
53. Fu, S. F., Wang, F., Yuan, X. Z., Yang, Z. M., Luo, S. J. and Wang, C. S. (2015a). The thermophilic (55°C) microaerobic pre-treatment of corn straw for anaerobic digestion. Bio-resource Technology, 175:203-208.
54. Fu, S. F., Shi, X. S., Xu, X. H., Wang, C. S., Wang, L. and Dai, M. (2015b) Secondary thermophilic microaerobic treatment in the anaerobic digestion of corn straw. Bioresource Technology, 186:321-324.
55. Garba, A. and A.S. Sambo. (1992) Nig. J. Solar Energy, 3: 36-44.
56. Garba, A. and Uba, A. (2002) Biogas Generation from Ornamental Plants, Nig. J. Renewable; 15:61-63.
57. Gashaw, A. (2014). Anaerobic Co-Digestion of Biodegradable Municipal Solid Waste with Human Excreta for Biogas Production: A Review. American Journal of Applied Chemistry, 4:55-62.
58. Gelegenis, J., Georgakakis, D., Angelidaki, I. and Mavris, V. (2007).Optimization of Biogas Production by Co-digesting Whey with Diluted Poultry Manure. Renewable Energy, 32: 2147–2160.
59. Glanpracha, N. and Annachhatre, A. P. (2016). Anaerobic co-digestion of cyanide containing cassava pulp with pig manure. Bioresource Technology. 214:112-121.
60. Guo, J., Cui, X., Sun, H., Zhao, Q., Wen, X. and Pang, C. (2018). Effect of glucose and cellulase addition on wet-storage of excessively wilted maize stover and biogas production. Bioresource Technology, 259:198-206.
61. Hamad, M. A., Dayem, A. and El-Hawagi, M. M. (1983). Rural Biogas Technology: Effect of Digester Pressure on Gas Rate and Composition. Journal of Engineering and Applied Sciences, 2:49-57.
62. Hoefnagels, R. and Germer, S. (2018) Supply potential, suitability and status of ligno-cellulosic feedstocks for advanced biofuels. Advance fuel 14:12-21
63. Itodo, I. N., E. B. Lucas and F. I. Kucha (1992) The Effects of Media Material and its Quantity on Biogas Yield. Nig. J. Renewable Energy, 3:45-49.
64. Ivo Achu, N. (2012) Anaerobic Digestion of Crop and Waste Biomass: Impact of Feedstock Characteristics on Process Performance. PhD Thesis, Lund University;
65. Jena, S., Mishra, S., Acharya, S. and Mishra, S. (2017). An Experimental Approach to Produce Biogas from Semi Dried Banana Leaves. Sustainable Energy Technologies and Assessment, 19: 173-178.
66. Kacprzak, A., Krzystek, L., Ledakowicz, S. (2010). Co-digestion of agricultural and industrial wastes. Chem. Pap. 64(2):127-131.
67. Kalyanasundaram, G. T., Ramasamy, A., Blesy, G., Ramesh, D. and Karthikeyan, S. (2020). Prospects and Challenges in Biogas Technology: Indian Scenario. In: Biogas Production: From Anaerobic Digestion to a

Sustainable Bioenergy Industry Springer Nature: Switzerland.
68. Karp, S. G., Woiciechowski, A. L., Soccol ,V. T., Soccol, C. R. (2013). Pretreatment strategies for delignification of sugarcane bagasse: a review. Braz Arch Biol Technol 56(4):679–689.
69. Kaur, Harmanjot (2017) Designing of Small Scale Fixed Dome Biogas Digester for Paddy Straw. International Journal of Renewable Energy Research, 7(1): 422–434.
70. Kazemi, S., Panahi, H., Dehhaghi, M., Kinder, J. E. and Ezeji, T. C. (2019) A review on green liquid fuels for the transportation sector: a prospect of microbial solutions to climate change. Biofuel Research Journal 23:995-1024.
71. Kozo, I., Hisajima, S. and Dangh, R. J. (1996). Utilization of Agricultural wastes for biogas production in Indonesia, In: Traditional technology for environmental conservation and sustainable development in the Asia Pacific region. 9th Ed.,Pp.134 – 138
72. Lemmer, A., Merkle, W., Baer, K. and Graf, F. (2017). Effects of High-Pressure Anaerobic Digestion Up to 30 bar on pH-value, production kinetics and specific methane yield. Energy, 138, 659-667.
73. Li, L., Zhang, R., He, Y., Wang, W., Chen, C., and Liu, G. (2015).Anaerobic Digestion Performance of Vinegar Residue in Continuously Stirred Tank Reactor. Bio-resource Technology, 18: 338-342.
74. Li, Y., Liu, H., Yan, F., Su, D., Wang, Y., and Zhou, H. (2017). High-Calorific Biogas Production from Anaerobic Digestion of Food Waste Using a Two-phase Pressurized Biofilm (TPPB) System. Bio-resource Technology, 224:56-62.
75. Li, W., Siddhu MAH, A. F., He, Y, Zhang, R. and Liu, G. (2018). Methane production through anaerobic codigestion of sheep dung and wastepaper. Energy Conversion and Management.156:279-287.
76. Lin, L., Chunli, W., Xiang, L., Duu-Jong, L., Zhongfang, L., Zhang, Y., and Tay, J. H. (2013). Effect of Initial pH on Mesophilic Hydrolysis and Acidification of Swine Manure. Bio-resource Technology, 136:302–308.
77. Mancini, G., Papirio, S., Lens P. and Esposito G. (2018). Increased biogas production from wheat straw by chemical pretreatments. Renewable Energy.119:608-614.
78. Marin Batista J, Salazar L, Castro L, Escalante-Hernández H. (2015). Co-digestión anaerobia de vinaza y gallinaza de jaula: alternativa para el manejo de residuos agrícolas colombianos. Revista Colombiana de Biotecnología1 8(2):6-12.
79. Martín, Juárez J, Riol Pastor E, Fernández Sevilla J. M, Muñoz Torre R, García-Encina PA, Bolado Rodríguez S (2018). Effect of pretreatments on biogas production from microalgae biomass grown in pig manure treatment plants. Bioresource Technology. 257:30-38.
80. Mata-Alvarez, J., Dosta, J., Romero-Güiza, M. S., Fonoll, X., Peces, M. and Astals, S. (2014). Renewable and Sustainable Energy Reviews.A critical review on anaerobic co-digestion achievements between 2010 and 2013, Energy J. 36: 412-427.
81. Mateescu, C. (2016). Influence of the Hydrostatic Pressure on Biogas Production in Anaerobic Digesters. Romanian Biotechnological Letters. Romania.
82. Mitchell, D. (2008) A note on rising food prices. World Bank Policy Research Working Paper Series.
83. Mosier, N. S. and Ladisch, M. R. (2009). Modern Biotechnology: Connecting Innovatioins in Microbiology and Biochemistry to Engineering Fundamentals. Canada: John Wiley & Sons.
84. Mustafa, A. M., Li, H., Radwan, A. A., Sheng, K. and Chen, X.. (2018). Effect of hydrothermal and Ca(OH)2 pretreatments on anaerobic digestion of sugarcane bagasse for biogas production. Bioresource Technology. 259:54-60.
85. Ofoefule, A. U. and Onukwuli, O. D. (2010) Biogas production from blends of bambara nut (Vigna subterranea) chaff with some animal and plant wastes. Advances in Applied Science Research, 1 (3): 98-105.
86. Ofoefule, A. U. and Uzodinma, E. O. (2006) In Proceedings of the IX World Renewable

Energy Congress University of Florence, Italy, 19-25 UK: Elsevier Publishers.
87. Ofoefule, A. U. and Uzodinma, E. O. (2009) Int. J. Phy Sci. 4 (7): 398-402.
88. Ofoefule, A. U., Uzodinma, E. O. and Onukwuli, O. D. (2009) Int. J. Phy. Sci, 4(8): 535-539.
89. Okoroigwe, E. C. and Agbo, S. N. (2007) Gas Evacuation on the Quantity of Gas Production in a Biogas Digester, Trend in Applied Sciences Research 2(3): 246-250.
90. Okoroigwe, E. C. (2005). Adaptation of Plastic Technology in the Manufacture of Biodigester. M.Eng. Dissertation, University of Nigeria, Nsukka.
91. Oparaku, N. F., Ofomatah, A. C. and Okoroigwe, E. C. (2013) Biodigestion of cassava peels blended with pig dung for methane generation Academic Journal, 12 (40):5956 -5961.
92. Patel, V. R. (2017). Cost-effective Sequential Biogas and Bioethanol Production from the Cotton Stem Wastes. Process Safety and Environmental Protection, 111:335-345.
93. Pisutpaisal, N., Nathoa, C. and Sirisukpoca, U. (2014) Production of Hydrogen and Methane from Banana Peel by Two-Phase Anaerobic Fermentation. Energy Procedia, 50: 702 – 710
94. Ryckebosh, E. (2011). Techniques for Transformation of biogas to biomethane. Biomass and Bioenergy, 1633-1645.
95. Safley, L. and P. Westerman (1990) Psychrophilic Anaerobic Digestion of Animal Manure: Proposed Design Methodology. Biological Wastes, 34 ( 2):133–148.
96. Steffen, R., Szolar, O., Braun, R. (1998). Feedstocks for anaerobic digestion. Institute of Agro-biotechnology Tulin, University of Agricultural Sciences, Vienna.
97. Tasnim, F., Iqbal, S. A. and Chowdhury, A. R. (2017). Biogas Production from Anaerobic Co-digestion of Cow Manure with Kitchen Waste and Water Hyacinth. Renewable Energy, 109: 434-439.
98. Tchobanoglous G; Burton F. L; Stensel, D. H. (2003).Wastewater Engineering, Treatment and Reuse. Fourth edition. Metcalf & Eddy, Inc., McGraw - Hill Science Engineering pp 629-632, 983-1026.
99. Teng, Z., Hua, J., Wang, C. Lu, X. (2014). Design and optimization principles of biogas reactors in large scale applications. 4th edition Singapore: MCGraw Hill.
100. Uzodinma, E. O., Ofoefule, A. U., Eze, J. I. and Onwuka, N. D. (2007) Trends Appl. Sci. Res. 2(6): 554-558.
101. Vazifehkhoran, A. H., Shin, S. G. and Triolo, J. M. (2018). Use of tannery wastewater as an alternative substrate and a pretreatment medium for biogas production. Bioresource Technology, 258:64-69.
102. Velázquez-Martí, B., Meneses-Quelal, O. W., Gaibor-Chavez, J. and Niño-Ruiz, Z. (2019). Review of Mathematical Models for the Anaerobic Digestion Process In: Intechopen. DOI: http://dx.doi.org/10.5772/ 80815.
103. Vivekanandan, S. and Suresh, R (2017) Two Stage Anaerobic Digestion Over Single Stage on Biogas Yields from Edible and Non-Edible De-Oiled Cakes Under the Effect of Single and Co-Digestion System. International Journal of Civil Engineering and Technology, 8(3):. 565–574.
104. Wall, D., Allen, E., P. O'Kiely. and Murphy, J. (2014). Optimisation of digester performance with increasing organic loading rate for mono and co-digestion of grass silage and dairy slurry. Bioresource Technology 173 (0): 422-428.
105. Wang, S., Dai, G., Yang, H. and Luo, Z. (2017).Lignocellulosic Biomass Pyrolysis Mechanism: A State-of-the-Art Review. Progress in Energy and Combustion Science, 62:33-86.
106. Xu, W., Fu, S., Yang, Z., Lu, J. and Guo, R. (2018) Improved methane production from corn straw by microaerobic pretreatment with a pure bacteria system. Bioresource Technology. 259: 18-23.
107. Zahan, Z., Othman, M. Z. and Muster, T. H. (2018). Anaerobic digestion/co-digestion kinetic potentials of different agroindustrial wastes: A comparative batch study for C/N optimisation. Waste Management.71:663-674.
108. Zahan ,Z., Othman, M. Z., Muster, T. H. (2018). Anaerobic Digestion/Co-Digestion Kinetic Potentials of Different Agro-Industrial Wastes: A Comparative Batch Study for C/N Optimisation. Waste Manag. 71:663–674.

109. Zhang, J. (2017). Three-Stage Anaerobic Digester for Food Waste. Applied Energy, 194: 287–295.
110. Zhu, B., Zhang, R., Gikas, P., Rapport, J., Jenkins, B. and Li, X. (2010). Biogas Production from Municipal Solid Wastes Using an Integrated Rotary Drum and Anaerobic-Phased Solids Digester System. Bio-resource Technology, 101, 6374–6380.
111. Zuru, A. A., Saidu, H. Odum, E. A. and Onuorah, O. A. (1998) Nig. J. Ren. Ener, 6 (1 and 2): 43 – 47.

# Paradigm Shift from Waste to Wealth through Biomass Conversion Technologies: A Panacea for Energy, Health and Environmental Challenges in Nigeria

*Benedict Edenseting, Minister Obonukut, Innocent Oboh & Jock Alexander*

*University of Uyo*

## ABSTRACT

The over-dependence on fossil fuel, estimated to be exhausted in less than five decades, is not sustainable and economical to the most populous country in Africa. Currently, Nigeria is battling with insufficient energy, polluted environment, and health challenges due to inequality in energy generation and consumption which promote the use of generators in the country. Meanwhile, biomass has been successfully exploited and adopted by advanced countries to break the fossil fuel monopoly and curtail its adverse effects on the environment and health. This paper projected biomass conversion technology as a panacea to the energy, environmental and, health challenges. Of the conversion technologies reviewed, bio-digestion has great potential in biogas production. The technology is cheap and, the feedstock is readily available for exploitation at a communal or individual level, making it an attractive alternative to attain energy self-sufficiency. Presently, there are several collaborative efforts between Nigeria and several countries concerning biogas generation. About 20 biogas pilot plant has been found to be operational within the country. However, replication of the technology in a different part of the country has been challenged by a lack of technical know-how, inadequate fund, and lack of awareness. Hopefully, much can be achieved as the low-level development of the technology is not encouraging.

*Keywords:* biomass, conversion technology, biodigestion, and biogas.

*Classification:* DDC Code: 333.9539, LCC Code: TP339

*Language:* English

London Journals Press

LJP Copyright ID: 392973
Print ISSN: 2631-8474
Online ISSN: 2631-8482

London Journal of Engineering Research

Volume 22 | Issue 1 | Compilation 1.0

# Paradigm Shift from Waste to Wealth through Biomass Conversion Technologies: A Panacea for Energy, Health and Environmental Challenges in Nigeria

Benedict Edenseting[α], Minister Obonukut[σ], Innocent Oboh[ρ] & Jock Alexander[Ↄ]

## ABSTRACT

*The over-dependence on fossil fuel, estimated to be exhausted in less than five decades, is not sustainable and economical to the most populous country in Africa. Currently, Nigeria is battling with insufficient energy, polluted environment, and health challenges due to inequality in energy generation and consumption which promote the use of generators in the country. Meanwhile, biomass has been successfully exploited and adopted by advanced countries to break the fossil fuel monopoly and curtail its adverse effects on the environment and health. This paper projected biomass conversion technology as a panacea to the energy, environmental and, health challenges. Of the conversion technologies reviewed, bio-digestion has great potential in biogas production. The technology is cheap and, the feedstock is readily available for exploitation at a communal or individual level, making it an attractive alternative to attain energy self-sufficiency. Presently, there are several collaborative efforts between Nigeria and several countries concerning biogas generation. About 20 biogas pilot plant has been found to be operational within the country. However, replication of the technology in a different part of the country has been challenged by a lack of technical know-how, inadequate fund, and lack of awareness. Hopefully, much can be achieved as the low-level development of the technology is not encouraging. With government interventions and support from non-governmental organizations and others in the country, biogas plants can be constructed in all communities to replace generators thus eliminating the energy, environmental, and health challenges.*

*Keywords:* biomass, conversion technology, biodigestion, and biogas.

*Author α σ ρ Ↄ:* Department of Chemical and Petroleum Engineering, University of Uyo, Nigeria.

## I. INTRODUCTION

The trio of energy, health and environmental issues in Nigeria constitutes a serious challenge to all aspects of her economy. They are related subjects of concern for decades and much research effort has been devoted towards addressing these issues for decades. This paper projects biomass conversion technology as a panacea for energy, health and environmental challenges in Nigeria. The conversion technology exploits mostly biomass/organic materials 'once regarded as waste' to proffer solution to the hydra-headed problems confronting Nigeria and beyond as energy, health and environment are global issues – a paradigm shift from waste to wealth.

Energy is the power required for transportation, heat, light and even in manufacture of products. It drives all sectors of the economy in terms of powering of heavy duty manufacturing and agricultural machinery in the industries, lighting, space heating and cooling in commercial and household buildings, powering electronic appliances, charging of phone and fuelling airplanes, ships and vehicles in the transport sector (Ampomah-Benefo, 2018; Edenseting *et al.,* 2020). Insufficiency in energy supply is the

worst tragedy that can befall any 21st century society since life itself revolves around energy (Kosmo, 1989; Galadima *et al.*, 2011; Ampomah-Benefo *et al.,* 2013; Haiwen *et al.,* 2015). Obviously, there is no sector in the economy that is not powered by energy hence; it is a veritable indicator of the level of development of a country as such an ailing energy sector translates to ailing economy (Linnhoff and Dhole, 1992; Koh *et al.*, 2008; Mitchell, 2008).

Globally, energy sources exploited generally are either non-renewable (conventional) or renewable (non-conventional). These energy sources are utilized worldwide but in different proportions according to availability and geographical location (Sorensen, 2004). Nigeria is endowed with inestimable renewable energy resources (hydro, geothermal, biomass and solar) and huge renewable energy resources (Table 1) mostly fossil fuel (Obonukut *et al.,* 2016).

*Table 1:* Renewable Energy Reserves in Nigeria

| Fossil Fuel | Reserves | |
|---|---|---|
| | Natural Units | Energy Units (Btoe) |
| Crude Oil | 36.22 billion barrels | 5.03 |
| Natural Gas | 187 trillion SCP | 4.19 |
| Lignite and Coal | 2.175 billion tonnes | 1.52 |
| Tar Sand | 31 billion barrels equivalent | 4.31 |

*Source: Ozoegwu et al (2017)*

The country is ranked 10$^{th}$ and the highest crude oil and Natural Gas producer in Africa indicating her significant contribution to the world's fossil-based energy supply (Obonukut *et al.,* 2016). Presently, the country depends mostly on fossil fuel regarded as conventional energy (Anowor *et al.,* 2014; Oyedepo *et al.,* 2019; Edenseting *et al.,* 2020). With the exponential growth rate in the population, the energy consumption rate does not commensurate with the energy production rate. Consequently, the over-dependence on fossil fuel in order to meet the soaring energy needs leads to over-exploitation of the country's hydrocarbon reserves as aggressive exploration strategies (enhanced oil recovery, subsea exploration) have been explored (Obonukut *et al.*, 2016). In the quest to address the energy issue, plunge us into a twin issue relating to environment and health. The genesis of these issues is extensively discussed (section 2) in order to address them from the root. Biomass resource in Nigeria is discussed in section 3. However, the aim of this review is to present the panacea to these challenging issues. To achieve this aim, the conversion technology required (section 4) and its prospect and challenges (section 5) of executing the technology in Nigeria are discussed. The way forward to successful take off of the project is addressed (Section 6) prior to conclusion.

## II. THE GENESIS OF ENERGY, ENVIRONMENTAL AND HEALTH CHALLENGES IN NIGERIA

Nigerian has huge energy resources (e.g. oil, gas, hydro and solar) but exploited few of them (Obonukut *et al.,* 2016). With the potential to generate 12,522MW of electric power from existing plants, the country is only able to distribute about 4000 MW which is insufficient to more than 200 million people (Sambo, 2006; Udoh, 2020). As the largest economy in the sub-Saharan Africa, this insufficiency in energy has adverse impact on the industrial growth of the country (Ofoefule and Uzodinma, 2009; Abila, 2012). In order to improve the sector, Nigeria privatized the power sector leading to creation of 11 distribution companies (DISCOS), yet no remarkable positive impact as both the government and the Discos have continued to blame each other for the poor and unstable energy supply (Udoh, 2020). Consequently, most businesses have folded up while others relocated leaving the country to neighboring countries.

To prevent businesses from crippling and as well cater for domestic energy needs, Nigerians have resorted to the use of generators for energy supply (Wjst and Boakye, 2007). This has led to increase in generator budget for many households and businesses within the country. Research shows that as at 2019, the number of generators (mostly petrol and some diesel) was between 22 million and 60 million in Nigeria (Ebrima, 2019). According to CBN report, Nigerian spent about USD 12 billion in 2019 and USD 14 billion in 2020 fueling generators (Ebrima, 2021). This increment (USD 2 billion) shows that all is not well with the sector, hence, the need to direct research effort toward this sector.

Furthermore, in an attempt to address the shortfall in energy with the procurement of generators especially diesel powered generators plunged the citizens into a serious environmental and health issues. Specifically, the cluster of generators in both residential, commercial and industrial building across Nigeria significantly contribute to noise and air pollution in the form of GHG emissions with associated health impacts such as asthma (Wjst and Boakye, 2007; Awofeso, 2016). It is worse if the generator (petrol) is in bad condition or diesel powered as their exhaust emits more than 40 toxic air contaminants in the fume including known/suspected carcinogenic substances such as benzene, arsenic and formaldehyde in addition to the GHG (Awofeso, 2016; Zhang, 2017; Vivekanandan, 2017). Wjst and Boakye (2007) reported that Nigeria has the highest prevalence of asthma in Africa. This perhaps is attributed to generators' fume.

Obviously, the capital flight associated with importation of generators and fuel coupled with the health and environmental issues are strong indicators that the use of generators is not a solution to the Nigerian energy challenge. Meanwhile, the over-dependence on fossil fuel in order to meet the soaring energy needs leads to over-exploitation of the country's hydrocarbon reserves (Obonukut *et al.*, 2016). This appears to be the solution to meet the energy demand, yet the resources are purely government-owned and are cheaply sold out abroad as Nigerian refineries gulped 1.64 trillion NGN in cumulative losses in 5 years (Udoh, 2020). As a last resort, Nigeria considers importation of petroleum products as cheaper than refining the product in the country's refineries (NNPC, 2015; Eboh, 2016). The government may not exploit the hydrocarbon resources wholly for domestic usage when it is actually the proceeds of these resources that are used to finance the economy especially when refining operation in the country is not economical.

Obviously, Nigerians will still pay heavily for fuel. However, this is not the issue as these resources would not be available forever. Recently, it was reported that Nigeria has 41 billion barrels of untapped crude oil reserves (NNPC, 2015; Ebrima, 2019; Udoh, 2020). Based on this data and with the level of average daily production (2 million barrels/day), the proven oil reserve will be exhausted within the next six decades. Similar prediction is applicable to Nigerian gas reserves as these hydrocarbon reserves take millions of years to replenish. Hence, research focus should be directed to finding alternative but renewable (infinite) sources of energy with minimal adverse impact on our environment in order to promote energy security and health.

Waste treatment/disposal is another challenge confronting the country. As expected, based on her population, the domestic, industrial and commercial activities generate huge waste. These wastes are seen to litter the street claiming more lands as number of dumping sites keeps increasing. Waste treatment/disposal is one of the environmental challenges confronting the modern societies not only Nigeria. Bio-waste (organic waste) constitutes over 60% of these wastes in the advanced nations and even more in the developing nations (Arvanitoyannis *et al.,* 2007; Cheng *et al.,* 2010; Mata-Alvarez *et al.*, 2014). However, these biological material (biomass) includes not only bio-waste but all materials from natural processes which in most cases are nuisance to our environment constituting waste (Babatola and Ojo, 2020; Edenseting *et al.,* 2020).

## III. AVAILABILITY OF BIOMASS IN NIGERIA: INTEGRATING ENERGY AND ENVIRONMENTAL NEEDS

Biomass is organic material that comes from plants and animals related materials and it includes: crops, waste wood and trees (Bamgboye, 2012; Bruni *et al.,* 2010; Pisutpaisal *et al.,* 2014; Patel, 2017). It extended to household, municipal solid waste (Zhu *et al.,* 2010), industrial waste as well as waste waters (Gelegenis *et al.,* 2007). Biomass refers to energy derivable from sources of plant origin such as trees, grasses, agricultural crops and their derivatives, as well as animal wastes, wastes from food processing, aquatic plants and algae (Duku *et al.,* 2011; Edenseting *et al.*, 2020). Based on population and intense agricultural activities, Nigeria is the highest biomass producer in Africa (Babatola and Ojo, 2020). Table 2 shows the renewable energy reserves in Nigeria.

*Table 2:* Shows the renewable energy reserves in Nigeria

| Energy sources | Reserves |
|---|---|
| Solar radiation | 3.5–7.0 kWh/m2/day (4.2 million MWh/day using 0.1% land area) |
| Animal waste | 211 million assorted animal (285.065 million tons/yr of production |
| Small hydropower | 3,500 MW |
| Large hydropower | 11,250 MW |
| Energy crops and agriculture residue | 28.2 million hectares of arable land (30% of total land) |
| Wave and tidal energy | 150,000 TJ/(1,759.6 toe/yr) |
| Fuel wood | 11 million hectares of forest and wood land |
| Wind | 2–4 m/s at 10 m in height (main land) |
| Crop residue | 83 million tons/yr |

*Source: Ozoegwu et al. (2017)*

Obviously, biomass is currently the largest renewable energy source with wider geographical spread than other renewable energy sources (solar, hydro, etc.). However, fossil fuel has been extensively exploited for many centuries while biofuel despite its availability, has been neglected perhaps rarely exploited conventionally (Abila, 2010; Ben-Iwo *et al.*, 2016). Biofuel is one of the renewable energy sources' competing with fossil fuel as its energy content is captured through natural processes and it is potentially renewable indefinitely. while fossil fuel is a non-renewable energy source as its energy content is captured through geological processes which take longer time to replenish hence continuously depleted (Sambo, 2006; Mohammed *et al.*, 2013). Unlike biofuel, fossil fuel is found in specific parts of the world making them more plentiful in some nations than others (Abila, 2012; Galadima *et al.*, 2011). To achieve more in meeting the energy need of the country as well as derive maximum benefit from utilization of vast available renewable resources, the over-dependence of the energy sector on fossil fuel that has slowed down the development of alternative fuels must be reversed (Giwa *et al.,* 2017). There is the need for diversification to achieve a wider energy supply mix which will ensure greater energy security for Nigeria. The way forward is the exploration of biomass which is abundant all over the country. As a renewable energy source, biomass products (Figure 1) are sustainable, limitless and environment friendly. Bioenergy sources have significant potential to improve and make a difference on the low level access to clean energy and electricity in Nigeria (Aliyu *et al.*, 2015; Oyedepo *et al.,* 2019).

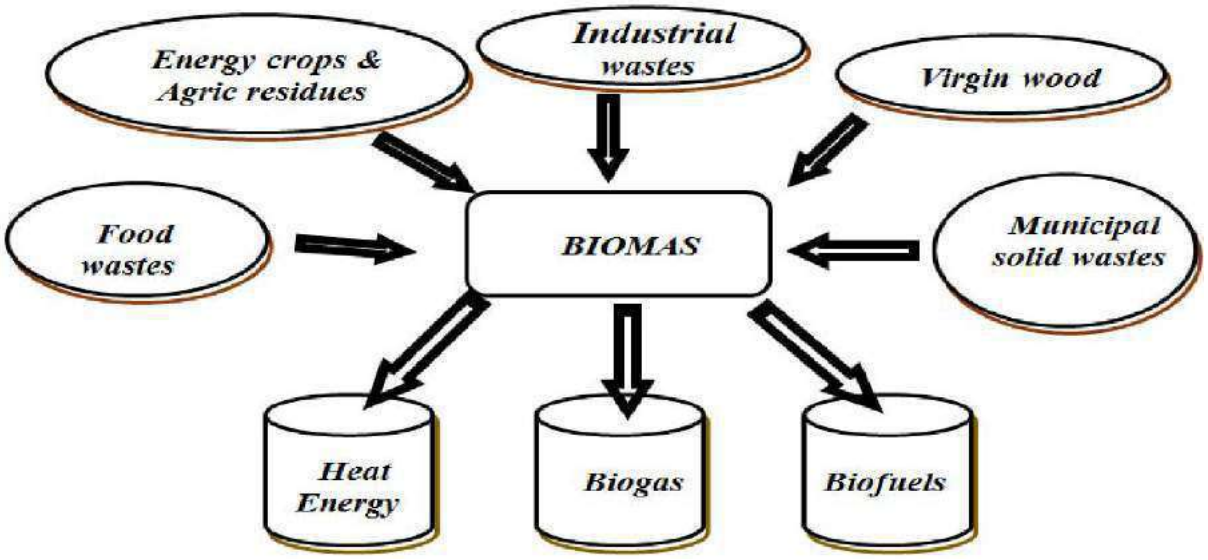


*Figure 1:* Biomass sources and products

*Source: Oyedepo et al., 2019*

Generally, biomass is compounds of carbon, oxygen, nitrogen and sulphur with high energy content (Aliyu *et al.,* 2015). It can be exploited depending on the type of conversion technology to generate energy which is environmental friendly and healthy. The conversion technology is presented next..

## IV. BIOMASS CONVERSION TECHNOLOGY: MITIGATING ENERGY, ENVIRONMENTAL AND HEALTH CHALLENGES

Bio-sourced feedstocks can be converted into chemical, electrical or heat energy using various conversional processes. The energy obtained can be utilized onsite or stored and transported for future use. Generally, fuel generated from biomass can be in solid form as seen in charcoal and briquette; liquid form as seen in bioethanol; or gaseous form as seen in biogas (methane-rich gas). Myriads of biomass have been exploited for fuel and these include: agricultural and forest product residues (Bruni *et al.,* 2010; Patel, 2017), household and municipal solid waste, (Zhu, *et al.,* 2010) and industrial waste and waste waters (Gelegenis *et al.,* 2007).

Research effort should be directed towards harnessing these materials using appropriate technology to increase the rate of integration of renewable energy into the existing energy supply mix of Nigeria (McKendry, 2002; Evans and Furlong, 2003; Ullah *et al.,* 2015; Ben-Iwo *et al.* 2016). There are various technologies for biomass conversion and some of them are more advanced than others. A review of these technologies is critical to this study in order to assess which of them is suitable and adaptable for energy generation by developing countries.

### *4.1 Thermochemical Conversion*

It involves thermal decomposition of carbonaceous material (biomass) to energy and other products. Specifically, this biomass conversion technological process exploits heat in transforming the bio-sourced feedstocks. The thermochemical conversion processes exploited are: incineration, pyrolysis and gasification. A brief review of these processes is necessary.

#### *4.1.1 Incineration (combustion)*

This involves burning of bio-sourced feedstocks in excess Oxygen. This technology involves the combustion (complete oxidation) of biomass in the presence of Oxygen. This is required for onsite consumption as the main product of incineration, heat energy, which cannot be easily stored but has to be consumed immediately. The process is favored when the moisture content of the feedstock is low and the oxidizer is oxygen-rich

air. In view of this, the moisture content of the biomaterial must be assessed prior to incineration. The moisture content of the feedstock can be reduced or drive off by drying or heating (Komilis *et al.,* 2014). However, incomplete combustion of the feedstocks has been reported producing intermediate products like polycyclic aromatic hydrocarbons and dioxins in addition to CO (Ampomah-Benefo, 2018). This undesired development usually occurred when there is limited supply of air.

### 4.1.2 Pyrolysis

This process utilizes several process variables (temperature, rate of heating, particle size and residence time) to transform bio-sourced feedstocks in a reactor chamber to solid, liquid and gaseous fractions (Mohan *et al.,* 2006). Pyrolysis is an endothermic, irreversible process that occurs in absence of oxygen. Depending on the process condition, the process can be a slow pyrolysis or fast pyrolysis. The former (slow pyrolysis) occurs at about 350°C producing about 10 % oil (volatile component) and the rest being biochar. The latter (fast pyrolysis) occurs at about 700°C. In this case, bio-sourced feedstock decomposed rapidly to produce more than 70% biofuel and very little biochar (Bolalumi, 2016). However, biofuel production through this technology is energy intensive and alternative should be explored for economic and environmental impacts purpose.

### 4.1.3 Gasification

This is another conversion technology for exploitation of bio-sourced feedstock. Synthesis gas (syngas), a combustible gas mixture is produced by partial oxidation of biomaterials (fuel). The temperature is relatively high (about 1000°C) with variable air to fuel ratio ranging from 1.5:1 to 1.8:1 producing mostly CO mixed with $H_2$ (Obonukut *et al.,* 2016; Wang *et al.,* 2017; Bassey *et al.,* 2020).

## 4.2 Biochemical Conversion

This is a conversion process in which bio-sourced feedstocks are turned into energy by microbial activities. It involves breakdown (catabolic processes) of substrates (biomass) into simple compounds that can be absorbed and used as nutrients by the microorganisms (Ampomah-Benefo, 2018). However, the process equally goes beyond catabolism as new substances are also formed through anabolic process as combustible gas (biogas) is formed. In addition, the microorganisms metabolize nutrients (substrates) for their survival and growth by producing enzymes (protein molecules) that break down specific substances. The factors exploited include: carbon source, pH, temperature, retention time, and adequate moisture content.

Enzymes are found in thousands from living cells of animals, plant microbes and from fungi and yeast. They can be intracellular (located inside the cell) or extracellular (located outside the cell). Their functions are specific in nature as they reduce the activation energy of biochemical reactions, thereby increasing reaction rates. Enzymes are used repeatedly as they remain unaffected structurally at the end of the chemical reactions (Grassian, 2005). Consequently, proteases and peptidases split proteins into small peptides and amino acids. Lipases split fat into three fatty acids and glycerol. Amylases split carbohydrates (polysaccharides and disacchari des). Enzymes (E) and substrates (S) combine to form an intermediate state, called enzyme–substrate complex (ES). A new product (P) is formed and the unchanged enzyme is ready to react again with the substrate (Equation 2.1).

$$E_S + S_S \rightleftharpoons ES_s \rightleftharpoons E_S + P_S \qquad 2.1$$

The process is economical with less adverse impact on the environment. It mimics the digestion process that occurs especially in human and ruminant animals where microbial actions in their intestines lead to the breakdown of food to release energy. It is the foundation on which this research is built as such in-depth discussion is necessary.

## 4.3 Biodigestion of Biomass

Digestion is a biology term relating to eating of food and biodigestion connotes a special type of eating by microbes. Digestion is a biological process whereby micro-organisms convert

biological material (organic matter) into volatile components and water resulting to mass loss, destruction of pathogens. The process was formulated mainly for waste treatment/disposal just like pyrolysis, gasification, thermal incineration (combustion) and others. As waste treatment/disposal is another global concern in addition to energy crisis, an attempt to handle these two challenges plunged us into climate change (Arvanitoyannis *et al.,* 2007; Cheng *et al.,* 2010). Sludge digestion may involve decomposition of biological material by microbes in the presence of oxygen (aerobic digestion) or in the absence of oxygen (anaerobic digestion) as discussed next.

### *4.3.1 Aerobic Digestion of Bio-Sourced Feedstocks*

This type of digestion by microbes utilizes bio-sourced feedstocks in the presence of oxygen and the end products are mainly $CO_2$ and water which are stable oxidized forms of carbon and hydrogen. However, if the organic contains Nitrogen and Sulphur, the end product may also include Ammonia/Nitrate and Sulphate. The process is cheap and it is useful in disposing waste as mass of the digestible waste reduces. The effluent is stable but not much useful to crops as fertilizers as Nitrogen is converted to ammonia gas (Bhat *et al.,* 2001). The process is not efficient for energy generation.

### *4.3.2 Anaerobic Digestion of Bio-Sourced Feedstocks*

In this section, a brief description of the anaerobic biodigestion technology is presented (section 4.3.2.1). This is followed by biogas production and purification (section 4.3.2.2). In the concluding section, utility of anaerobic biodigestion technology is discussed (section 4.3.2.3).

*Description of the Anaerobic Biodigestion Technology:* It is a digestion of biomaterials by microbes in an oxygen-deficient chamber (digester). Anaerobic digestion produces methane, a major combustible constituent in biogas, in addition to $CO_2$. There are two types of anaerobic digestions depending on the solid content of the slurry to process. These wet digestion and dry digestion. A digestion is considered dry if the total solid content is above 50% of the slurry. On the other hand, a wet digestion involves more than 50% of water in the slurry (Teng 2014). Wet digestion is more efficient than the dry counterpart as it gives high quality products and this study seeks to achieve an improved biogas production by exploiting wet digestion (Zhang, 2017).

Specifically, research has shown that the advantage of using anaerobic over aerobic (though cheaper) is that it generates biogas and its effluent is a nutrient-rich biol (bio-fertilizer) with essential inorganic elements for plant growth like Nitrogen, Phosphorus, etc. which enriches not only the crops with nutrient but also the soil structure with no adverse effect on the environment (Bhat *et al.,* 2001; Vavilin *et al.*, 2008). Anaerobic Digestion (AD) is the most promising way as it has the least aggressive effect on the environment compared to others (Suh and Roussaux, 2002). Anaerobic digestion process proffer solution to the energy crisis and climate change leaving the environment pollution-free when properly handled.

*Biogas Production and Purification:* Biogas is methane-rich gas produced during anaerobic digestion as microorganisms break down (eat) biomaterials in the absence of air (oxygen). The gas made up of methane $CO_2$, $H_2S$ and water plus other trace gases. Methane is about 60-70% while others constitute the remaining 30 to 40%. The effluent or left over sludge after anaerobic digestion of the organic matter is called digestate. It is rich in plants nutrient used as liquid fertilizer for crop production. Other gases can be removed leaving only methane which is highly combustible as seen in natural gas (the primary component of the natural gas) during purification.

Biogas purification process is synonymous to biogas cleaning and scrubbing. The essence of purifying biogas is to remove other associated gases leaving only methane which is the most valuable energy component in biogas due to energy content. There are processes for removing $CO_2$, $H_2S$ and moisture. These gases are more prevalent in biogas yet they have little value to the gas and need to be removed to improve the calorific value of the gas.Biogas is used for as fuel

for cooking, run generator for production of electricity and stored as refrigerant in the compressor. The gas competes highly with liquefied petroleum gas (LPG) and even the more preferred as it is found to be: cheaper to produce, less explosive. LPG leads to high emission of $NO_2$ and $CO_2$ during combustion while biogas releases minimal emission of $CO_2$ during combustion in the burner. The differences between LPG and biogas are tabulated in Table 3.

*Table 3:* Differences between biogas and LPG

| | Biogas | LPG |
|---|---|---|
| Source | Biomass (biofuel) | Hydrocarbon (fossil fuel) |
| Sustainability | Renewable | Non-renewable |
| Environment Impact | It releases pollutant ($CH_4$, $NO_2$, $CO_2$, $SO_2$, and NO) in negligible quantity which does not lead to global warming due to its low production rate | It releases pollutant ($CO_2$, CO, $SO_2$ and $NO_2$) in large quantity which increases global warming potential due to its high production rate |
| Pressure | It can be stored at atmospheric pressure which leads to higher level of safety and less explosive as relatively small quantity of biogas is stored- too little to pose any serious threat and a minuscule amount compared to any other gas connection | It is stored at 14 to 17 bar pressure and used in store at 0.2 bar pressure using a regulator |
| Risk factor | Safer as the storage pressure (1.0 atm) and low moisture content make it less explosive | Highly risky as leakage or improper usage has high possibility for explosion |
| Burner Efficiency | 50 – 55% | 60 -65% |
| Odorant | $H_2S$ naturally present in the biogas is used to detect any leakage | Ethyl Mercaptan is additionally added as the odorant to detect any leakage |
| Availability | As long as organic waste is available, it can be generated any time and the biogas is readily available for use | Based on the market demand as the availability may vary. At times, one may wait for more than a month for LPG cylinder after booking |
| Cost | it is a onetime investment and lifetime enjoyment | It requires monthly expenses and frequent price hike |
| Thermal Expansion | Expansion is negligible | The ratio between the volume of the vaporized gas and the liquefied gas varies depending on the composition, pressure and temperature |
| Auto ignition | 580°C | 405°C |
| Health Impact | Neglible health hazards | Carbon particles are emitted during combustion. Prolong or repeated exposure causes serious health related problems |

*Source: Ampomah-Benefo (2018)*

*Utility of Anaerobic Biodigestion Technology:* This is discussed in terms of treatment and disposal of fecal waste through biological filtration (Biofil digester toilet system and other bio-degradable wastes) and source of fertilizer for crop production.

*Biofil Digester/Biodigester Toilet:* It exploits science of anaerobic digestion to treats human feces (undigested waste) in the most environmental friendly manner devoid of odor, flies and cockroaches. This technology requires no sewage as such it takes very small space to install. Biodigestion of fecal waste is a sequence of process where micro - organisms/anaerobes decompose feces in the absence of oxygen. The microbe degrades the feces into biogas and water (liquid fertilizer). Air is prevented from entering into the system from the outside environment into the digester. The anaerobes access oxygen from the feces itself or alternatively from inorganic oxide from within the inbuilt material of the system.

The biodigestion technology exploited for fecal waste treatment provides an enclosed

environment for natural process of anaerobic decomposition of feces and other biodegradable materials. The biodigester box achieves this through a process called RAB system. This system comprises: rapid separation of solid (feces) and liquid (water); anaerobic digestion of solid aided by bio-catalyst (enzyme) and bio-filtration of waste water. The system decomposes and digests waste very fast and turns toilet from water closet (WC) system into green water every minute. This is achieved through anaerobic digestion (biochemical reactions) caused by fusion of internally generated gas and natural heating elements that are sealed and tightly fixed into the system.

Millions of environmental friendly microbes (anaerobes) feed on the toilet waste till it (the waste) disappear completely leaving traces of organic fertilizer (sludge) in the anaerobic chamber. Meanwhile, the biodigester chamber itself is a filter bed. Thus, as the toilet waste water passes through several layers with grades of sand, fiber net and other porous materials, a clean, non-toxic and odorless water leaves the chamber into a the drainage (soaked pit, gutter or garden). The technology has an edge over the traditional septic tank toilet system. The benefits of biodigester toilet are enumerated next

1. Biodigester is cheap as it requires low cost of construction and installation compare to septic tank/soaked away system.
2. No dislodging of sewage evacuation because it does not get full. Thereby saving money spent on sewage disposal.
3. It last for over 50 years and requires zero or little maintenance.
4. Biofil toilet can be constructed in water logged area, dry land and any land irrespective of its topography.
5. It consumes small space and can be constructed in few days.
6. Flies, cockroaches and rodents are not attracted to biofil digester toilet hence pollution free.
7. It is odorless, smart compact and promotes good health as it does not contaminate underground water.
8. Biofill digester toilet has the capacity to generate cooking gas and gas to run generator

*Bio-Fertilizer Production:* Bio-fertilizer (organic fertilizer) is a product of anaerobic fermentation process, containing specific individual or group of soil microorganisms which improve plant growth and productivity through supply of easily utilizable form of nutrients. Food shortage is a global issue as hike in food prices caused millions to either reduce their rations while others are starved. Nigeria is not exempted as the country is not self-sufficient in food production. Generally, there is a global crusade for increased per capital agricultural production to alleviate food security challenges due to the expanding world population (Amigun and Musango, 2011). Farmers, a major stakeholder in food production have been encouraged to increase production in order to alleviate the impact and prevent the impending famine.

However, the poor soil, harsh climatic conditions, including high temperature and drought, the poor economic situation, lack of technological development and inefficient farming practices have significantly affected crop productivity in Nigeria (Galadima *et al.*, 2011). Presently, increasing crop productivity requires fertilizer (organic/inorganic) application to provide the necessary nutrients for plant growth. This has been major nutrient management method to alleviate the impact of poor soil as tons of fertilizers are imported into the country each year. Organic fertilizers, which are made from bio-sourced feedstocks have been used for centuries for improving plant productivity. However, challenges bordering on availability, cost, and management have limited the use of organic fertilizers in Nigeria. Chemical fertilizers are costly, unsustainable and contribute to the environmental pollution and soil structure degradation (Bhattacharyya and Palit, 2016). The several ecological damages caused by the overuse of chemical fertilizers have become increasingly uncontrollable and most times, irreversible, causing significant nutrient loss to soils.

Moreover, the demand for green agriculture and high-quality food supply has suggested a shift or a reduction in the application of chemical fertilizer. The world desires a chemical-free material and the quest for organic cosmetic, food and related products keeps increasing. There are several organic farms including the Obasanjo organic farms in Nigeria. The production process of bio-fertilizer via anaerobic biodigestion technology is economical and straight forward when compare to chemical fertilizers. However, key factors, including microbial strains, formulation type, carrier materials and field applications are critical during bio-fertilizer production (Manlay, 2000; Dioha *et al.*, 2005; Ndiaye *et al.*, 2010).

It is necessary to characterize the biol in order to assess potentially active and non-toxic microbes which can promote plant growth. The functional characterization of the biol is carried-out using general laboratory techniques, including differential culture media or qualitative testing. Functional characteristics are used as a general quality control factor for inoculants because they are quicker and cheaper than strain-specific assessment (Ndiaye *et al.,* 2010). Generally, digestion processes irrespective of types (aerobic and anaerobic) produces bio-fertilizer. The difference between the fertilizer from aerobic and that of anaerobic digestion is the availability of Nitrogen. This particular element (Nitrogen) is essential to plant growth as it constitutes the highest proportion in most of the fertilizers (chemical and organic).

In aerobic bio-fertilizer, most of the Nitrogen held in the sludge is lost to the air in the form of ammonia gas or dissolved in surface run-off in the form of Nitrate (leaching/erosion). In this case, the Nitrogen is not available to plants. This is a similar scenario where inorganic fertilizer on application is leached to Lakes, Lagoon and other water sources depriving plant of essential nutrients (Ndiaye *et al.,* 2010). This is not applicable to bio-fertilizer from anaerobic digestion process. In this process, the Nitrogen is converted to ammonium ions when its effluent is used as fertilizer. These ions affix themselves readily to the soil particles which make it difficult to oxidize to ammonia gas or dissolve in run-off water as Nitrate. Thus, much of the Nitrogen is accessible to plant as nutrient. Hence, bio-fertilizer from anaerobic biodigestion process is more superior to that of aerobic digestion.

However, bio-fertilizer from aerobic digestion has an edge over bio-fertilizer from anaerobic counterpart in terms of offensive odor emission. The offensive odor from the anaerobic bio-fertilizer during application is a critical issue as it pollutes the environment. Strategy to reduce or eliminate the odor while maintaining its fertilizing effect should be examined.

### *4.4 Biochemical Processes of Anaerobic Bio-Digestion Technology*

The nitty-gritty of anaerobic biodigestion technology in terms of its biochemical and physicochemical processes are broken down into four stages: hydrolysis, acidogenesis (acidification), acetogenesis and methanogenesisn (Krich, 2005; Zhang, 2017). These are schematically represented in Figure 2.

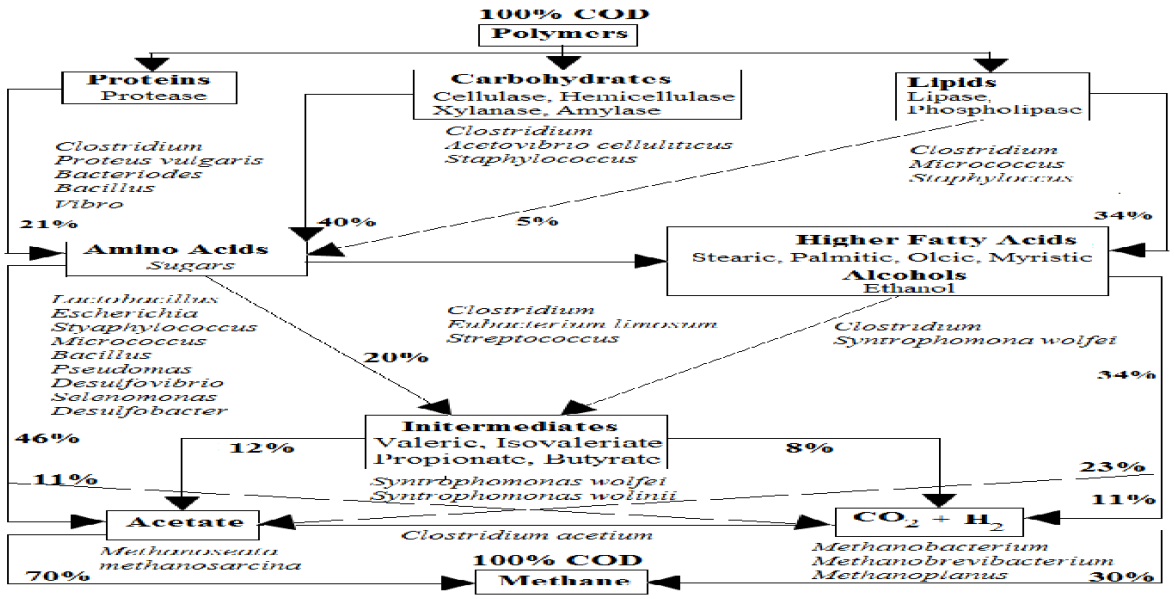


*Source: Mara and Horan (2003)*

*Figure 2:* Metabolic pathways and microbial groups in anaerobic digestion

This process requires little energy while the rest of the energy is stored as biogas and nutrient-rich sludge (Wagner *et al.*, 2009; Herrmann *et al.*, 2016). These stages (Figure 3) are described in the following sections under the sub-headings hydrolysis (section 4.4.1), acidogenesis (section 4.4.2) acetogenesis (section 4.4.3) and methanogenesis (section 4.4.4).


*Figure 3:* Stages in anaerobic digestion

### *4.4.1 Hydrolysis of Bio-Sourced Materials*

This stage initiates the biodegradation/ biodigestion process and it mainly a catabolic process. Complex biopolymer constituting starch, protein, fat and oil (21 % proteins, 40 % of carbohydrates, and 39 % of lipids) are digested by fermentative bacteria to monosugar, amino acid, peptides, etc. (monomers and oligomers). The complex biomaterials are insoluble and difficult to be digested by microbes (Vavilin *et al.*, 2008). The hydrolytic microbes have to secrete different types of enzymes, mostly extracellular enzymes, which break down the larger molecules (polymers) into simpler soluble components (monomers).

Carbohydrates are broken down into simple sugars such as monosaccharides and disaccharides by cellulase, cellobiase, xylanase and amylase. Hydrolytic anaerobe called protease degrades proteins into amino acids, while lipase split lipids into short chain fatty acids and glycerol (Saha and Cotta, 2007). This stage is usually the rate limiting stage for lignocellulosic materials.

### 4.4.2 Acidogenesis of Monomers

This is the second stage after hydrolysis considered to be the stage with fastest reaction rate (Saha and Cotta, 2007). This is attributed to the fact that many organisms are more active during this stage than during the other 3 stages.

The products from the previous (hydrolysis) stage which are soluble monomers are the substrate exploited by different microbes (acidogens). As the name implies, the acid formers microbes include: bacteriodes, bifidobacterium, clostridium, lactobacillus, and streptococcus. They thrive in acidic medium at optimum pH range of 5.5 and 6.5. The substrates are mainly converted into various short chain volatile organic acids (acetic, propionic, butyric, succinic, lactic acid etc.), alcohols (methanol and ethanol), ammonia (from amino acids), carbon dioxide, and hydrogen.

### 4.4.3 Acetogenesis of Acidogen Substrates

This is the third stage where the digested monomers and oligomers in hydrolysis become acetate or Hydrogen and Carbondioxide in the presence of fermentative bacteria. This stage intertwines the second and the fourth stages. The acetogens which are hydrogen producing and consuming anaerobes convert the substrates which are the products from the second stage (propionates and butyrates lactate and ethanol) to produce $H_2$, $CO_2$, and acetate. Acetate can also be formed from $CO_2$ and $H_2$.

### 4.4.4 Methanogenesis and the Production of Biogas

This is the last step of the anaerobic digestion process and perhaps the rate limiting stage. It is strictly anaerobic and methane forming step. It is dominated by microorganisms called methanogens (methanobacterium, methanococcus, methanosarcina, and methanosaeta). The products of acetogenesis stage (Hydrogen, Acetate, and $CO_2$) constitute the substrates exploited to produce biogas (mostly $CH_4$ and $CO_2$). However, there are three main pathways leading to methane production in this stage. These are: acetoclastic methanogenesis, hydrogenotrophic methanogenesis and homoacetogenesis (Ampomah-Benefo, 2018).

Most of the methane (above 60%) is formed by acetoclastic methanogens (methanosarcina and methoanosaeta), where methanosarcina utilize acetate, hydrogen, formate, methylamines and methanol to form $CH_4$, and methanosaeta exploits only acetate to form $CH_4$ (Conrad, 1999; Ferry, 2011). Hydrogenotrophic methanogenesis converts $H_2$ and $CO_2$ to produce $CH_4$ and $H_2O$, as homoacetogenesis converts the same reactants ($H_2$ and $CO_2$) to produce $CH_3COOH$ and $H_2O$. Ampomah-Benefo (2018) stated that due to the comparatively high Gibb's free energy of hydrogenotrophic pathway (-135 KJ mol-1), its forward reaction is thermodynamically more favorable than the homoacetogenic pathway (-104 KJ mol-1). It is crystal clear that the hydrogenotrophic pathway has a potential to keep the $H_2$ pressure low in the digester through its consumption. Table 4 shows the main methanogenic reactions pathways indicating some of the microorganisms exploited as well as their corresponding standard Gibb's free energies.

*Table 4:* Reactions pathways in methanogenesis

| Pathway | Reaction | Microorganism | $\Delta G^o$ at 25°C (KJ $mol^{-1}$) |
|---|---|---|---|
| Hydrogenotrophic methanogenesis | $4H_2 + CO_2 \rightarrow CH_4 + 2H_2O$ | Methanobacterium, Methanobrevibacter | -135.0 |
| Acetoclastic methanogenesis | $CH_3COOH \rightarrow CH_4 + CO_2$ | Methanosaeta, Methanosacina | -31.0 |
| Homoacetogenesis | $4H_2 + CO_2 \rightarrow CH_3COOH + 2H_2O$ | Clostridium acetium | -104.0 |

*Source: Ampomah-Benefo (2018)*

The maximum biogas yield can be evaluated through the digestion efficiency of the biomass. The theoretical evaluation of the maximum yield of methane when the elementary composition of bio-sourced feedstock is known can be determined using approximate Buswell's equation (Ampomah-Benefo, 2018) Equation 2.2 is the modified form of Buswell's equation, which is a stoichiometric equation of biogas production from bio-sourced feedstock.

$$C_nH_hO_oN_nS_s + yH_2O \longrightarrow xCH_4 + nNH_3 + sH_2S + (c - x)CO_2 \quad 2.2$$

Where $x = \frac{1}{8}(4c + h - 2o - 3n - 2s)$ and $y = \frac{1}{4}(4c - h - 2o + 3n + 3s)$

The evaluation requires stoichiometric reactions of the biomaterial constituents (carbohydrates, fats, and proteins). These are shown in Table 5.

*Table 5:* Stoichiometric reaction of biomass to produce biogas

| Substrate | Chemical reaction |
|---|---|
| Carbohydrates | $C_6H_{12}O_6 \longrightarrow 3CO_2 + 3CH_4$ |
| Fats | $C_{12}H_{24}O_6 + 3H_2O \longrightarrow \frac{9}{2}CO_2 + \frac{15}{2}CH_4$ |
| Proteins | $C_{13}H_{25}O_7N_3S + 6H_2O \longrightarrow \frac{13}{2}CO_2 + \frac{13}{2}CH_4 + 3NH_3 + H_2S$ |

*Source: Ampomah-Benefo (2018)*

The prospect and challenges of executing the technology in Nigeria are discussed next.

## V. THE PROSPECT AND CHALLENGES OF EXECUTING CONVERSION TECHNOLOGY IN NIGERIA

In this section, the challenges confronting its execution (section 5.1) are highlighted and the prospect of executing the technology is discussed (section 5.2).

### *5.1 Challenges of Executing Conversion Technology in Nigeria*

The conversion technology is not widespread in Nigeria despite its significance. This is attributed to:

1. *Lack of Technical Know-how*: Only limited number of skilled labor and specialists are available. Most Engineers are not well trained in the conversion technology and are not conversant with executing related projects. Skilled labors are required to operate and maintain renewable energy equipment. The absence of such ones especially in the rural areas is a major deterrent to the widespread adoption of the technology in Nigeria. Oyedepo *et al.* (2019) stated that remote areas with restricted access where on-hands maintenance is needed in terms of frequent visits by repair and maintenance staff is most affected. Consequently, failure to provide regular maintenance of the equipment when it is required leads to their complete breakdown, thereby defeating the purpose of the initial investment.
2. *Inadequate Fund:* Inadequate financial capacity to execute biomass conversion project is a serious barrier to the rapid uptake and development of renewable energy technologies in Nigeria. Access to loan facilities to execute these projects is unavailable. Government incentives are also inadequate. The cultivation of biofuel crops requires long-term loans and greater incentives. The NNPC sugarcane and cassava energy project can be replicated especially in the rural areas as the poverty level in these areas impedes farmers from getting loans, thus affecting their productivity.
3. *Lack of Awareness:* Generally, most Nigerians are not aware of the conversion technology. There is lack of awareness about what conversion technology options are available for exploitation and what benefits can be obtained from each of these options. This is the main issue, as the end users are ignorant of biomass potential for energy development.

This is attributed to improper means of information dissemination as people living in rural areas find it difficult to obtain relevant information on the technology.

### *5.2 The Prospect of Executing Conversion Technology in Nigeria*

The technology exploited for the conversion of biomass to energy has been practiced for decades in the developed countries. China, Brazil, USA, Japan and others have invested hugely and had successfully added the technology to their energy mix. Generally, biofuel is mainly used for household heating, cooking and lighting, as well as energy production for agricultural and industrial processes. However, Nigeria is yet to breakeven since 1982 when biogas research started (REMP, 2005). The prospect is great as the country is endowed with huge bio-sourced feedstock irrespective of its category (Edenseting *et al.*, 2020). The research activity has been slow but steady as such not strong enough to make the technology attain commercial status in the country (Oyedepo *et al.*, 2019).

There is a growing interest in harnessing bio-resources for biofuel production in Nigeria. Consequently, the country along with the United States was the third and fourth largest bioenergy producers with shares of over 80% and below 4% respectively (Oyedepo, 2012; Ben-Iwo *et al.*, 2016; Edenseting *et al.*, 2020). This motivated Clean Development Mechanism (CDM) of the Kyoto Protocol to persuade 15 rich countries to invest in developing green energy in Nigeria through the Nigerian National Petroleum Corporation (NNPC) renewable energy program (Automotive Biomass Programme). Germany through Germany's Renewable Energy, Energy Efficiency Partnership (REEEP) has responded with 70,000 Euros grants to NNPC (Nwokeji, 2007). In Nigeria, Energy crops have been the only bio-sourced feedstock dedicated to biofuel production (Ben-Iwo *et al.*, 2016). There are dedicated sugarcane commercial farm by Nigerian National Petroleum Corporation (NNPC) and other investors for Automotive Biofuel Program (Ibeto *et al*, 2011; NNPC, 2015). This is follow up with the construction of 10,000 units of mini refineries and 19 ethanol bio-refineries for the annual production of 2.66 billion liters of fuel grade ethanol (Ohimain, 2010; Ben-Iwo *et al.*, 2016). Table 6 summarized several emerging projects harnessing bio-sourced feedstock for biofuel production in Nigeria.

*Table 6:* Emerging biofuel projects in Nigeria

| Project | Cost | Location | Owners | Feedstock | Feedstock quantity (tonnes / year) | Project summary, ethanol production / year | Land take (ha) | Project phase |
|---|---|---|---|---|---|---|---|---|
| Automotive biofuel project | $306M | Agasha, Guma, Benue State | NNPC/private sector | Sugarcane | 1.8 million | 75 million litres, 116,810 metric tonnes (sugar), 59 MW (electricity) | 20,000 (16,000 will be cultivated) | Planning |
| Automotive biofuel project | $306M | Bukaru, Benue State | NNPC/private sector | Sugarcane | 1.8 million | 75 million litres, 116,810 metric tonnes (sugar), 59 MW (electricity) | 20,000 (16,000 will be cultivated) | Planning |
| Automotive biofuel project | $306M | Kupto, Gombe state | NNPC/private sector | Sugarcane | 1.8 million | 75 million litres, 116,810 metric tonnes (sugar), 59 MW (electricity) | 20,000 (16,000 will be cultivated) | Planning |
| Automotive biofuel project (Kwali Sugarcane ethanol project) | $80 - 100M | Abuja, FCT | NNPC/private sector | Sugarcane | 1.8 million | 120 million litres, 10–15 MW (electricity) | 26,374 estimated | Planning |
| Automotive biofuel project | $125M | Ebenebe, Anambra State | NNPC/private sector | Cassava | 3–4 million | 40–60 million litres | 15,000 | Planning |
| Automotive biofuel project | $125M | Okeluse, Ondo State | NNPC/private sector | Cassava | 3–4 million | 40–60 million litres | 15,000 | Planning |
| Ethanol refinery and Sorghum farm | $70M | Arigidi Akoko, Ondo State | Global biofuel Ltd. | Sweet sorghum | 1.05 million estimated | 84 million litres bio-refineries + farm estimated | 30,000 acquired | EPIC |
| Ethanol refinery and Sorghum farm | $92M | Illemso, Ekiti State | Global biofuel Ltd. | Sweet sorghum | 385,000 estimated | 30.8 million litres bio-refineries + farm estimated | 11,000 acquired | EPIC |
| Ethanig (via Starcrest Nigeria Energy) | $300M estimated | Kastina Ala/Benue River Basin of Benue State | Private | Sugarcane | 3.25 million estimated | 100 million litres, sugar, and electricity | 50,000 | Planning |
| Ethanig (via Starcrest Nigeria Energy) | $300M estimated | Kebbi State | Private | Sugarcane | 3.25 million estimated | 100 million litres, sugar, and electricity | 50,000 | Conception |
| Savannah sugar company | $167M | Numan, Adamawa State | Dangote Industries Ltd | Sugarcane | 1 million | Expansion to produce 100 million litres, 1 billion tonnes sugar, 100,000 metric tonnes fertilizer and 300 MW electricity | 36,000 (Lau, Taraba State) | Planning |
| Kwara Casplex Ltd. | $90M estimated | Kwara State | Private/government | Cassava | 300,000 estimated | 38.86 million litres | 15,000 | EPIC |
| Oke-Ayedun Cassava ethanol project | $18M | Oke-Ayedun, Ekiti State | Ekiti State Government/ Private | Cassava | 238,500 | 38.1 million litres bio-refinery + farm | 15,000 | EPIC |
| CrowNet Green Energy ethanol plant | $122M | Iyemero, Ekiti State | Ekiti State Government/ Private | Cassava | 150,000 | 65 million litres, (100 t of starch and 50 t $CO_2$/ day) | 12,500 | Operational (4 Sept. 2008) |
| Cassava ethanol plant | $115M | Taraba State | Taraba State | Cassava | 300,000 | 72 million litres, 360,000 t of cassava flour, 1.87 million tonnes $CO_2$ and 57 MGy of liquid fertilizer, 1600 MW electricity | 30,000 | EPIC |
| Niger State Government ethanol plant | $90M estimated | Niger State | Niger State | Cassava | 150,000 | 27 million litres, bio-refinery + farm estimated | 15,000 | EPIC |
| Cassava bioethanol project | $138M | Niger Delta region | NA | Cassava | 0.32 million estimated | 58 million litres/year bio-refinery + farm | 20,000 | Conception |
| Bioethanol from sugarcane/ molasses | $85M | Niger Delta region | NA | Sugarcane | 0.857 million estimated | 60 million litres | 67,692 estimated | Conception |
| Cassava industrialization project | $16.4M | Ogun State | Private + Government | Cassava | 75,000 | 3 million litres | 5000 | Conception |
| National Cassakero cooking fuel programme | $1B | 36 states + Abuja | Private | Cassava | 8 million | 1.44 billion litres | 400,000 | EPIC |

*Source: Ohimain (2010)*

Presently, about twenty biogas pilot projects are domiciled in the country (Akinbomi *et al.*, 2014). The prominent ones among them include: biogas plants at Zaria prison in Kaduna, Ojokoro in Lagos, Mayflower School Ikene in Ogun State and a biogas plant at Usman Danfodiyo University in Sokoto with capacity of the digesters ranges between 10 and 20 $m^3$ (Akinbomi *et al.*, 2014). Furthermore, with collaboration with UNDP's "Africa 2000 Low Technology Biogas System", the UNDP introduced to Yobe, Jigawa and Kano States the floating drum, plastic balloon and tube types of biogas digesters. Since 2003, Kwachiri community in Kano state depended on the UNDP biogas project (using cow dung) for their daily cooking needs (Oyedepo *et al.*, 2019). Similarly the UNDP introduced biogas technology at some market abattoirs in some Northern States. However, most of the pilot bioenergy programs have not been successful. It is hoped that more can be achieved as the low level development of the technology is not encouraging. With government interventions and support from non-governmental organization and other individual in the country, biogas plant can be constructed in all communities to generate energy thereby replacing generators thereby eliminating the energy, environmental and health challenges.

## VI. CONCLUSION

The potential of exploring biomass for energy development in Nigeria is huge. The effect is beyond achieving sustainable energy as a cleaner energy translates to a cleaner environment and sound health. The biomass conversion technology is cheap and the feedstock is readily available for exploitation at communal or individual level making it an attractive alternative to attain energy self-sufficiency. Consequently, rural to urban migration would be curtailed as individual community/household can exploit commonly found biomaterial to generate electricity making life more comfortable and positive impact to businesses.

The asthma and other related health challenges can be curtailed as the problem of generator noise and smoke would be fully addressed. This is true as country's hydrocarbon resources are state-owned as such no citizen is expected to harness it if even if the technology is cheap. The government does not have the political will to exploit these resources for energy development rather these resources are cheaply sold to other countries for immediate financial needs. Consequently, Nigerians have resorted to use of generators to meet their domestic and industrial energy needs. The impact of these generators on the environment in terms of noise and smoke contribute immensely on GHG emission.

Bioenergy has a major role as a source of dispatchable/portable energy and with high penetration of intermittent renewable commonly found in every household. The target of the project is to make the technology flexible and portable such that individual household or community can generate biogas and manage its effluent efficiently. This will ameliorate the problem of deforestation as it would be unreasonable to bypass these wastes generated within the community to cut trees in the forest for firewood. The time used to fetch firewood can be used for more profitable endeavor.

Generally, clean cooking using biogas eliminates smoke and inhalation of poisonous gases such as CO, NOx and Sox from incomplete combustion of firewood, diesel and poorly designed kerosene stoves thus eliminating health challenges associated with such fumes. In addition, age-long problem associated with open defecation, environmental pollution, contamination of water source, emission of odor would be eliminated as people will be conscious of transforming these wastes to wealth.

## REFERENCES


1. Abila, N. (2010) Biofuels adoption in Nigeria: a preliminary review of feedstock and fuel production potentials. *Manag Environ QualInt J*; 21:785–95.
2. Abila, N. (2012) Biofuels development and adoption in Nigeria: synthesis of drivers, incentives and enablers. *Energy Policy*; 43: 387–95.
3. Akinbomi, J., Brandberg, T., Sanni, S.A. and Taherzadeh, M.J. (2014) 'development and

dissemination strategies for accelerating biogas production in Nigeria', *BioResources*, Vol. 9, No. 3, pp.5707–5737.
4. Aliyu, A.S., Dada, J.O. and Adam, I.K. (2015) 'Current status and future prospects of renewable energy in Nigeria', *Renewable and Sustainable Energy Reviews*, Vol. 48, pp.336–346.
5. Amigun, B., Musango, J.K. and Stafford, W. (2011) 'Biofuels and sustainability in Africa', *Renewable and Sustainable Energy Reviews*, Vol. 15, pp.1360–1372.
6. Ampomah-Benefo, K., Boafo-Mensah, G., Animpong, M. A., Oduro, W. O., Kotey, E. N., Akufo-Kumi, K. and Laryea, G. N. (2013). Thermal Efficiency of Charcoal Fired Cook stoves in Ghana.*Global Advanced Research Journal of Engineering, Technology and Innovation, 2*(3), 102-110.
7. Ampomah-Benefo, Kofi (2018) A Prototype of an Adaptive, Multi-Feedstock, Anaerobic Biomass Digester for Biogas Production, PhD Thesis, University of Ghana, Legon.
8. Anowor, O.F., Achukwu, I.I. and Ezekwem, O.S. (2014) 'Sustainable sources of energy and the expected benefits to Nigerian economy', *International Journal of Sustainable Energy and Environmental Research*, Vol. 3, No. 2, pp.110–120
9. Arvanitoyannis, I. S., Kassaveti, A and Stefanatos, S. (2007) *Int. J. Food Sci. Tech.* 42 (7): 852 – 867.
10. Awofeso, Niyi (2016) Generator Diesel Exhaust: A major Hazard to Health and Environment in Nigeria: *Environ. Health Propect.* 115: 1160-1168.
11. Babatola, J. O. and Ojo, O. M. (2020) Dung-Aided Water Hyacinth Digestion Mixes: Association between Biogas Quality and Digester Temperature for Selected Animal *J. Appl. Sci. Environ. Manage.* Vol. 24 (6) 955-959.
12. Bamgboye, I. A. (2012). The potential of producing fuel from biomass in Nigeria In: Jekayinfa S. O. (Ed). Building a non-oil export based economy for Nigeria: the potential of value-added products from agricultural residues. *Cuvillier Verlag Gottingen*. pp. 35-41.
13. Bassey, P. G., Esu, C. O. and Obonukut, M. E. (2020) Simulation and Optimisation Study on Exploitation of Coal/Biomass (Rice Husk) Synergy for Production of Syngas. *Journal of Scientific and Engineering Research*. Vol. 7 Issue 10. pp. 77-89.
14. Ben-Iwo, Juliet, VasilijeManovic, and Philip Longhurst (2016)Biomass resources and biofuels potential for the production of transportation fuels in Nigeria.*Renewable and Sustainable Energy Reviews* 63; 172–192.
15. Bhat P.R., Chanakya H.N. and Ravindranath N.H. ( 2001) *J. Energy Sust. Dev.*, 1:39 – 41.
16. Bhattacharyya, S. C., and Palit, D. (2016). Mini-grid Based Off-grid Electrification to Enhance Electricity Access in Developing Countries: What Policies May be Required? *Energy Policy,* 94, 166-178.
17. Bolalumi, D. (2016). Preliminary Study of Pyrolysis and Gasification of Biomass and Thermosetting Resins for Energy Production. *Energy Procedia,* 101, 432 – 439.
18. Bruni, E., Jensen, A. P., Pedersen, E. S. and Angelidaki, I. (2010).Anaerobic Digestion of Maize Focusing on Variety, Harvest Time and Pretreatment *Applied Energy,* 87, 2212–2217.
19. Cheng, L-L, Lee, Y-H, Lin, J-H, Chou, M-S. (2010). Treatment of mixture of sewage and partially treated swine wastewater by a combination of UASB and constructed wetlands. Practice Periodical of Hazardous, Toxic, and Radioactive Waste Management, 14 (4), 234-239.
20. Dioha, I. J., Eboatu, A. N., Akpuaka M.U., Abdullahi .D. Arinze R.U. and Okoye P.A.C. (2005). Comparative studies of the Effects of Brands of cow dung and NPK fertilizers on the growth of okra plants. *Nigerian Journal of Solar Energy* 16: 15 – 18.
21. Duku, M., Gu, H., Hagan, S. and Ben, E. (2011) A comprehensive review of biomass resources and biofuels potential in Ghana. *Renew Sustain Energy Rev*; 15: 404–15.
22. Eboh, M. (2016) 'It is cheaper to import petrol than refine locally'- Kachikwu. Available at: http//: www.vanguardngr.com. Date accessed: 20th January 2020.
23. Ebrima, F. (2019) Nigerians spend 14billion USD on generators, fuel in Business News,

Stock market and Financial Literacy www.nairametrics.com accessed on 17/3/20 21.
24. Edenseting, B. O., Obonukut, M. E. and Oboh, I. O. (2020) Bio-Sourced Feedstocks for Biofuel Production: Nigeria as a Case Study. *bJournal of Scientific and Engineering Research*. Vol. 7 Issue 12 pp. 1-18.
25. Evans, G. M. and Furlong, J. C. (2003). *Environmental Biotechnology: Theory and Application*. Chichester: Johy Wiley and Sons.
26. Galadima A., Garba, Z. N., Ibrahim, B. M., Almustapha, M. N., Leke, L. and Adam, I. K. (2011) Biofuels production in Nigeria: the policy and public opinions. *J Sustain Dev*;4: 22–31
27. Gelegenis, J., Georgakakis, D., Angelidaki, I. and Mavris, V. (2007).Optimization of Biogas Production by Co-digesting Whey with Diluted Poultry Manure. *Renewable Energy,* 32, 2147 –2160.
28. Giwa, A., Alabi, A., Yusuf, A. and Olukan, T. (2017) 'A comprehensive review on biomass and solar energy for sustainable energy generation in Nigeria', *Renewable and Sustainable Energy Reviews*, Vol. 69, pp.620 –641.
29. Grassian, V. (2005).*Environmental Catalysis*. New York: Taylor and Francis.
30. Haiwen, S., Lin, D., Jing, S., Xin, J., Zhiyong, R. and Haiyang, Y. (2015).Field Measurement and Energy Efficiency Enhancement Potential of a Sea Watera Source Heat Pump District Heating System. *Energy and Buildings,* 105, 352-357.
31. Herrmann, C., Idler, C. and Heiermann, M. (2016). Biogas Crops Grown in Energy Crop Rotations: Linking Chemical Composition and Methane Production Characteristics. *Bio-resource Technology,* 206, 23-35.
32. Ibeto, C. N., Ofoefule, A. U., Uzoma, , C. C. and Oparaku, O. U. (2011) Biomass technology: A key driver for improving climate change and socio-economic life in Nigeria. *Int. J. Environ. Sci.* 5:54-58.
33. Koh, L. P. and Ghazoul, J. (2008) Biofuels, biodiversity, and people: understanding the conflicts and finding opportunities. *Biol Conserv*. 141:2450–60.
34. Komilis, D., Kissas, K., &Symeonidis, A. (2014). Effect of Organic Matter and Moisture on the Calorific Value of Solid Wastes: An Update of the Tanner Diagram. *Waste Management,* 34, 249–255.
35. Kosmo, M. (1989) Commercial Energy Subsidies in Developing Countries. *Energy Policy,* 17(3).
36. Krich, K. (2005) *Biomethane from Dairy Waste A Sourcebook for the Production and Use of Renewable Natural Gas in California* Singapore: Prentice Hall.
37. Linnhoff, B. and Dhole, V. R. (1992) Targeting for $CO_2$ emissions for Total Sites, *Chemical Engineering & Technology*, vol. 16, No.4: p. 252-259.
38. Manlay R. (2000) Organic matter dynamics in mixed-farming systems of the West African savanna: A village case study from south Senegal. In *Ecole Nationale du Genie Rural, des Eaux et Forets Centre de Montpellier,* vol Doctorat. Montpellier.
39. Mara, D. and Horan, N. (2003). *The Handbook of Water and Wastewater Microbiology*. London: Academic Press.
40. Mata-Alvarez, J., Dosta, J., Romero-Güiza, M. S., Fonoll, X., Peces, M. and Astals, S. (2014). Renewable and Sustainable Energy Reviews. A critical review on anaerobic co-digestion achievements between 2010 and 2013, *Energy J*. 36, 412-427.
41. McKendry, P. (2002). Energy Production from Biomass (part 1): Overview of Biomass. *Bioresource Technology,* 83, 37–46.
42. Mitchell, D. (2008) A note on rising food prices. World Bank Policy Research Working Paper Series.
43. Mohammed, Y. S, Mustafa, M. W., Bashir, N. and Mokhtar, S. (2013). Renewable energy resources for distributed power generation in Nigeria: A review of the potential. *Renew Sustain Energy Rev* 22:257–68.
44. Mohan, D., Pittman, C. U. and Steele, P. H. (2006). Pyrolysis of Wood/Biomass for Bio-oil: A Critical Review. *Energy & Fuels,* 20, 848-889.
45. Ndiaye, M. L., Niang, S., Pfeifer, H. R., Peduzzi, R., Tonolla, and M. and Dieng, Y. (2010) Effect of irrigation water and

processing on the microbial quality of lettuces produced and sold on markets in Dakar (Senegal). In: Sons JW, ed. *Irrigation and Drainage*, vol Wiley Online Library.
46. NNPC (2015) Refineries and Petrochemicals. Nigerian National Petroleum Corporation www.nnpcgroup.com/NNPCBusiness/MidstreamVentures/RefineriesPetrochemicals. Date accessed 21.06.2020.
47. Nwokeji, G. U. (2007). The Nigerian National Petroleum Corporation and the development of the Nigerian oil and gas industry: history, strategies and current directions. Houston: James A. Baker III Institute for Public Policy Rice University.
48. Obonukut, M. E., Alabi, S.B. and Bassey, P.G. (2016) Steam Reforming of Natural Gas: Value Addition to Natural Gas Utilization in Nigeria. *Journal of Chemistry and Chemical Engineering*. Volume 10, No. 1 pp. 28 - 41.
49. Ofoefule, A. U. and Uzodinma, E. O. (2009) *Int. J. Phy Sci.* 4 (7): 398-402.
50. Ohimain E. I. (2010) Emerging bio-ethanol projects in Nigeria: their opportunities and challenges. *Energy Policy*; 38:7161–8.
51. Oyedepo, S. O., Dunmade, I. S., Adekeye, T., Attabo, A., Olawole, O., Babalola, P. O., Oyebanji, J. A., Udo, M., Kilanko, O. and Leramo, R. (2019) Bioenergy technology development in Nigeria –pathway to sustainable energy development. *Int. J. Environment and Sustainable Development,* Vol. 18, No. 2.
52. Oyedepo, S.O. (2012) 'On energy for sustainable development in Nigeria', *Renewable Sustainable Energy Review*, Vol. 16, pp.2583–2598.
53. Ozoegwu, C.G., Ezeb, C., Onwosi, C.O., Mgbemene, C.A. and Ozor, P.A. (2017) 'Biomass and bioenergy potential of cassava waste in Nigeria: estimations based partly on rural-level garri processing case studies', *Renewable and Sustainable Energy Reviews*, Vol. 72, pp.625–638.
54. Patel, V. R. (2017). Cost-effective Sequential Biogas and Bioethanol Production from the Cotton Stem Wastes. *Process Safety and Environmental Protection,* 111, 335-345.
55. Pisutpaisal, N., Nathoa, C. and Sirisukpoca, U. (2014) Production of Hydrogen and Methane from Banana Peel by Two-Phase Anaerobic Fermentation. *Energy Procedia,* 50, 702 – 710.
56. Saha, B. C. and Cotta, M. C. (2007). Enzymatic Hydrolysis and Fermentation of Lime Pretreated Wheat Straw to Ethanol. *Journal of Chemical Technology and Biotechnology,* 82, 913-919.
57. Sambo, A. S. (2006). Renewable energy electricity in Nigeria: The way forward. Paper presented at the Renewable Electricity Policy Conference held at Shehu Musa Yarádua Centre, Abuja. pp. 11-12.
58. Sorensen, B. (2004). *Renewable Energy, its Physics, Engineering, use, Environmental Impact, Economy and Planning Aspects*. Elsevier Science.
59. Suh, Y. J. and Roussaux, P. (2002). An LCA of alternative wastewater sludge treatment scenarios", Resources, Conservation and Recycling, Vol. 35, pp. 191-200.
60. Teng, Z., Hua, J., Wang, C. Lu, X. (2014). *Design and optimization principles of biogas reactors in large scale applications*. 4th edition Singapore: MCGraw Hill.
61. Udo, Bassey (2020) Three refineries lost N1.6 trillion in 5 years. Premium Times June 17 2020.
62. Ullah, K., Sharma, V. K., Dhingra, S. and Braccio, G. (2015). Assessing the ligno-cellulosic biomass resources potential in developing countries: A critical review. *Renewable and Sustainable Energy Reviews,* 51, 682–698.
63. Vavilin, V. A., Fernandez, B., Palatsi, J. and Flotats, X. (2008). Hydrolysis Kinetics in Anaerobic Degradation of Particulate Organic Material: An Overview. *Waste Management,* 28, 939–951.
64. Vivekanandan, S. and Suresh, R (2017) Two Stage Anaerobic Digestion Over Single Stage on Biogas Yields from Edible and Non-Edible De-Oiled Cakes Under the Effect of Single and Co-Digestion System. *International Journal of Civil Engineering and Technology,* 8(3), 2017, pp. 565–574.

65. Wagner, A. O., Malin, C., Gstraunthaler, G. and Illmer, P. (2009). Survival of Selected Pathogens in Diluted Sludge of a Thermophilic Waste Treatment Plant and in NaCl-solution under Aerobic and Anaerobic Conditions. *Waste Management,* 29, 425–429.
66. Wang, S., Dai, G., Yang, H. and Luo, Z. (2017).Lignocellulosic Biomass Pyrolysis Mechanism: A State-of-the-Art Review. *Progress in Energy and Combustion Science,* 62, 33-86.
67. Wjst, M. and Boakye, D. (2007) Asthma in Africa. *PLoS Med* 4:e72.
68. Zhang, J. (2017) Three-Stage Anaerobic Digester for Food Waste. *Applied Energy*, vol. 194, pp. 287–295.
69. Zhu, B., Zhang, R., Gikas, P., Rapport, J., Jenkins, B. and Li, X. (2010). Biogas Production from Municipal Solid Wastes Using an Integrated Rotary Drum and Anaerobic-Phased Solids Digester System. *Bio - resource Technology,* 101, 6374–6380.

*This page is intentionally left blank*

# Simulation and Optimization of a Natural Gas Dehydration Plant with Triethylene Glycol

*Perpetua Bassey, Godslove Johnson & Minister Obonukut*

*University of Uyo*

## ABSTRACT

Dehydration of Natural Gas has been a subject of interest for decades due to the effect of wet gas on the system. Specifically, the gas' heating value and its flow assurance are challenged coupled with not meeting markets' specification. Besides these flow assurance and related issues, the hydrate in the gas quickly deactivate catalyst and burn less. This study attempts to economically dehydrate the gas using Triethylene Glycol (TEG) which has to be optimally regenerated and used for further dehydration process. The simulation and optimization of the dehydration process through absorption with TEG was carried out using Aspen HYSYS software and Design-Expert software respectively. The simulation was carried out using Glycol and Peng-Robinson as the thermodynamic fluid package. Effects of parameters such as TEG circulation rate, equilibrium stages of absorption column, operating conditions on the process efficiency were investigated. It was found that, lowering the pressure in the absorption column reduces the amount of hydrocarbons trapped in the wet TEG stream leaving the bottom of the absorber. The optimization of the Recycled TEG was carried out using the numerical optimization of the Design-Expert software, the experimental design was based on the Central Composite Design of the Response Surface Methodology of Design-Expert version 10, this optimization yield a relative increase in TEG recycled stream from 99.59 mole% to 99.89 mole% at an optimum operating parameters of 250C, 6320 kpa and 1883 kgmole/h of the wet gas stream.

*Keywords:* natural gas, dehydration, triethylene glycol, absorber, regenerator.

*Classification:* DDC Code: 665.7 LCC Code: TN884

*Language:* English

London Journals Press

LJP Copyright ID: 392974
Print ISSN: 2631-8474
Online ISSN: 2631-8482

London Journal of Engineering Research

Volume 22 | Issue 1 | Compilation 1.0

# Simulation and Optimization of a Natural Gas Dehydration Plant with Triethylene Glycol

Perpetua Bassey[α], Godslove Johnson[σ] & Minister Obonukut[ρ]

## ABSTRACT

*Dehydration of Natural Gas has been a subject of interest for decades due to the effect of wet gas on the system. Specifically, the gas' heating value and its flow assurance are challenged coupled with not meeting markets' specification. Besides these flow assurance and related issues, the hydrate in the gas quickly deactivate catalyst and burn less. This study attempts to economically dehydrate the gas using Triethylene Glycol (TEG) which has to be optimally regenerated and used for further dehydration process. The simulation and optimization of the dehydration process through absorption with TEG was carried out using Aspen HYSYS software and Design-Expert software respectively. The simulation was carried out using Glycol and Peng-Robinson as the thermodynamic fluid package. Effects of parameters such as TEG circulation rate, equilibrium stages of absorption column, operating conditions on the process efficiency were investigated. It was found that, lowering the pressure in the absorption column reduces the amount of hydrocarbons trapped in the wet TEG stream leaving the bottom of the absorber. The optimization of the Recycled TEG was carried out using the numerical optimization of the Design-Expert software, the experimental design was based on the Central Composite Design of the Response Surface Methodology of Design-Expert version 10, this optimization yield a relative increase in TEG recycled stream from 99.59 mole% to 99.89 mole% at an optimum operating parameters of 25°C, 6320 kpa and 1883 kgmole/h of the wet gas stream.*

*Keywords:* natural gas, dehydration, tri- ethylene glycol, absorber, regenerator.

*Author α σ ρ:* Department of Chemical and Petroleum Engineering, University of Uyo, Nigeria.

## I. INTRODUCTION

Natural gas provides a great portion of the world growing energy need and the situation is likely to remain so for the next few decades (Appah, 2014). In terms of energy, natural gas consumption represents more than half of the total petroleum consumed and may likely double as natural gas reserved are being discovered at twice the rate of petroleum (Gray *et al.,* 1990; Partho and Ruhul, 2011; Ahmed *et al.,* 2019). This trend indicates the increasingly important role that gas will play in the future world energy (Obonukut *et al.,* 2016). As oil shortage looms in the future, it becomes a concern for scientists and engineers to use natural gas as an alternative source of energy (Patel *et al.,* 2005). This is the way to go as gas reserves with the increasing trend in gas than crude oil and it is anticipated that this trend will extend well into the 21st century (Holmen, 2009; Ahmed *et al.,* 2019).

Over the years, large quantities of natural gas are located in remote areas (isolated from centers of commerce and dense population), where no distribution network exists for its transportation. Transportation cost of remote natural gas is relatively the expensive part of the final delivered price and it is serious as most of the world natural gas reserves are in remote locations (Saeid *et al.*, 2006). In these regions, pipelines are not economical to bring natural gas to the market. Consequently, most natural gas is consumed in the country where it is produced. In some cases, natural gas associated with crude oil is often flared for convenience (Obonukut *et al.*, 2016). The gas needs to be converted to liquid fuels in order to make it easier for transportation to market.

Specifically, Liquefied natural gas (LNG) terminals and vessels can bring remote gas to market. Compressed natural gas (CNG) can be transported from short remote distances using tankers with pressurized containers/vessels. Alternatively, depending on the economic conditions, on-land and subsea pipelines can be constructed to transport the remote gas. However, gas interaction with the aggressive substances within the reservoir influences not only its flow integrity but also its property adversely.

The natural gas, produced from underground reservoir, contains huge quantity of light hydrocarbon mainly methane together with ethane, propane and butane. However, traces of the heavy hydrocarbon compounds (pentane and hexane) and non-hydrocarbon compounds such as: water, nitrogen and hydrogen sulphide are equally found in the gas (Siti and Abdul, 2012; Mokhatab *et al.*, 2014). Consequently, natural gas must be treated to enrich its light hydrocarbon content. This could be achieved by dehydration (where water vapour is removed) and separation of the heavy hydrocarbon components (Kong *et al.*, 2018; Shoaib *et al.*, 2018). The water content in natural gas is a big problem in the oil and gas industry as it can accelerates corrosion in the gas pipe lines and as well reduces the heating value of the natural gas.

The flow integrity of wet gas is challenged as its water content especially at subsea condition becomes 'hydrate' leading to slugging flow conditions thus lowering flow efficiency of the pipelines (Akpabio *et al.,* 2021). Downstream processing of this gas especially in chemical processes involving catalyst would create undesired side reactions, foaming or catalyst deactivation (Obonukut *et al.,* 2016). Therefore, to prevent such problems, natural gas treatment is inevitable. The water in the natural gas contains dissolved aggressive compounds including mineral/inorganic salts (Stewart and Arnold, K. (2011). Thus removing water from the gas implies eliminating these aggressive compounds.

An overview of the gas production activities as well as its formation is necessary. Different offshore processes need to be applied for the gas dehydration, avoiding subsequent problems caused by the wet gas such as corrosion or gas hydrate formation. During offshore oil production, the reservoir fluid coming from the well is typically a mixture of three distinct phases: an aqueous phase (produced water), a liquid hydrocarbon phase (crude oil) and a gas phase with some suspended solids in the mixture. Normally, the three phases must be separated and then further processed in the topside facilities, before being discharged or exported to onshore (Figure 1.1).

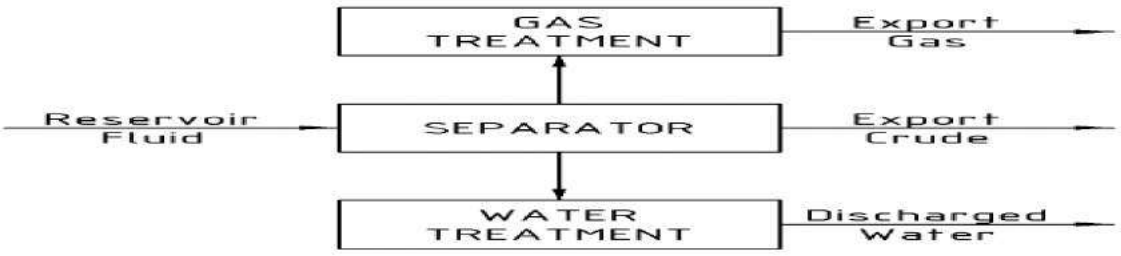


*Figure 1.1:* Overview of upstream processes in the oil and gas industry

The separation of the three phases is carried out in 3-phase separators. These vessels slow down the reservoir fluid by reducing its momentum. Then, the phases are separated by means of gravitational force. There are normally three separators on offshore facilities, the first being high pressure, the last being low pressure and the pressure of the middle separator is in between. This arrangement serves to stabilize the crude oil by removing volatile components. The produced water is treated in water treatment facilities. The objective is to remove the dispersed hydrocarbons from the water to meet environmental regulations for the produced water discharge quality. The

water purification facilities mostly consist of hydrocyclones and skimmers.

The produced gas must be recompressed and exported to onshore facilities. The high-pressure (9 - 14 MPa) pipelines (Bothamley, 2004) used for exporting, lay on the seabed where the fluid can cool down to as low as -1°C (Skjoldal, 2007). At this low temperature and high pressure, if there is water in the gas phase it may form solid crystalline hydrates with the light hydrocarbons. The hydrates can cause severe damage to the pipelines. The gas phase in the reservoir fluid is saturated with water because it was previously in contact with the brine and other aggressive substances. Therefore, one of the purposes of the gas treatment is the removal of water from the gas (dehydration).

Dehydration is the main operation employed in the industry to remove the contaminated moisture from the natural gas (Mokhatab *et al,* 2019). This is necessary for hydrocarbon dew point control which is to maintain the water content specification, prevent corrosion, separate the heavy hydrocarbons, prevent the formation of hydrate, avoid side reactions, prevent catalyst deactivation and eliminate condensation of the water and heavy hydrocarbon in the gas transport pipeline (Bahadori, 2014; Abdulla, 2015). There are several ways of removing the water content of the raw natural gas (Rahimpour *et al.*, 2013), one is preferred over the other based on factors such as the composition of the wet natural gas, the condition of the wet natural gas, the operating cost and how effective it is in removing the water content from the wet natural gas, one of such is dehydration of the raw natural gas using the absorption process with glycol as the absorbent.

Industrially, three methods of dehydration are usually adopted, these are: adsorption, absorption by using glycol solvent and condensation by raising the dew point temperature of the hydrocarbon and the water (Netusil and Ditl, 2011). However, there are supersonic method and membrane method for the natural gas dehydration process (Pezman and Roya, 2011). The aim of this paper was to optimize natural gas dehydration process using triethylene glycol (TEG) as the absorbent. This involved simulation of Natural gas dehydration process using Aspen HYSYS. Industry data available in this direction was generously exploited to investigate the effect of operating parameters on the efficiency of the process. Design Expert was used to optimize the solvent regeneration of gas dehydration plant (Luyben, 2011). Thus, optimizing the regeneration of TEG is economical as fewer quantity of the solvent (TEG) and eventually maximize the profitability of natural gas dehydration (Chebbi *et al.*, 2019).

## II. MATERIALS AND METHODS

In this study, dehydration process of a typical natural gas from one of the Niger Delta oil field is presented. The plant as simulated using one of the popular commercial software in the oil and gas industry (Aspen HYSYS) explores the real industrial experience of the researcher while in the field.

### *2.1 Simulation of Natural Gas Dehydration Plant*

Basically, a natural gas dehydration plant is divided into two sections. These are mainly the Absorbing/Contacting section where the hydrated gas is contacted with TEG to have a dry gas and the Regeneration/Stripping section where the TEG is recovered and recycled for further absorption operation. Specifically, Triethylene Glycol (TEG) based dehydration process as depicted in absorption unit and the extraction of the solvent (TEG) as presented in regeneration unit singled out the necessary equipment required to model the plant. The gas used is a partially treated natural gas which has bad compositions such as acid gas, mercury and heavy hydrocarbons removed (Sanggyu *et al.*, 2011) as well as its process condition as shown in Table 2.1 and 2.2 respectively.

*Table 2.1:* Wet Natural Gas Composition

| Composition | Mole Fraction |
|---|---|
| Methane | 0.8565 |
| Ethane | 0.0614 |
| Propane | 0.0494 |
| i-Butane | 0.0100 |
| n-Butane | 0.0095 |
| i-Pentane | 0.0083 |
| n-Pentane | 0.0040 |
| Water | 0.0010 |

*(Source: Afaiko, 2014)*

*Table 2.2:* Condition of the Wet Gas

| Property | Value |
|---|---|
| Inlet Pressure | 7201Kpa |
| Inlet Temperature | 25°C |
| Flow Rate | 1883Kgmole/hr |

*(Source: Afaiko, 2014)*

A combined fluid package (Glycol and Peng-Robinson) was used for the HYSYS simulation as it is commonly used for hydrocarbon systems applications and studies (Elliot and Lira, 1999). It is specifically used for gas phase components that handle the complex thermodynamics that occur during compression, and is useful in both upstream and downstream industries.

The simulation on HYSYS commences with passing wet gas to the flash tank (Separator) at 7201 kpa where some of the water in the mixture is separated. The gas is then fed to the absorber (contactor) through the bottom. The absorber was operated with 9 stages for higher purity (Pezman and Roya, 2011; Affandy *et al.,* 2020). The mixed TEG (fresh and recycled TEG) inlet and Dry gas outlet are located at the top of the column while the TEG outlet (Rich TEG) and Natural gas with hydrate (Hydrated gas) inlet are located at the bottom of the column Figure 2.1.

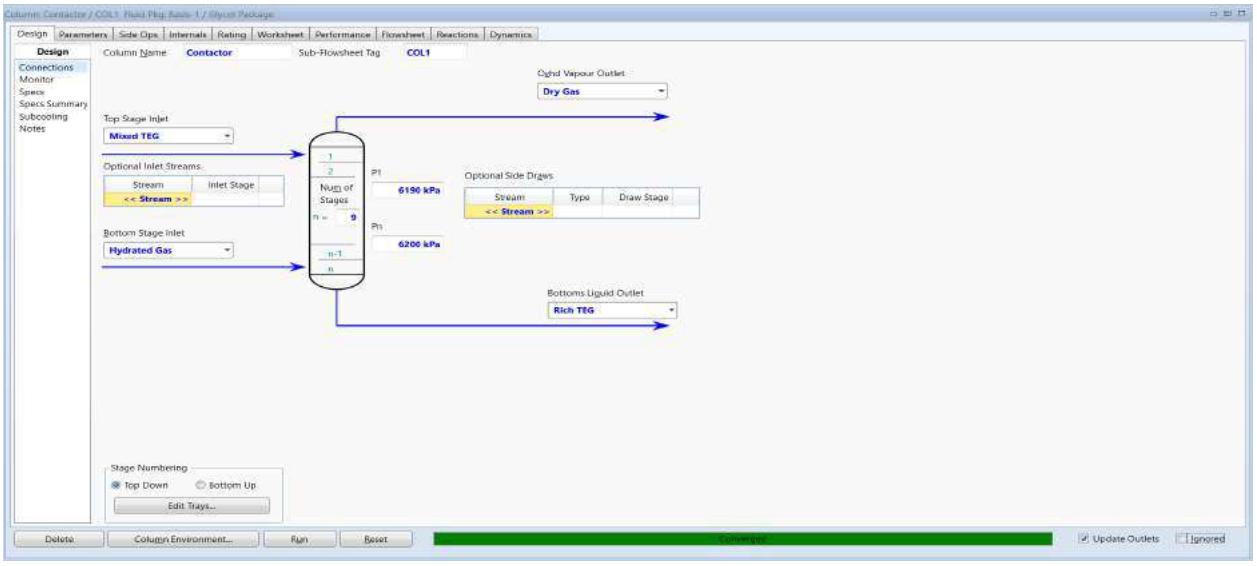


*Figure 3.1:* The Contactor control screen on HYSYS

The TEG flow is dependent on the water (hydrate) content in the hydrated gas. Rich TEG leaves the bottom by level control and is depressurized by a valve. The rich stream flows through a cartridge filter to remove solid particles coming from corrosion or TEG degradation (Affandy *et al.*, 2017). However, solid particles and degradation are not taken into account in this model. Hence, it is not represented in the simulated plant. Consequently the filtration does not have serious impact on the process. Once filtered, the depressurized TEG stream is subjected to heat exchange with the hot regenerator bottom product (lean TEG) coming out of the TEG regenerator at the Rich/Lean TEG Exchanger before it then becomes feed for the regenerator. The Regenerator is used to strip water from the lean TEG (Figure 2.2).

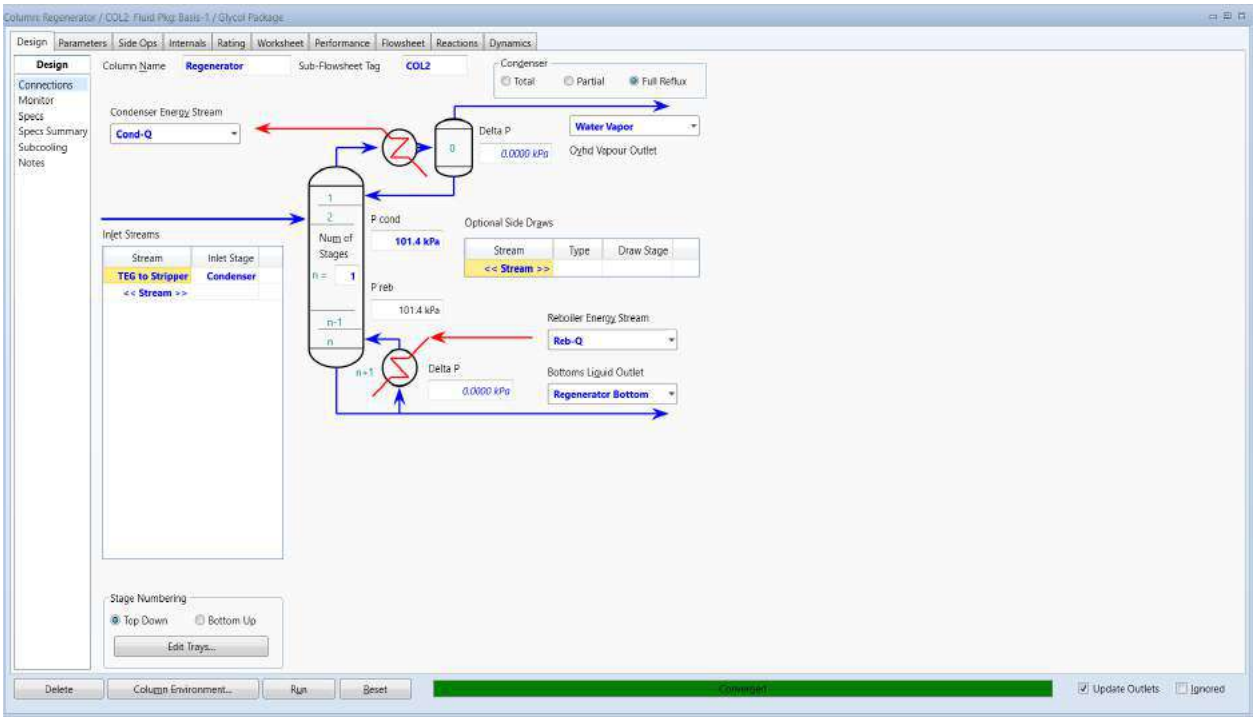


*Figure 2.2:* The Regenerator control screen on HYSYS

The temperatures given for the reboiler and condenser are 205°C and 102°C respectively. After leaving the regenerator, the lean TEG is once again cooled and stored in a surge drum. At this point there will also be some kind of TEG makeup system to replace the TEG lost to the gas phases in the dehydration plant before it is finally recycled to the start point. Figure 2.3 shows the composition of the rich glycol stream leaving the absorber.

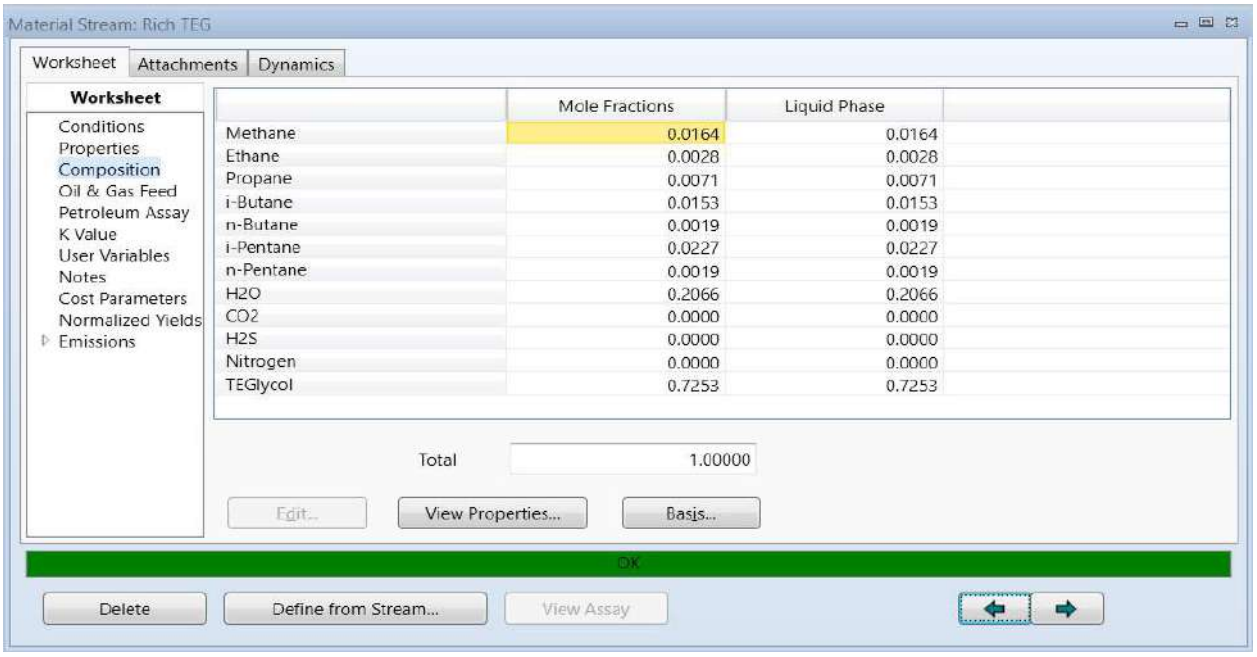


*Figure 2.3:* Composition of Rich TEG control screen on HYSYS

The Process achieved high water removal and is reflected in zero water composition in the natural gas outlet stream (Sale Gas) shown in Figure 2.4.

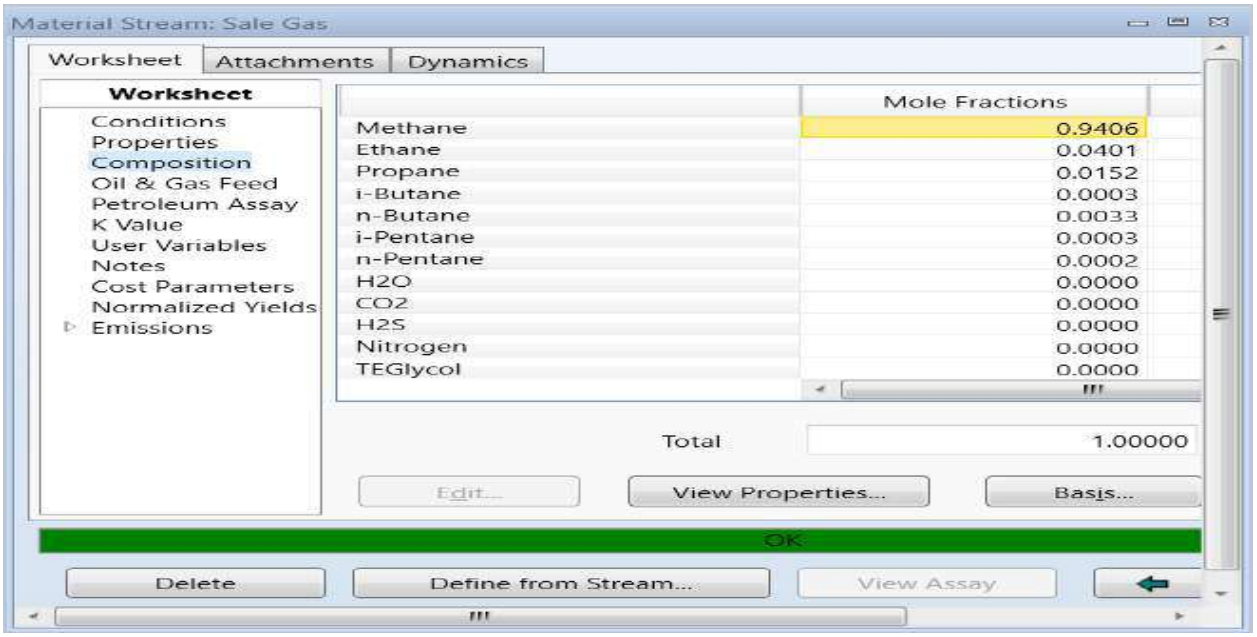


*Figure 2.4:* Composition of the Dehydrated (Sale Gas) control screen on HYSYS

Waste gases consisting of water and the hydrocarbons dissolved in the TEG leave the regenerator at the top. The lean TEG then enters a Surge drum in which gaseous hydrocarbons that were absorbed along with the water in the separator is vaporized as flash out. The Lean TEG is then cooled, pumped (Glycol Circulation Pump) and recycled back to the contactor as it mixes with fresh lean TEG in a mixer (TEG Mixer) and fed to the contactor. Figure 2.5 shows Process Flow Diagram (PFD) of the HYSYS simulation of the Natural gas Dehydration process.

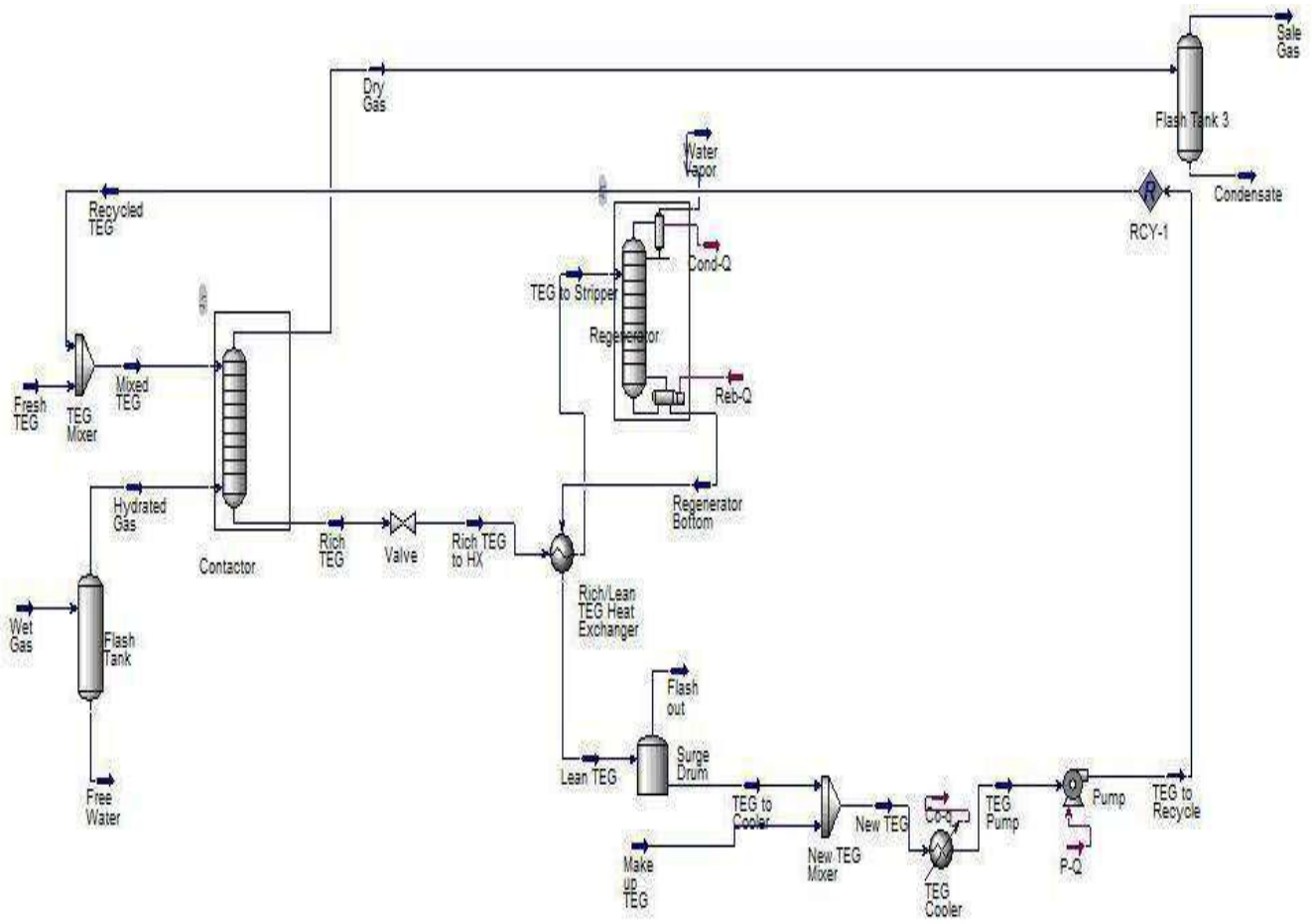


*Figure 2.5:* Process Flow Diagram of Natural Gas Dehydration Plant in Aspen HYSYS

### *2.2 Optimization of the Natural Gas Dehydration Plant*

Optimization of the natural gas dehydration plant was carried out using Design Expert version. 10 to maximize the yield of recycled TEG that will be used for further dehydration process. The Response Surface methodology (RSM) using the Central Composite Design (CCD) of design expert was adopted for the optimization process, the process variables of the wet natural gas stream were used to evaluate the optimum operating condition at which maximum recycled TEG yield could be achieved. By using design expert version 10, low and high values of the process variables (temperature, pressure and flow rate) were specified and the response set to be Recycled TEG. A total of 15 runs were generated from the specified low and high values of the process variables to generated different ranges of the process variables at which one should give the maximum yield of the regenerated TEG. This generated process variables were then taken to Aspen HYSYS to simulate the dehydration plant, the values of Recycled TEG using the new process variables were used as response variable to analyze the maximum Recycled TEG yield using Design Expert numerical optimization method.

## III. RESULTS AND DISCUSSION

### *3.1 Effects of Process Parameters on Natural Gas Dehydration Plant*

In the quest to maximize the absorption efficiency of TEG in the contactor, the impacts of the key parameters were evaluated using the simulation model presented in this study. These parameters were:

i. The number of contactor theoretical trays
ii. TEG circulation rate
iii. Temperature of the reboiler in the regenerator

It was found that lowering the pressure in the absorption column reduces the amount of hydrocarbons trapped in the wet TEG stream

leaving the bottom of the absorber. The Wet TEG stream also has a low pressure and thus the valve is no more needed. Figure 3.1 shows the composition of the Rich TEG.

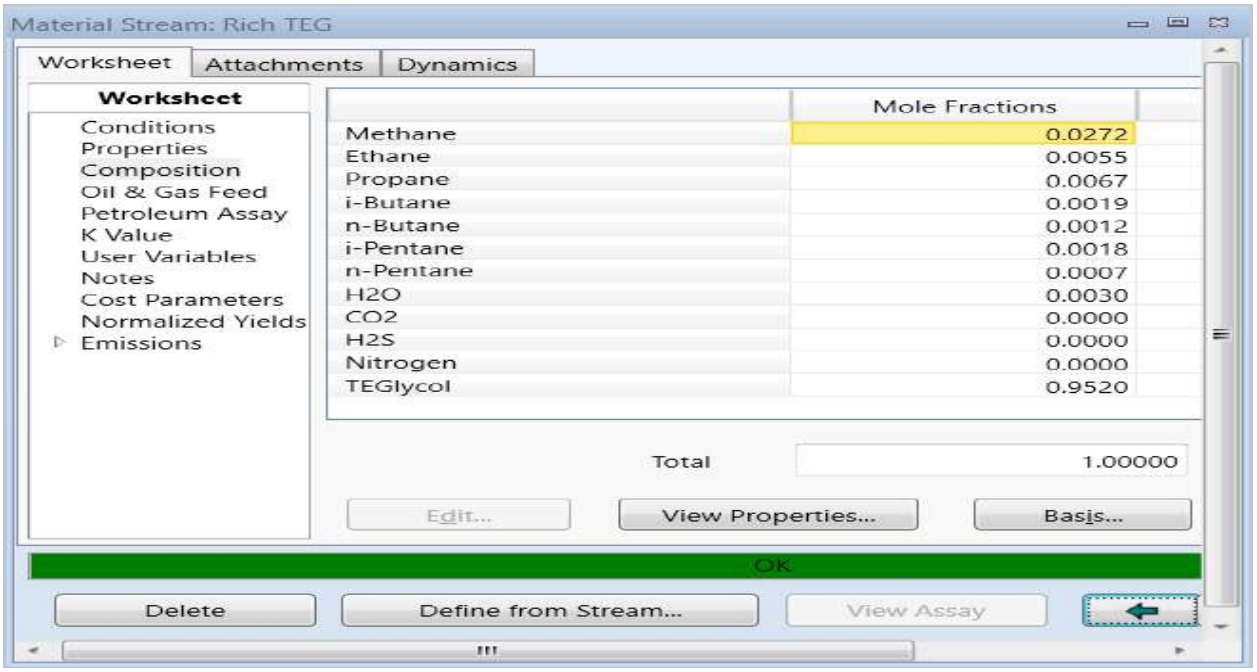


*Figure 3.1:* Composition of the Rich TEG stream after simulation in HYSYS

However, other parameters may have also a limited impact. It was also observed that increasing the number of trays in the regenerator has no effect on the outlet stream composition. It was observed that increasing the flowrate of the TEG above the minimum requirement is not necessary as maximum separation has already been achieved. TEG is known to decompose at a temperature of 206°C which is far lower than its boiling point of 284°C and this limits the temperature of the TEG regenerator reboiler (Kamin *et al.,* 2017; Neagu and Cursaru, 2017).

### *3.2 Optimization of TEG Regeneration of the Natural Gas Dehydration Plant*

The optimization of TEG regeneration of the natural gas dehydration plant was carried out using Design Expert ver. 10 so as to recover maximum TEG for further dehydration process. This section discusses the Analysis using Response Surface Methodology based on Central Composite Design Model (section 3.2.1), Anova for Response Surface Reduced Quadratic Model (section 3.2.2).

#### *3.2.1 Analysis using Response Surface Methodology (RSM)*

After performing the dehydration plant simulation, it was found that recycled TEG yield depends on different parameters of the natural gas dehydration process. So, by controlling these parameters, optimum recycled TEG yield was obtained. Response Surface Methodology (RSM) based on Central Composite Design (CCD) was used to monitor the yield of Recycled TEG with response to the process variables. The variables and their corresponding coded values for the process are analyzed (Table 3.1) and the Response parameter (Table 3.2) as follows:

*Table 3.1:* Process variables and their corresponding coded values

| Factor | Name | Units | Type | Subtype | Minimum | Maximum | Coded | Values | Mean | Std. Dev. |
|---|---|---|---|---|---|---|---|---|---|---|
| A | Temperature | oC | Numeric | Continuous | 20.0522 | 53.8378 | -1.000=25 | 1.000=48.89 | 36.945 | 9.02957 |
| B | Pressure | kPa | Numeric | Continuous | 6137.54 | 7383.46 | -1.000=6320 | 1.000=7201 | 6760.5 | 332.987 |
| C | Flow rate | kgmole/h | Numeric | Continuous | 92.1477 | 12320.9 | -1.000=1883 | 1.000=10530 | 6206.5 | 3268.26 |

*Table 3.2:* Response parameter

| Response | Name | Units | Obs | Analysis | Minimum | Maximum | Mean | Std. Dev. | Ratio | Trans | Model |
|---|---|---|---|---|---|---|---|---|---|---|---|
| R1 | Recycled TEG | mole | 15 | Polynomial | 0.9984 | 0.9989 | 0.998593 | 0.000109978 | 1.0005 | None | RQuadratic |

The experimental design using the central composite design consisted of a total of 15 base runs, comprising of 3 factorial points, and 1 response point, Table 3.3 shows the experimental design of TEG regeneration optimization.

*Table 3.3:* Experimental design of TEG regeneration optimization

| | | Factor 1 | Factor 2 | Factor 3 | Response 1 |
|---|---|---|---|---|---|
| Std | Run | A: Temperature | B: Pressure | C: Flow rate | Recycled TEG |
| | | oC | kPa | kgmole/h | Mole |
| 8 | 1 | 36.945 | 7383.46 | 6206.5 | 0.9987 |
| 10 | 2 | 36.945 | 6760.5 | 12320.9 | 0.9984 |
| 15 | 3 | 36.945 | 6760.5 | 6206.5 | 0.9986 |
| 5 | 4 | 20.0522 | 6760.5 | 6206.5 | 0.9986 |
| 3 | 5 | 25 | 7201 | 10530 | 0.9985 |
| 6 | 6 | 53.8378 | 6760.5 | 6206.5 | 0.9986 |
| 7 | 7 | 36.945 | 6137.54 | 6206.5 | 0.9986 |
| 9 | 8 | 36.945 | 6760.5 | 92.1477 | 0.9986 |
| 14 | 9 | 36.945 | 6760.5 | 6206.5 | 0.9986 |
| 11 | 10 | 36.945 | 6760.5 | 6206.5 | 0.9986 |
| 12 | 11 | 36.945 | 6760.5 | 6206.5 | 0.9986 |
| 13 | 12 | 36.945 | 6760.5 | 6206.5 | 0.9986 |
| 4 | 13 | 25 | 6320 | 1883 | 0.9989 |
| 2 | 14 | 48.89 | 6320 | 10530 | 0.9985 |
| 1 | 15 | 48.89 | 7201 | 1883 | 0.9985 |

### *3.2.2 Anova for Response Surface Reduced Quadratic Model*

Analysis of variance table (Table 3.4), the model F-value of 134.47 implies the model is significant.

There is only a 0.01% chance that an F-value this large could occur due to noise. Values of "Prob > F" less than 0.0500 indicate model terms are significant. In this case B, C, AB, AC, BC, $B^2$, $C^2$ are significant model terms. Values greater than 0.1000 indicate the model terms are not significant. The summary of fit of the Factor and Coefficient Estimates are presented in Table 3.5. The best fit model proposed by the software was the quadratic model.

*Table 3.5:* Fit summary of Factor and Coefficient Estimate

| | Coefficient | | Standard | 95% CI | 95% CI | |
|---|---|---|---|---|---|---|
| Factor | Estimate | df | Error | Low | High | VIF |
| Intercept | 1.00 | 1 | 5.051E-006 | 1.00 | 1.00 | |
| B-Pressure | 3.536E-005 | 1 | 6.682E-006 | 1.956E-005 | 5.115E-005 | 2.00 |
| C-Flow rate | -7.071E-005 | 1 | 6.682E-006 | -8.651E-005 | -5.491E-005 | 2.00 |
| AB | 2.929E-005 | 1 | 9.449E-006 | 6.946E-006 | 5.163E-005 | 2.00 |
| AC | 1.354E-004 | 1 | 9.449E-006 | 1.130E-004 | 1.577E-004 | 2.00 |
| BC | 1.000E-004 | 1 | 6.682E-006 | 8.420E-005 | 1.158E-004 | 1.00 |
| $B^2$ | 3.125E-005 | 1 | 4.808E-006 | 1.988E-005 | 4.262E-005 | 1.00 |
| $C^2$ | -4.375E-005 | 1 | 4.808E-006 | -5.512E-005 | -3.238E-005 | 1.00 |

The empirical relationship between response parameter (recycled TEG) and the process variables is represented in Equations 3.1 where A, B, and C are coded terms used for temperature, pressure and flow rate of the wet gas.

$$Y = +1.00 + 3.536E\text{-}005*B - 7.071E\text{-}005*C + 2.929E\text{-}005*AB + 1.354E\text{-}004*AC + 1.000E\text{-}004*BC + 3.125E\text{-}005*B^2 - 4.375E\text{-}005*C^2 \quad 3.1$$

Where;
Y = Recycled TEG yield
A = Temperature
B = Operating Pressure
C = Flow rate
Intercept = 1.00

The equation in terms of coded factors above can be used to make predictions about the response for given levels of each factor. By default, the high levels of the factors are coded as +1 and the low levels of the factors are coded as -1. The coded equation is useful for identifying the relative impact of the factors by comparing the factor coefficients.

Graphical representation of how the individual process variables affect the yield of recycled TEG as well as a three-dimensional plot (3D plot) and contour plot were generated by the Design-Expert software. The 3D and the contour plots (Figures 3.1 - are used to estimate the effects of the combination of variables (temperature, pressure and flow rate of the wet gas) on the response (recycled TEG yield).

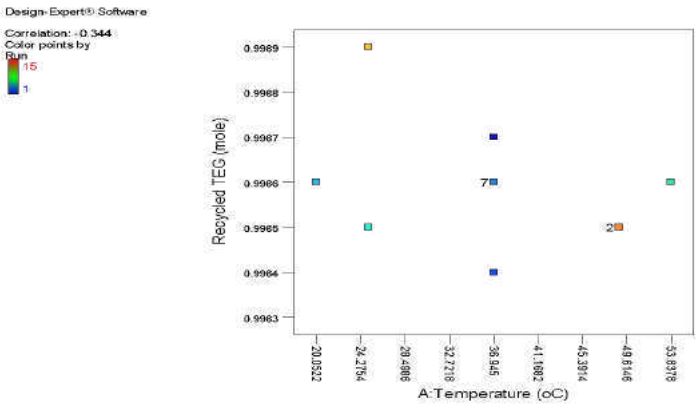


*Figure 3.1:* Graphical representation of the effect of temperature on Recycled TEG

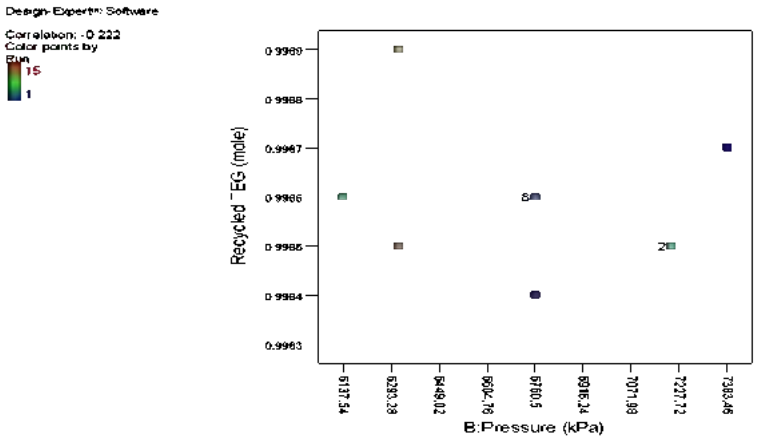


*Figure 3.2:* Graphical representation of the effect of pressure on Recycled TEG

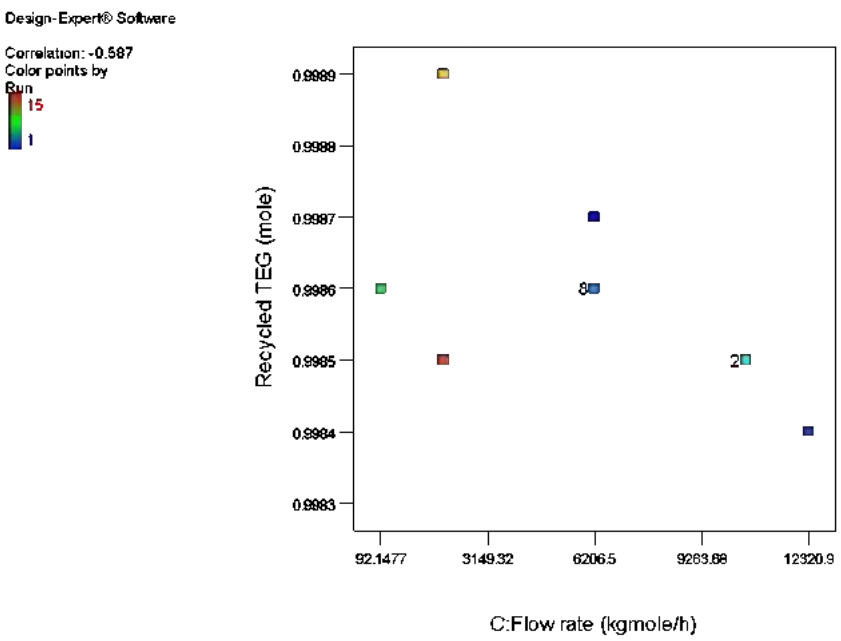


*Figure 3.3:* Graphical representation of the effect of pressure on Recycled TEG

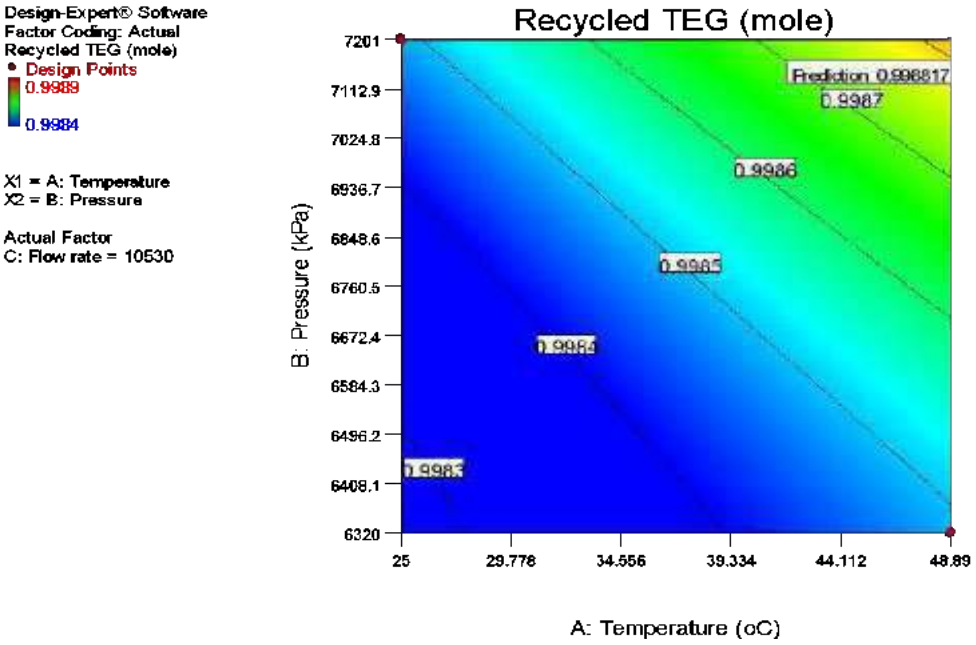


*Figure 3.4:* Contour Plot showing the effect of temperature and pressure on the Recycled TEG

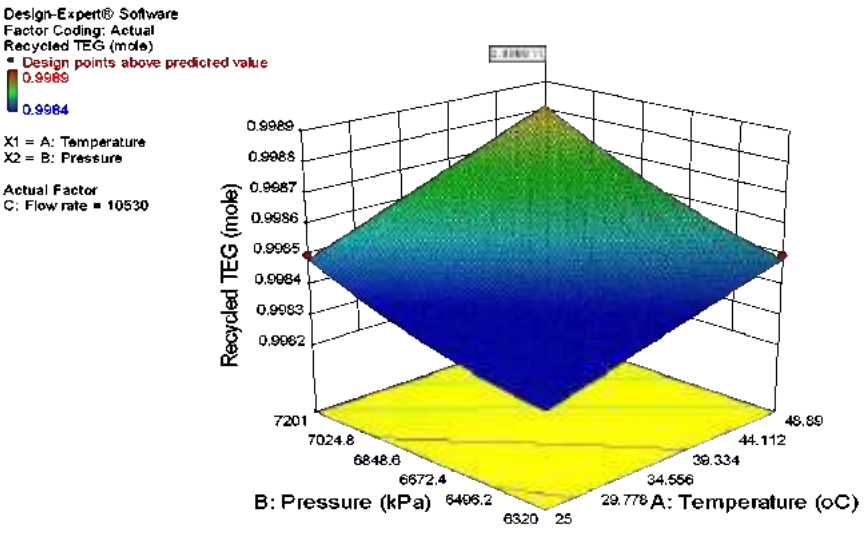


*Figure 3.5:* 3D Plot showing the effect of wet gas temperature and pressure on recycled TEG response

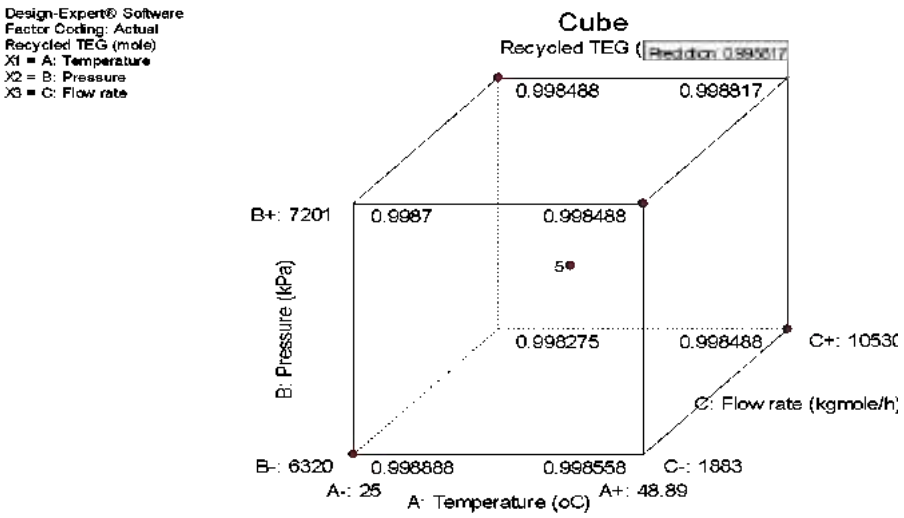


*Figure 3.6:* A cube showing the effect of wet gas parameters on the response

From the result of the optimization, it was seen that temperature, pressure and flow rate has significant effect on the process, the optimum operating temperature, pressure and flow rates were found to be 25°C, 6320 kpa and 1883 kgmole/h respectively, this process variable values gives an optimum yield of Recycled TEG of 99.89 mol%.

## IV. SUMMARY, CONCLUSION AND RECOMMENDATION

### *4.1 Summary*

Dehydration of Natural Gas has been a subject of interest for decades due to the effect of the wet gas on the system, gas' value and market specification. Specifically, dehydration is carried out to prevent formation of hydrates which are known to corrode pipelines and block valves. Besides these flow assurance issues, the hydrate in the gas quickly deactivate catalyst and burn less. Several studies emerged with an attempt to economically dehydrate the gas. In this study, TEG, proven to be the best and less aggressive on the environment has been exploited. This study evaluated the dehydration of Natural gas through absorption with Triethylene glycol and HYSYS simulation of the process was carried out using

Glycol and Peng-Robinson as the thermodynamic fluid package.

Optimization of the process was done using the Central Composite Design approach of Response Surface methodology (RSM) of the Design Expert software. The process variables of the wet gas stream were used as design parameters for the experiment based on central composite design. It was found that, at a temperature of 25°C, pressure of 6320 kpa and a flow rate of 1883 kgmol/h, a maximum recycled TEG yield of 99.89 mol% of the recycled stream was obtained.

### 4.2 Conclusion

Based on the results obtained from the optimization of Natural gas Dehydration plant with TEG, it can be concluded that:

i. The column pressure of the absorption column should be minimized to reduce the amount of hydrocarbons trapped in the wet TEG stream leaving the bottom of the absorber.
ii. The number of theoretical trays of the TEG regenerator has a little impact on lean TEG content; a minimum possible number of trays should be used.

### 4.3 Recommendation

Based on the findings of this work, it is recommended that the TEG regenerator reboiler temperature should not exceed 206°C as triethylene glycol degrades at this temperature which is far less than its boiling point of 285°C. Also, for Optimum TEG regeneration operation, the temperature, pressure and flow rate of the wet gas stream should be 25°C, 6320 kpa and 1883 kgmole/h respectively as maximum yield of the Recycled TEG is achieved at this operating condition.

## REFERENCES


1. Abdulla, S. (2015). Simulation of Pumps by Aspen Plus. *International Journal of Engineering Science,* 4 (3): 2 -45.
2. Afaiko, D. U. (2014). *Maximizing the efficiency of natural gas dehydration process with triethylene glycol using Aspen HYSYS.* B. Eng Project, University of Uyo, Nigeria.
3. Affandy, S., Renanto, J., and Chien, L. (2017). Simulation and optimization of structured packing replacement in absorption column of natural gas dehydration unit using triethylene glycol (TEG). Paper presented at 6th International Symposium on Advance Control of Industrial Processes, AdCONIP 2017.
4. Affandy, S., Kurniawan, A., Handogo R., Sutikno, J., and Chien, I. (2020). Technical and economic evaluation of triethylene glycol regeneration process using flash gas as stripping gas in a domestic natural gas dehydration unit. *Engineering Reports* 2 (4):1-3.
5. Ahmed, S., Nadia, A. and Said, A. (2019) Gas Condensate Stabilization Methods: Optimum Operating Conditions. *International Journal of Recent Technology and Engineering*, 8 (3): 1643-1648.
6. Akpabio, J., Bassey, P., Ajie, O. and Obonukut, M. E. (2021) Development of a Model Predicting Rate of Wax Deposition in Production Tubing: A Flow Assurance Study. *Journal of Petroleum Technology and Alternative Fuels* (in press)
7. Appah, D. (2014). Energy Challenge for Nigerian Industrial Revolution Plan: The Way Forward. Paper presented at the 44th Annual Conference of Nigerian Society of Chemical Engineers, Owerri, Nigeria, 2 - 6 November, 2014.
8. Bahadori A. (2014). *Natural gas processing: Technology and Engineering Design*. Gulf Professional Publishing.
9. Chebbi, R., Qasim, M. and Abdel N. (2019). Optimization of Triethylene Glycol Dehydration of Natural Gas. *Energy Report.* 5: 723-732.
10. Elliot J. R. and Lira C. T. (1999). *Introduction to Chemical Engineering Thermodynamics*. Prentice Hall.
11. Gray, David, Tomlinson, Glen and Shen, John (1990). Direct Methane Conversion: An Assessment. *Hydrocarbon processing,* 432-435.

12. Holmen, A. (2009). Direct Conversion of Methane to Fuels and Chemicals. *Catalysis Today*, 142: 2 – 8.
13. Kamin. Z., Bono, A., and Leong, L. (2017). Simulation and optimization of the utilization of triethylene glycol in a natural gas dehydration process. *Chemical Product and Process Modelling*. 12(4):1-9.
14. Kong, J., Mahmoud, Z., Liu, A. and Sunarso, S. (2018) Revamping existing glycol technologies in natural gas dehydration to improve the purity and absorption efficiency: Available methods and recent developments. *Journal of Natural Gas Science and Engineering*, 56: 486 -503.
15. Luyben W. (2011). *Principles and Case Studies of Simultaneous Design*. Hoboken, NJ: John Wiley & Sons.
16. Mokhatab, S., Mak, J. Y., and Poe, W. A. (2019). *Process Modelling and Simulation of Gas Processing Plants*. Handbook of Natural Gas Transmission and Processing. Gulf Professional Publishing; 4th edition.
17. Neagu, M. and Cursaru, D. (2017). Technical and economic evaluations of the triethylene glycol regeneration processes in natural gas dehydration plants. *Journal of Natural Gas Science and Engineering*. 37:327-340.
18. Netusil, M. and Ditl, P. (2011). Comparison of three methods for natural gas dehydration. *Journal of Natural Gas Chemistry* .20(5): 471-476.
19. Obonukut, M. E., Alabi, S. B. and Bassey, P. G. (2016). Steam Reforming of Natural Gas: Value Addition to Natural Gas Utilization in Nigeria. *Journal of Chemistry and Chemical Engineering* 10 (1): 2841.
20. Partho, S. and Ruhul, A. (2011) Aspen-HYSYS Simulation of Natural Gas Processing Plant. *Journal of Chemical Engineering IEB* 26: 62-65.
21. Patel, M. S., Wong, S. F. and Storm, D. A., (2005). Retrofitting Methanol Plants for Higher Alcohols. 78th American Institute of Chemical Engineer's, National Meeting, New Orleans, LA.
22. Pezman K. and Roya H. (2011). Sensitivity Analysis of a Natural Gas Triethylene Glycol Dehydration Plant in Persian Gulf Region. *Petroleum and Coal* 53(1): 71-77.
23. Rahimpour, M. R., Jokar, S. M., Feyzi P., Asghari, R. (2013). Investigating the performance of dehydration unit with Coldfinger technology in gas processing plant. *Journal of Natural Gas Science and Engineering*. 1:471-476.
24. Saeid, M., William A., Poe J. and Speight, G. (2006). *Handbook of Natural Gas Transmission and Processing*. Gulf Professional Publishing, Oxford, United Kingdom.
25. Sanggyu I., Sung-heechoi, Yeongbeom I., Kyusang C. and Young-myung Y. (2011). The study on a new liquefaction cycle development for LNG plant. International Gas Union Research Conference, Seoul, Korea, October 2011.
26. Shoaib, T., Bhran, A., Awad, A. and El-Sayed, M. (2018). Optimum operating conditions for improving natural gas dew point and condensate throughput. *Journal of Natural Gas Science and Engineering*, 49: 324–330.
27. Siti, N. and Abdul G. (2012). Simulation of Typical Natural Gas Dehydration Unit using Glycol Solutions. *Engineering Reports* 8 (2): 27-31
28. Stewart, M. and Arnold, K. (2011). *Gas Sweetening and Processing Field Manual*. Houston: Gulf Professional Publishing, pp. 51–52.

# Instability of Ice Mass Balance and Climate Change Induced Sea Level Rise-An Appraisal

*Chakraborty Sudipta, A. R. Kambekar & Sarma Arnab*

*The Assam Royal Global University, Guwahati, India*

## ABSTRACT

It is found from literature on impact of changes in climate and the resultant rise in sea level, that the scenarios, which are presumed for estimating the rise in Sea Level are stranded on a lot of doubts. Projections by different teams of scientists and real time data from IPCC's predictions do not always match and mostly rather differ. Various models so far considered, grounded on mathematical and statistical methods are anticipated to experience unforeseen variation due to the present unpredictable behaviour of the ice sheets. Studies about the contribution from Antarctica itself towards rise in Sea Level predicts abrupt variations in different projections and accordingly the importance of detailed study on Marine Ice Instability has been highlighted in this paper. The phenomenon related to MISI and MICI has been stressed upon to arrive at more correct projections on Sea Level Rise in coming decades and centuries.

*Keywords:* global warming, sea level rise, melting of ice, ice sheet, ice cliff, uncertainty, instability.

*Classification:* DDC Code: 551.458, LCC Code: GC89

*Language:* English

London Journals Press

LJP Copyright ID: 392975
Print ISSN: 2631-8474
Online ISSN: 2631-8482

London Journal of Engineering Research

Volume 22 | Issue 1 | Compilation 1.0

# Instability of Ice Mass Balance and Climate Change Induced Sea Level Rise-An Appraisal

Chakraborty Sudipta[α], A. R. Kambekar[σ] & Sarma Arnab[ρ]

## ABSTRACT

*It is found from literature on impact of changes in climate and the resultant rise in sea level, that the scenarios, which are presumed for estimating the rise in Sea Level are stranded on a lot of doubts. Projections by different teams of scientists and real time data from IPCC's predictions do not always match and mostly rather differ. Various models so far considered, grounded on mathematical and statistical methods are anticipated to experience unforeseen variation due to the present unpredictable behaviour of the ice sheets. Studies about the contribution from Antarctica itself towards rise in Sea Level predicts abrupt variations in different projections and accordingly the importance of detailed study on Marine Ice Instability has been highlighted in this paper. The phenomenon related to MISI and MICI has been stressed upon to arrive at more correct projections on Sea Level Rise in coming decades and centuries.*

*Keywords:* global warming, sea level rise, melting of ice, ice sheet, ice cliff, uncertainty, instability.

*Author* α: Chakraborty Sudipta, Research Scholar, Department of Civil Engg., The Assam Royal Global University , Guwahati , India.
e-mail: diptasu@gmail.com
σ: Kambekar A.R. Dr., Department of Civil Engg., Sardar Patel College of Engineering, Mumbai University, Andheri (W), Mumbai- 400058, India.
ρ: Sarma Arnab Dr., Prof., Head , Department of Civil Engg., The Assam Royal Global University, Guwahati, Assam-781035, India.

## I. INTRODUCTION

One of the most important effects of anthropogenic warming in our globe is Rise in Sea Level, which appears as a major challenge to the Civilization as all coastal places with human habitation are likely to face catastrophic inundation threatening migration, health and economic challenges around the world. Due to the complex nature of interactions within seas, troposphere, ice and land, profound doubts remain about the resultant rise in sea level arising out of changes in climate. Scale of longstanding GMSL rise for coming centuries is essential to be known for effective planning of adaptation and mitigation pathways and policies.

## II. BACKGROUND

It is highlighted in IPCC's AR-VI (2021), that the global rise in temperature would reach 1.5°C in the 2030s, then again will increase to 1.6°C, and then show a downward trend with temperatures dropping back down to 1.4°C at the top of the century. The Agreement at Paris (2015) resolved the necessity of keeping warming in our globe below 2° C than pre-industrial levels by 2100, with an attempt to restrict the rise within 1.5°C by 2050 or before. However, as per Glasgow Climate Summit (2021), in the next two decades our planet is irrevocably heading towards warming by 1.5° C over preindustrial times. As per existing declarations by countries the globe is now in the direction of 2.7°C minimum rise in temperature by 2100. If this scenario doesn't change globally the rise in sea level will linger much after this century also [1]. From review of some papers presented below it's found that there are plenty of doubts in realistic estimation of Rise in Sea Level.

## III. LITERATURE REVIEW

Parris et al. (2012) found various possibilities in imminent rise of GMSL by 2100, up to a high-end of 2.0 m with a low-end of 0.2 m with two optimized intermediate high and low position

from 1.2 m to 0.5 m (Figure 1).It is stated that the low scenario represents the inferred trend in rise of GMSL adding an additional amount of about 5 cm over the rise in last century, while the high scenario represents another model under more extreme land-ice contributions with an upper limit of GMSL rise. The midway situations signify the upper-end predictions for rise as per IPCC AR4-B1 scenario (Intermediate-Low), and more than a few semi-empirical revisions (Intermediate-High) [2].

Bamber and Aspinall (2013) attempted to ascertain a consensus amongst numerous experts and presumed an unchanging rate of likely rise in sea level, by 2100. They considered the above pre-industrial temperatures up to an increase of 3.5°C, matching with a medium range scenario for emissions of carbon. The average proportion of rise in the seawater level was considered to be 5.4 mm per year by 2100, just only from the Antarctic and Greenland ice sheets, as agreed upon by these experts. After merging the consequences of molten ice and glaciers, along with that from expansion of ocean due to warming, the average estimation for rise in sea level by 2100 was predicted by them to be within the range of 33 to 132 cm. Although they did not rule out the uncertainty on this guesstimate, it was stated to be the best estimate, according to them [3].

Golledge et. al. (2015) observed that the runaway ice loss from Antarctica will cross a tipping point prior to 2100, pledging the planet to have a rise in sea level up to 2 m by 2100 and 15 m by 2300 [4]. Whereas the currents in the top 100 m of the ocean's surface are driven by winds, they stated that currents flowing thousands of meters below surface are driven by thermohaline circulation. This happens due to differences in the water's density, temperature (thermo) and salinity (haline) and inter hemispheric atmospheric cooling at local level is triggered due to reduction of temperature in the bottom water level at Antarctic [4].

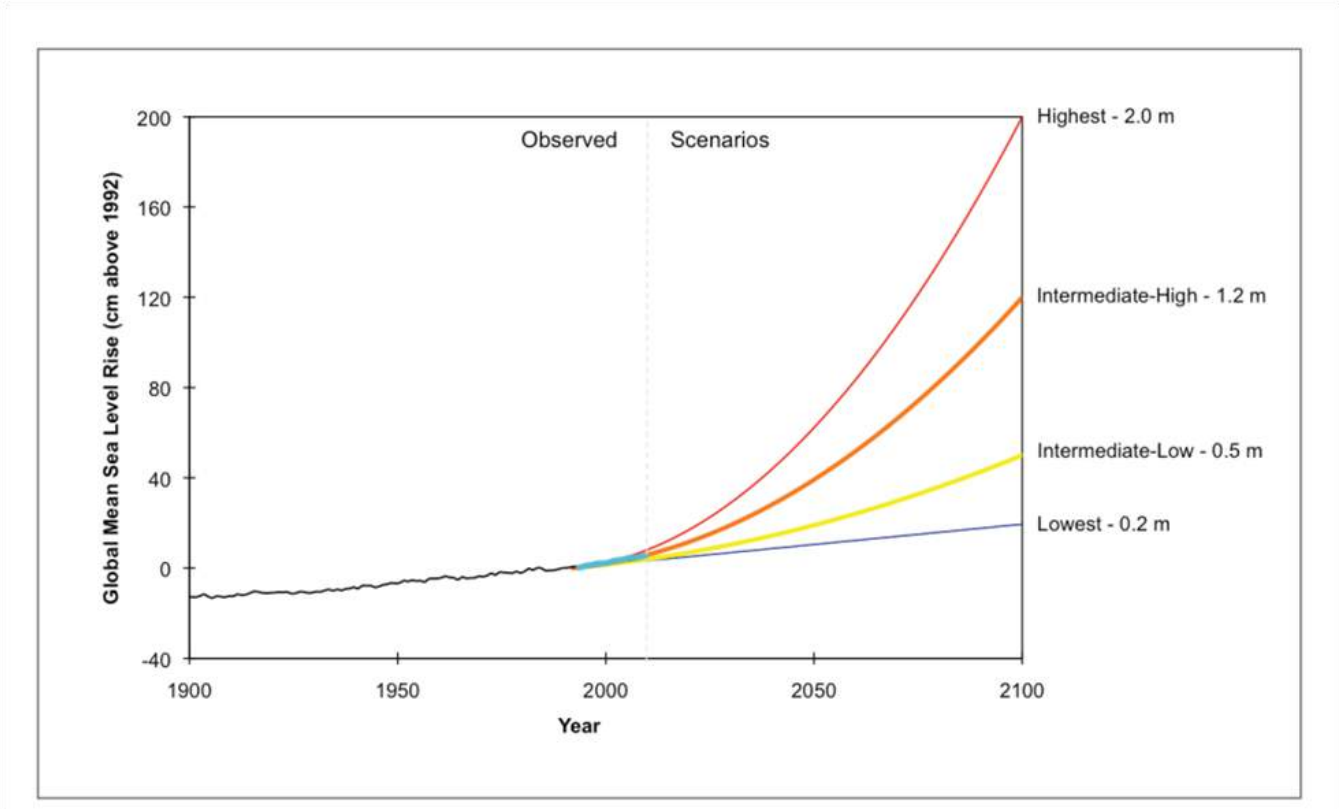


*Figure 1:* The rise scenarios in Global mean sea level. Source: NOAA - 2012 [ 2]

Pollard et al. (2015) explained that as per physical characteristics, the subaerial ice cliffs are prone to collapse due to their self-weight when the height of the cliff exceeds 90 meters. Such instability called MICI (Marine Ice Cliff Instability) leads to failure of ice-cliffs and retreat of ice sheets [5].

Landerer, F. W et. al (2015) revealed that Sea-level rise is accelerating, but the future rate is uncertain. Acceleration is mostly due to increased thermal expansion of the top two kilometers of the oceans which amplified melting of icebergs. A large portion of Antarctica below sea level is subject to melting from below, due to warm water. It causes the ice sheet to peel off the ocean floor, accelerating the flow of the glacier towards the sea. According to reports from the satellite named-GRACE (Gravity Recovery and Climate Experiment), the melting of Antarctica has fast-tracked by a factor of five in recent decades. Uncertainty in forecasting Sea level rises from Antarctica is emphasized [6].

J. Hansen et.al. (2016) highlighted a layer of the cold meltwater at the ocean's surface layer which acts like a lid and facilitates ice melting by increasing subsurface ocean warming. The layer of lid with low-density detains the warming below especially at ice shelf grounding lines where a restraining force develops which limits discharge of the ice sheet [7].

David Docquier (2016) pointed out that warm water at the base of ice shelves (basal) increases the melting, which in turn pushes back the grounding line and the resultant thinned ice-shelves exert less buttressing effect which causes perturbation to Ice sheet and disturbs the stability [8].

Sweet et.al. (2017) on scrutiny of several peer-reviewed publications came out with a physically plausible rise in GMSL due to instability of Antarctic ice-sheet itself within 2.0 m to 2.7 m. The values considered by Paris et al. [2] were revised and they recommended an upper-bound "extreme" scenario for rise in GMSL up to 2.5 m (0.5 m higher) by the year 2100 [9].

Garner et al. (2018) found projections of SLR vacillates and somewhat are usually found more than IPCC's projections. Windows for upper projection regarding SLR predictions are not same across various studies, in reality projections persist to remain ambiguous. According to them a gap in scientific knowledge related to assessing the probable rise in seawater level is evident as per the widely varying results obtained from different studies [10].

Andrew Shepherd et. al. (2018) from the IMBIE team, an international collaboration of scientists known as 'Ice-sheet Mass-Balance Inter-Comparison Exercise' investigated the Antarctic Ice-Sheet and its balance of mass. Regarding the processes responsible for active loss of the AIS, they found absence of proper technical explanations existed till the recent AR5 estimates, Subsequently the integration of the concept of instabilities particularly regarding numerical models for ice sheet was in progress. A high-impact scenario (with low-probability) for future sea level rise resulted in IPCC-AR6, where rise in GMSL up to 2 meters (Figure 1) was not ruled out by 2100 [11].

“Dow, Christine F et. al. (2018) explained MISI as one of the main catalysts for breaking and evacuation of the ice-sheets, stuck on sloping beds underneath sea level. Peripheral ice gets removed by ice cliff failure, which exposes taller ice cliffs more unstable and the process continues. Also, MICI can further increase because of surface melt through ponding and hydro fracture [12].

Jonathan L. Bamber (2019), based on the uncertainties of emission and melting ice volume, suggested that the rise in GMSL being up to 145 cm for contribution from Antarctic contribution by 2100 has 5% chances [13].

Horton et. al. (2020) documented that a group of scientists exercised a repeat survey in 2020, which was earlier conducted in 2014 to find projections for future GMSL rise. Relative 1986–2005, a team of 106 experts projected a rise of 0.30–0.65 m by 2100, and 0.54–2.15 m in GMSL by 2300, under RCP2.6.

This same team however, under RCP 8.5, projected a rise of 0.63–1.32 m by 2100, and a rise of 1.67–5.61 m by 2300 in GMSL. The

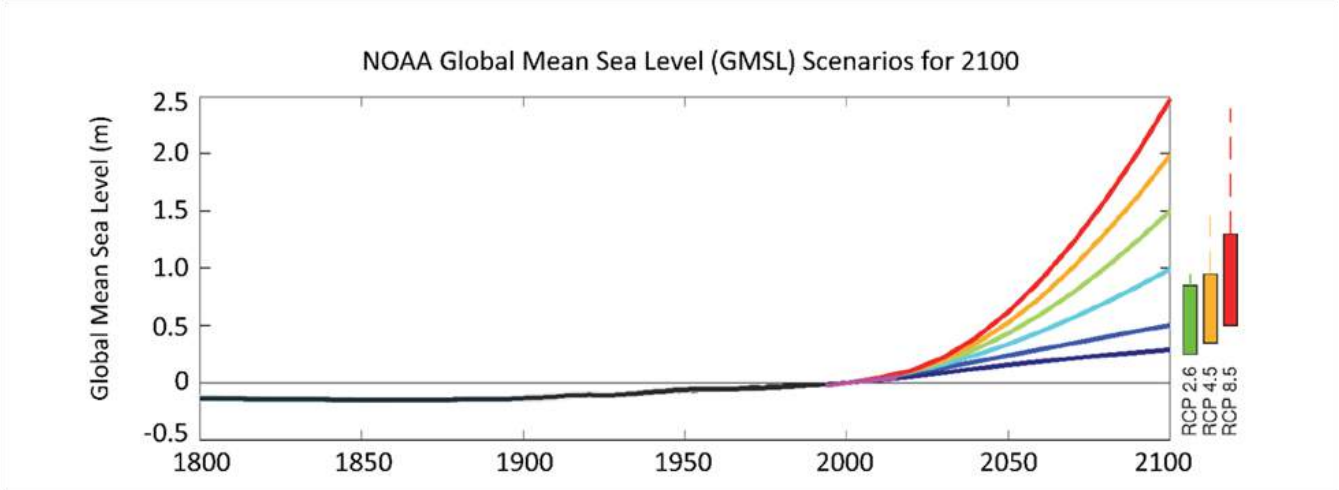


*Figure 2:* Scenarios for 2100 regarding rise in GMSL (6 coloured lines) [9]

projections for 2100 by these experts in 2020 remained similar with that obtained during the survey in 2014, whereas the projection for 2300 was more than that found in 2014. The experts projected that under the scenario of higher-emissions the rise in GMSL will cross the upper range estimated by IPCC AR5 (0.98 m) and the probability of such exceedance was 42% in the earlier survey (2014) whereas in the recent survey (2020), it was 45%. The cause of such uncertainties in upper-end estimates was diagnosed to be quantum of meltwater from the Antarctic Ice Sheet and its contribution to GMSL from the [14]. Frank Pattyn et al. (2020) had strong positive feedback that Antarctic Ice may yield a larger order of magnitude in Sea Level Rise. How quickly and how plentiful the quantum of melted water will be contributed from Antarctica remains a point of uncertainty. Being its base grounded below sea level on a slope towards inner, the West AIS is stated to have the volume with capacity to raise level of sea by 5.3 m, whereas the East AIS with marine basins has a far greater potential of contribution in rise in sea level up to 52.2 m [15].

Stef Lhermittea et al. (2020) mentioned that the glaciers in Antarctica are changing fast with possible large consequences in global sea level. They also stated that the processes controlling weakening of Ice-sheets and shifting of the contact position at ground is not fully clear. It was indicated by them that 'Thwaites Glacier' also known as 'Doomsday Glacier' will certainly contribute 65 cm. or more to global sea water, if it collapses, which will be sufficient to inundate New York, Shanghai, Miami, Tokyo and Mumbai etc. and will swallow islands like Kiribati, Tuvalu and Maldives. The glacier has already spewed ice into the ocean twice than that in the 1990s. More than 1000 billion tons of ice loss has happened since 2000, the flow speed being doubled in 30 years [16].

Lowry et al (2021) opined that the impact of scenarios of emission on future loss of ice from Antarctic is not expected to arise just within the 21st century. Dynamic ice sheet model simulations under various emissions scenarios of greenhouse gas had overlaps. The period was undis- tinguishable and it was inferred that the impact from the Ice Sheets of Antarctica towards rise of sea level in future is mostly indeterminable. Scientific community requires a focused effort to understand and identify the processes affecting the melting of the Antarctic Ice Sheet (AIS) which is the biggest capacity indefinite supplier to rise in sea level in future. It is indicated that the 21st century's warming situation will control the resulting long-term contribution on sea water- level from the Ice Sheets of Antarctica. It is possible that between the uppermost and lowermost scenarios of emissions in succeeding centuries, there can be multimeter differences in sea level [17].

Edwards et al. (2021) while projecting rise in sea level from the contributions of ice, showed a widespread variety of predictions for Antarctica's future contribution to rise in GMSL. According to a statistical assessment, relative to the 1995–2014 baseline, out of an overall rise in GMSL up to 62–101 cm, the melt water from ice of Antarctica will add 14–32 cm. Because of inadequate understanding of melting processes, it is seen that the IPCC AR6 projections [6] vary from these projections [18].

DeConto, R.M et al. (2021), recognized the deep uncertainties in probabilistic projections in sea level with contributions from Antarctica further to the middle of the 21st century after the Paris Agreement. For the SSP 5–8.5 scenario, when MICI and MISI are accounted for, a higher estimate in rise amounting to 20–53 cm for GMSL is likely by 2100 from Antarctic's contribution itself. The target set by the Paris agreement regarding emission will be met only if the global emissions trajectory tracks SSP 1–2.6, the lower-emission scenario. In that case ice loss to the ocean from Antarctica and its contribution

to Rise in Sea Level by 2100 is likely to be meaningfully lower i.e., 12–31 cm by 2100 and about 100 cm by 2300 [19].

Chakraborty et al (2021) observed that reports from different groups of scientists and their models have regenerated the ambiguity of uncertainty to a greater extent, although starting from studies through statistical forecast, numerical modeling including actual measurement of rise in sea level from Satellite Altimetry, scientists have taken recourse. There are comments which have either intensified or decreased the rate of the global rise in mean sea level. [20]

Colleoni et al. (2022) pointed out that as melting ice sheets do not lead to uniform Sea level Rises all over the globe, this further confounds understanding the niche contributions from Antarctic itself. Due to rearrangement of ocean water due to flow of melt ice into the ocean, the gravitational field and rotational state of Earth changes. Land also rises due to exertion of less pressure on the land below by the remaining ice. It is suggested that substantial loss of ice from Antarctica can be barred only by restricting emissions of greenhouse gasses within RCP 2.6 scenario. It was also opined that emissions in the coming decades will largely impact the quantity of melt water from the ice sheets of Antarctica for raising sea water level globally. In Higher-emission scenarios by the year 2300, ice loss from Antarctica is likely to contribute to an increase of sea level by 0.6–3 meters [21].

## II. MARINE ICE INSTABILITY

### *4.1 Marine Ice Sheet Instability*

A sheet of ice supported on the sea bed level is a marine ice sheet. Seawater being denser than ice, marine ice sheets can only remain stable when the mass of the ice sheet exceeds the mass of the seawater displaced by the ice (Archimedes' principle) and the ice below water level remains in place by the load of ice over it. The thinning of ice (due to melting) when it reaches a threshold value, the ice below water floats and warm water enters below it. After basal melting [8], thinning of the ice shelf decreases the buttressing effect supporting the interior grounded ice. Pollard et al. (2015) [5] and David Docquier (2016) [8] opined that in such conditions the retreat of Ice sheets gets accelerated. The grounding line shifts and such resultant retreat of the ice sheet was first termed as MISI or Marine Ice Sheet Instability by Mercer, J. H. (1978) [22]. Due to warming when surface meltwater increases, hydro fracture takes place causing ice-shelf calving and meltwater drainage into crevasses goes on. This hypothesis of Marine Ice Sheet Instability considers that due to warming in ocean melting of ice increases, particularly when the ice rests on a reverse slope gradient (from coast towards interior of marine sheet) due to lesser buttressing force from inside the ice and shifting of the grounding line controls the stability of ice sheet [25].

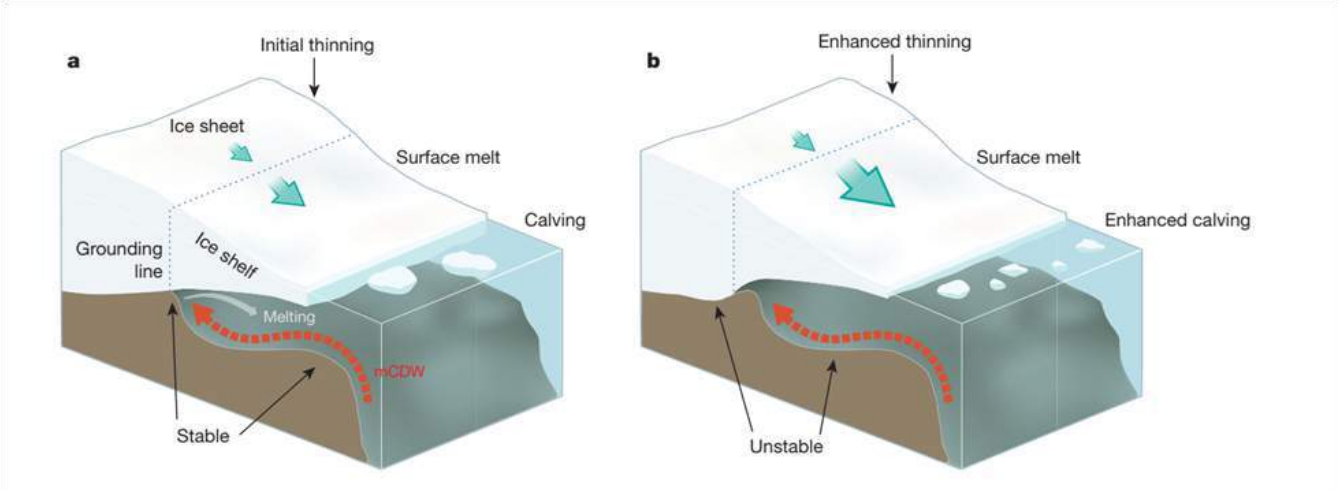


*Figure 3:* Schematic representation of MISI with (a) an initial stable grounding-line position and (b) an unstable grounding-line after the incursion of warm modified Circumpolar Deep Water (mCDW) [26]

Figure 4 shows the schematic representation of the phenomenon. When the ice at the grounding line is in upper position then the upstream grounding line retreats which stops only after a new stable position is reached. When the bedrock slopes down from the coast towards the interior of the marine ice sheet, the grounding line is not stable (in the absence of back forces provided by ice shelves). The position and migration of this grounding line control the stability of a marine ice sheet. Historically, blame for the sudden breakdown of the Larsen B ice shelf at Antarctica2002) into the ocean has been given to this mechanism by Vaughan et al. (2008) as summers (preceded the event [23].

### *4.2 Marine Ice Cliff Instability*

The section of ice exposed to the ocean or air above the waterline which actually becomes the calving face is known as the ice cliff. The formative and conceptual differences between Ice Sheet and Ice Cliffs are shown in the pictures in Figure 5. When the increasingly tall unstable ice cliffs are exposed due to reduction of buttressing effect at the bottom, the cliff collapses. When the strains ("stretching" forces) inside ice cliffs longitudinally are too large for it to sustain, the taller subaerial vertical cliff along the ice margins turns out to be structurally more unstable, which triggers catastrophic failure of the cliff into deep basins. The combined effect of surface melt, shifting of the grounding line as well as hydrofracturing is known as MICI [Marine Ice Cliff Instability]. Helsinki Discrete Element Model popularly known as 'HiDEM' is a particle model which is used for determining the fracture and resultant calving of retreating marine glaciers by simulation of the elastic behaviour through Finite Element Analysis. Such parameterization [27] assists for critical representation for retreat via ice-cliff failure in models. If certain conditions are met and ice-cliff height increases with each failure occurrence, the ice-cliff failure process can become self-sustaining. It is observed that glacier-retreat rates rise non-linearly with ice-cliff height. Figure 6 shows the schematic representation of MICI and the collapse of the ice cliff.

## V. CONCLUSION

Question remains whether Antarctica will empty itself into the ocean or as a cascading effect pull the adjacent ices also, which eventually may contribute towards a few meters of rise in sea-level. Satellite altimetry reports have already shown signs of fast depletion of ice. Prediction of the sea level rise by mid-century or top of it, happens to be an extremely complex task, which other than global warming in fact also basically depends on both MISI & MICI. Mercer, J. H. (1978) predicted these as a threat to disaster [22] and Vaughan, David G. (2008) reiterated the potential for ice destabilization in a runaway fashion which will contribute to comparatively faster rise in sea level [23]. Scientists are sure

about the acceleration of Rise in Sea Level in future decades and centuries. Currently there are limitations in our understanding in ice flow and sliding, with historical constrained iterative statistical ice sheet simulations. It is confirmed that under high- emissions scenarios, contribution towards sea water level from the Antarctic Ice Sheet will not be the same from low-emission scenarios for centuries. It is seen that there are plenty of concepts regarding scenarios and innumerable number of papers exist in literature with historical data and stochastically obtained projections regarding Sea Level Rise. There is no shortcut to save our planet from Sea Level Rise. With concerted effort, different nations have already started planning for reduction of burning fossil fuel, go for reducing emissions and thereby try to limit the warming.

Marine Ice Sheet (Source: Science.org)

Marine Ice Cliff (Source :SciTechDaily.com)

*Figure 4:* Marine Ice Sheet & Marine Ice Cliff

It may be said without hesitation that ironically the climate has started behaving erratically and the civilisation is heading towards catastrophe. In established cold countries, occasions of very high temperature are unprecedentedly seen to occur, whereas unexpected snowfall is found occurring intermittently even at the desert countries. Extreme weather events, storms are happening more frequently than expected.

On random review of the papers in the last decade it is observed that the expected global sea level rise till 2100 or beyond on account of global warming may lie in a range of say 25 cm to as high as 2.5 to 3 m or even more, which mainly will depend on Instability phenomenon of Marine Ice viz. MISI and or MICI. In this paper the authors intend to stress upon continuous elaborate studies on Instability phenomenon of Marine Ice as already highlighted by Chii Yun Tsai et.al. (2020); stating that improved knowledge about the interactions between climate scenario and ice sheets and also how ice sheets would react to future changes and variability in climate are extremely important for vigorously guesstimating the influence of AIS to SLR [24]. It is opined that even if the increase of temperature be kept under control as per Paris Agreement and Glasgow Summit, a severe uncertainty remains on how fast and how much the Icebergs will seriously melt, which can lead to a disaster in our world.

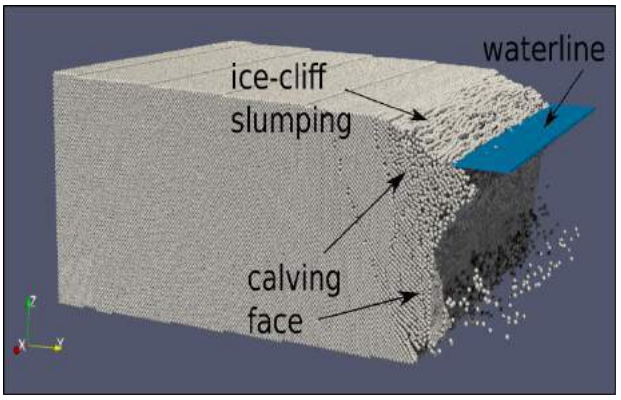


*Figure 5:* Schematic representation of collapse of an ice-cliff [27]

## REFERENCES


1. Masson-Delmotte, V., P. Zhai, A. Pirani, S.L. Connors, C. Péan, S. Berger, N. Caud, Y. Chen, L. Goldfarb, M.I. Gomis, M. Huang, K. Leitzell, E. Lonnoy, J.B.R. Matthews, T.K. Maycock, T. Waterfield, O. Yelekçi, R. Yu, and B. Zhou (eds.) Contribution of Working Group I to the Sixth Assessment Report IPCC, 2021: https:// www.ipcc.ch/report/ar6/wg1.
2. Parris, A., P. Bromirski, V. Burkett, D. Cayan, M. Culver, J. Hall, R. Horton, K. Knuuti, R. Moss, J. Obeysekera, A. Sallenger, and J. Weiss. 2012. Global Sea Level Rise Scenarios for the US National Climate Assessment. NOAA Tech Memo OAR CPO-1. 37 pp.
3. Bamber J, Aspinall W. An expert judgment assessment of future sea level rise from the ice sheets. Nature Clim Change 2013; 3:424–427.https://doi.org/10.1038/nclimate1778.
4. Golledge, N., Kowalewski, D., Naish, T. et al. The multi-millennial Antarctic commitment to future sea-level rise. Nature 526, 421–425 (2015). https://doi.org/10.1038/nature15706
5. Pollard et al. (2015). "Potential Antarctic Ice Sheet retreat driven by hydrofracturing and ice cliff failure" (https://doi.org/10.1016%2Fj.epsl.2014.12.035). Nature.412:112–121, (https://doi.org/10.1016%2Fj.epsl.2014.12. 035).
6. Landerer, F. W., D. N. Wiese, K. Bentel, C. Boening, and M. M. Watkins (2015), North Atlantic meridional overturning circulation variations from GRACE ocean bottom pressure anomalies, Geophys. Res. Lett.,42, 8114–8121, doi:10.1002/2015GL065730.
7. J. Hansen; M. Sato; P. Hearty; R. Ruedy; M. Kelley; V. Masson-Delmotte; G. Russell; G. Tselioudis; J. Cao; E. Rignot; I. Velicogna; E. Kandiano; K. von Schuckmann; P. Kharecha; A.N. Legrande; M. Bauer; K.-W. Lo (2016). "Ice melt, sea level rise and superstorms: evidence from paleoclimate data, climate modeling, and modern observations that 2 °C global warming could be dangerous". Atmospheric Chemistry and Physics. 16 (6): 3761–3812.; https://doi.or g/10.5194% 2Facp -16-3761-2016.
8. David Docquier (2016). "Marine Ice Sheet Instability "For Dummies" "https://blogs.egu.eu/divisions/cr/2016/06/22/marine-ice-sheet-instability-for-dummies-2/). EGU.
9. Sweet, W.V., R.E. Kopp, C.P. Weaver, J. Obeysekera, R.M. Horton, E.R. Thieler, and C. Zervas, 2017: Global and Regional Sea Level Rise Scenarios for the United States. NOAA Technical Report NOS CO-OPS 083. NOAA/ NOS Centre for Operational Oceano- graphic Products and Services.
10. Garner Andra J., Weiss Jeremy L., Parris Adam, Kopp Robert E., Horton Radley Overpeck Jonathan T., and Horton Benjamin P; Evolution of 21st Century Sea Level Rise Projections; Earth's Future; 10.1029/ 2018 EF00099.
11. Andrew Shepherd et.al.; IMBIE team. Mass balance of the Antarctic Ice Sheet from 1992 to 2017. Nature 558, 219–222 (2018). https://doi.org/10.1038/s41586-018-0179-y.
12. Dow, Christine F.; Lee, Won Sang; Greenbaum, Jamin S.; Greene, Chad A.; Blankenship, Donald D.; Poinar, Kristin; Forrest, Alexander L.; Young, Duncan A.; Zappa, Christopher J. . "Basal channels drive active surface hydrology and transverse ice shelf fracture" Science Advances. 4 (6),2018; https://www.ncbi.nlm.nih.gov/pmc/articles/ PMC6007161.
13. Jonathan L. Bamber, Michael Oppenheimer, Robert E. Kopp, Willy P. Aspinall, Roger M. Cooke; Ice sheet contributions to future sea-level rise from structured expert judgment Proceedings of the National Academy of Sciences Jun 2019, 116 (23) 11195-11200; DOI: 10.1073/pnas.1817205116
14. Horton, B.P., Khan, N.S., Cahill, N. et al. Estimating global mean sea-level rise and its uncertainties by 2100 and 2300 from an expert survey. npj Clim Atmos Sci 3, 18 (2020). https://doi.org/10.1038/s41612-020-0121-5
15. Frank Pattyn and Mathieu Morlighem ;The uncertain future of the Antarctic Ice Sheet SCIENCE • 20 Mar 2020 • Vol 367, Issue 6484 • pp. 1331-1335 • DOI: 10.1126/science. aaz5487
16. Stef Lhermittea, Sainan Sunb, Christopher Shumanc, Bert Woutersa, d, Frank Pattynb, Jan Wuitee, Etienne Berthierf, and Thomas

Naglere; Damage accelerates ice shelf instability and mass loss in Amundsen Sea Embayment; PNAS | October 6, 2020 | vol. 117 | no. 40 | 24735–24741; www.pnas. org/cgi/doi/10.1073/pnas.1912890117.
17. Lowry, D.P., Krapp, M., Golledge, N.R. et al. The influence of emissions scenarios on future Antarctic ice loss is unlikely to emerge this century. Commun Earth Environ 2, 221 (2021). https://doi.org/10.1038/s43247-021-00289-
18. Edwards, T.L., Nowicki, S., Marzeion, B. et al. Projected land ice contributions to twenty-first- century sea level rise. Nature 593, 74–82 (2021). https://doi.org/10.1038/s41586-021-03302-y.
19. DeConto, R.M., Pollard, D., Alley, R.B. et al. The Paris Climate Agreement and future sea-level rise from Antarctica. Nature 593, 83–89 (2021). https://doi.org/10.1038/s41586-021- 03427-0.
20. Chakraborty Sudipta, A. R. Kambekar, Sarma Arnab, "Uncertainties in Prediction of Future Sea Level Rise Due to Impact of Climate Change"; Journal of Geography, Environment and Earth Science International 25(7): PP:16-27, 2021; Article no. JGEESI. 70594 ISSN:2454-7352; DOI:10.9734/ JGEESI/2021/v25i730295.
21. Colleoni, F., T. Naish, R. DeConto, L. De Santis, and P. L. Whitehouse (2022), The uncertain future of Antarctica's melting ice, Eos, 103, https://doi.org/10.1029/2022 EO220014.
22. Mercer, J. H. (1978). "West Antarctic ice sheet and CO2 greenhouse effect: a threat of disaster". Nature. 271 (5643): 321–325. doi:10.1038/271321a0.
23. Vaughan, David G. (2008-08-20). "West Antarctic Ice Sheet collapse – the fall and rise of a paradigm" (http://nora. nerc.ac.uk/id/eprint/769/1/The_return_of_a_paradigm_16_-_nora.pdf) (PDF). Climatic Change. 91 (1–2): 65–79. doi:10.1007/s10584-008-9448-3.
24. Chii-Yun Tsai, Chris E. Forest, David Pollard; The role of internal climate variability in projecting Antarctica's contribution to future sea-level rise; Climate Dynamics (2020) 55:1875–1892; https://doi.org/10.1007/s00382- 020-05354-8.
25. Bamber, J.L., Riva, R.E.M., Vermeersen, B.L.A., and Le Brocq, A.M., 2009. Reassessment of the potential sea-level rise from a collapse of the West Antarctic Ice Sheet. Science, 2009. 324(5929): p. 901-903.
26. Hanna, E., Navarro, F., Pattyn, F. et al. Ice-sheet mass balance and climate change. Nature 498, 51–59 (2013). https://doi.org/10.1038/nature12238
27. Crawford, A.J., Benn, D.I., Todd, J. et al. Marine ice-cliff instability modeling shows mixed-mode ice-cliff failure and yields calving rate parameterization. Nat Commun 12, 2701 (2021). https://doi.org/10.1038/s41467-021-23070-7.

*This page is intentionally left blank*

# Research on Logistics Intelligent Unmanned Aerial Vehicle Combined Facial Recognition

*Hai Wu Lee*

*Xiangsihu College of Guangxi University for Nationalities*

## ABSTRACT

As unmanned aerial vehicle (UAV) starts to be frequently used in the fields of industry, agriculture, reconnaissance and logistics, flight research involving UAV also starts to cover a wider range. In the civil field, UAV is generally used as an auxiliary tool to deal with urban problems, but buildings are the main factors hindering the flight of UAV. The intelligent logistics UAV proposed in this paper is used to replace the courier to deliver small goods and process the fuzzy images taken along the way. It is a quad copter implementation plan integrating flight control, obstacle avoidance ultrasound, mobile APP control system and webcam. Gradient descent algorithm and Proportion-Integral-Differential (PID) controller are applied in UAV flight control system, MATLAB and wavelet transform to handle fuzzy image. Compared with the traditional PID controller, the improved PID controller eliminates the steady-state error and reduces the lag effect caused by the integral link. The denoising effect of wavelet transform is better than the traditional median filter and mean filter. The UAV can detect surrounding obstacles during flight, and the ground control station receives feedback information and makes emergency treatment to ensure safe flight.

*Index Terms:* intelligent logistics uav, improved pid algorithm, image processing, emergency treatment system, matlab.

*Classification:* DDC Code: 363.325, LCC Code: UG1242.D7

*Language:* English

London Journals Press

LJP Copyright ID: 392976
Print ISSN: 2631-8474
Online ISSN: 2631-8482

London Journal of Engineering Research

Volume 22 | Issue 1 | Compilation 1.0

# Research on Logistics Intelligent Unmanned Aerial Vehicle Combined Facial Recognition

Hai-Wu Lee

## ABSTRACT

As unmanned aerial vehicle (UAV) starts to be frequently used in the fields of industry, agriculture, reconnaissance and logistics, flight research involving UAV also starts to cover a wider range. In the civil field, UAV is generally used as an auxiliary tool to deal with urban problems, but buildings are the main factors hindering the flight of UAV. The intelligent logistics UAV proposed in this paper is used to replace the courier to deliver small goods and process the fuzzy images taken along the way. It is a quad copter implementation plan integrating flight control, obstacle avoidance ultrasound, mobile APP control system and webcam. Gradient descent algorithm and Proportion-Integral-Differential (PID) controller are applied in UAV flight control system, MATLAB and wavelet transform to handle fuzzy image. Compared with the traditional PID controller, the improved PID controller eliminates the steady-state error and reduces the lag effect caused by the integral link. The denoising effect of wavelet transform is better than the traditional median filter and mean filter. The UAV can detect surrounding obstacles during flight, and the ground control station receives feedback information and makes emergency treatment to ensure safe flight.

*Index Terms:* intelligent logistics uav, improved pid algorithm, image processing, emergency treatment system, matlab.

*Author:* Member, IEEE Xiangsihu College of Guangxi University for Nationalities, School of Science and Engineering. No.55, Youyi Road, Jiangnan District, Nanning City, Guangxi, P. R. China. CO: 530225.

## I. INTRODUCTION

With the continuous development of economy, science and technology, the circulation of goods and information is accelerating, so the logistics industry occupies a broad market space. Logistics UAV plays an increasingly important role in urban transportation [1-2]. UAV have also received increasing attention in recent years due to their applications in prospect, logistics, photography and communications [3]. These UAV are usually easy to control, even though WIFI smart phones and tablets [4]. Due to the development of low altitude UAV control policy and technology, the practical application of UAV is more and more [5]. Based on the development of mobile communication network, UAV further breaks through the limitation of information transmission distance. At present, the application demand of UAV in cities is increasing. Nowadays, with the rapid development of e-commerce, the volume of logistics business will continue to increase in the future. Logistics UAV can improve the delivery efficiency of e- commerce logistics and reduce the delivery cost [6-7]. Especially in the era of rapid development of the Internet, logistics industry needs to use informatization and technology to promote its development [8].

In June 2013, Matternet of the United States tested a network of drones in Haiti and the Dominican Republic. UAV were able to carry 1.9km of 2kg objects. The company hopes to build a large international drone transport network and a global supply system for drone accessories. At the same time, a charging base station is also established, so that the drone can be landed along the way for charging. Meanwhile, it can also ease the contradiction between express delivery requirements and express delivery capabilities.

Due to the complex imaging conditions on the UAV platform, such as jitter, frequent undefined motion, viewpoint changes and illumination changes [9], the problem of the logistics drones being blurred and unclear when shooting the

pick-up image Therefore, it is necessary to clear and identify the image [10]. In the paper, L. Meng et al. proposed a new method for real-time face recognition in video, which has been implemented in MATLAB [11]. In recent years, wavelets have become increasingly important for signal and image processing [12]. In the past literature, it has been studied to use different methods to sharpen blurred images, such as constrained least squares (CLS) and Wiener filters, which often lead to noise amplification or excessively smooth artifacts. In addition, advanced fuzzy image restoration techniques such as iterative regularization, Fourier domain threshold filtering and wavelet domain threshold filtering are not suitable for processing real-time problems due to the large amount of computation. In order to overcome these problems, S. Kim et al. proposed a fuzzy wavelet decomposition (VWD) method based on frequency adaptive contraction and directional wavelet basis, which can be used for real-time, space-frequency adaptive image restoration [13]. As early as 2012, Z. J. Xiang and P. J. Ramadge have studied a core issue: how to control edge retention in image denoising. They solved this problem from a machine learning perspective, using a tree classifier to support a new image regularizer [14]. Using this new regularizer, it provides a theoretical basis for the optimal selection of data-driven Dyadic wavelet decomposition structure. This proposed method proves to be superior to existing haar wavelet threshold algorithms that do not use adaptive trees. The choice of wavelet transform is determined by the symmetry and anti-symmetry of decomposition wavelet. Symmetry is considered an ideal property of wavelet, especially in image processing [15]. In the research of S. R. Dubey et al., a medical CT image feature description method based on local wavelet mode (LWP) is proposed. It also applies the symmetry of wavelet, has high recognition rate and efficiency, and can be effectively used in medicine CT image diagnosis [16]. Another advantage of wavelets is that they do not have a unique base like the Fourier transform, so a wavelet base with a given signal match is required at design time [17]. After a lot of literature research, the wavelet transform method has high value and advantage for the research of digital images. In addition, MATLAB and image processing algorithms have the advantages of compatibility and accuracy [18]. MATLAB can combine the Raspberry Pi embedded image processing technology to track and recognize faces [19].

Therefore, we have studied a logistics UAV, that is, an unmanned Low altitude aircraft operated by radio remote control equipment and its own program control device to carry packages while loading an image processing system. We embed the Raspberry Pi into the image processing technology, combined with wavelet transform to realize the contrast recognition of the picker on the MATLAB platform, and finally achieve safe and accurate delivery. The structure of this paper is as follows. In the second part, the system architecture of the logistics drone is proposed. The third part introduces related methodology, including PID - based flight control theory, wavelet transform and emergency system. In the fourth part, the principles and flow charts of UAV communication control, landing obstacle avoidance and image processing are described. The fifth and sixth parts compare and analyze different methodologies to give experimental and simulation results. Finally, the conclusion is drawn.

## II. SYSTEM ARCHITECTURE

Nowadays, the research on intelligent control has begun to turn from the ground to the air. Subsequently, UAV technology has become an important research direction of automatic control. However, since the birth of quad-rotor aircraft, due to poor control, low safety performance and other problems, it has reached a bottleneck state. This paper studies a four-rotor aircraft equipped with ultrasonic obstacle avoidance system. The aircraft architecture is shown in Figure 1, which mainly includes the following aspects:

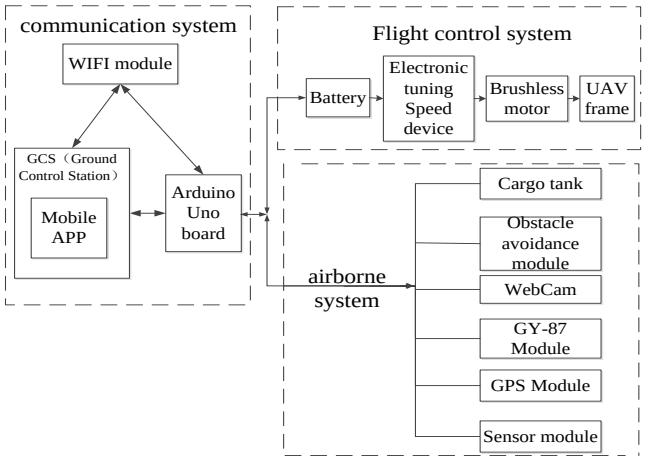


*Fig. 1:* System architecture diagram

a) *Ground Control Station (GCS):* This android-based mobile APP is designed on the basis of MIT APP Inventor 2 development environment. The operator connects the mobile device with the UAV through the WIFI module, so as to control the take-off, landing and flight direction of the UAV.

b) *Arduino Uno Board:* The flight control board of this system , which can achieve the bidirectional transmission of instructions between the ground control terminal, the flight control system and the airborne system.

c) *WIFI Module (ESP8266):* It is used for two-way communication between mobile phone and Arduino, so as to realize the function of sending and receiving information between mobile phone and UAV [20].

d) *Obstacle Avoidance Module:* It is mainly composed of HC-SR04 ultrasonic wave, SG90 steering gear and tri-color light. The steering gear combined with ultrasonic module can detect whether there are obstacles in the range of 180 degrees ahead [21]; the tricolor light displays different colors to reflect the distance between the quad and the obstacle.

e) *Webcam:* Image taken during a drone flight.

f) *GY-87 Module:* The 10-dof module, which is composed of a three-axis gyro, an accelerometer, a magnetic field and a pneumatic pressure, is used to calculate the current attitude of the four-axis aircraft so as to control its state.

g) *GPS Module* : The NEO-7N UBLOX satellite locator is used to obtain the position of the UAV.

h) *Motor Module:* Drive the brushless motor by Arduino output PWM to the electronic governor.

i) *Sensing Module:* Mainly consists of alarm buzzer, photosensitive resistor and LED lamp, among which the current light intensity is determined by the 5539 -type photosensitive resistor. When the light is dim, the LED light on the wing will be lit.

## III. METHODOLOGY

This system proposes three methods: flight control system , wavelet transform and emergency system.

### A. Flight Control System

The motor driver is a dc motor driver with current return. The UAV drive system in this paper uses the current control mode of the motor driver. The schematic diagram of the system is shown in Figure 2. The input voltage *ui* (*t*) represents the command value of the current.

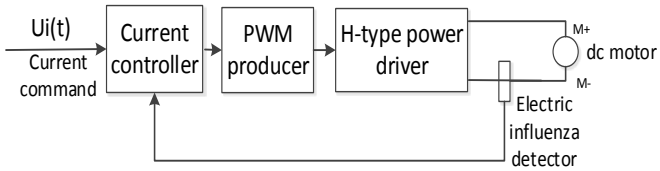


*Fig. 2:* Current control mode diagram of dc motor driver

The control system of the UAV uses the kinetic energy equation of the motor control system and the closed-loop PID controller to control the balance [22]. Its control input is dc motor current driver input voltage (*t*) and output is the Angle of reversion θ(t) of motor central axis.

We will first to obtain the characteristic equation of the motor linearization system is:

$$\Delta(s) = |sI - A| = s^4 + as^3 - \frac{g}{-}s^2 - \frac{g}{-}as = 0 \qquad (1)$$

If the state variable is x(t), the input variable is u(t), and the output variable is y(t), then the PID algorithm of the surrounding aircraft is shown in

the equation of state (2), where A and B are matrices, and t is the time coefficient.

$$\dot{x}(t) = Ax(t) + Bu(t) \quad (2)$$

$$y(t) = Cx(t) \quad (3)$$

Then, performance indicators were obtained using the optimal control under the LQR (Linear Quadratic Regulator).

The object is the linear system given in the form of state space in the present control theory, and the objective function is the quadratic function of object state and control input. LQR optimal design refers to the state feedback controller K designed to minimize the quadratic objective function J, and K is only determined by the weight matrix Q and R, so the choice of Q and R is particularly important. Let the state equation of the linear-time-varying system be:

$$x(t) = A(t)x(t) + B(t)u(t), x(t) = X0 \quad (4)$$

Performance index:

$$J = \frac{1}{2}\int_0^\infty [x^T(t)Qx(t) + u(t)Ru(t)]dt \quad (5)$$

In the formula, the vector x(t)∈ Rn, u(t)∈ Rm, the matrix A(t) is n x n dimensional time-varying system matrix, B(t) is n x m dimensional gain matrix, Q(t) is the semi-positive definite matrix, which is the weighted state, R(t) is the symmetric positive definite matrix, which is the weighted control input u(t).

For the time-varying state regulator problem in infinite time, if the matrix pairs {A(t), B(t)} are completely controllable, there exists A unique optimal control.

$$u(t) = -R - 1(t)BT(t)P(t)x(t) = -K(t)x(t) \quad (6)$$

Where the matrix P is the solution of Riccati algebraic equation (7), the matrix Q and the scalar R are the state variables and the proportion of the control input respectively.

$$PbR^{-1}b^TP - Q - PA - A^TP = 0 \quad (7)$$

The optimal performance index is:

$$J^* = \frac{1}{2}x^T(t)P(t)x(t) \quad (8)$$

## B. Wavelet Transform

Wavelet transform (WT) is a new transform analysis method. The WT can automatically adapt to the requirements of time-frequency signal analysis, and thus can focus on any detail of the signal. Wavelet transform is mainly divided into two parts, discrete and continuous transform [23].

### *1) Discrete Wavelet Transform*

Like the Fourier series expansion, if the function being developed is discrete (a string of Numbers), the coefficients are known as the discrete wavelet transform (DWT).Continuous wavelet in the treatment of the object will cause theory of coefficient of redundancy, what we need in the practical application in the removal of interference signals while preserving the original low redundancy, as discrete wavelet transform relatively continuous wavelet transform operation more convenient, and in the actual signal processing are discrete information stored on the computer. So the size parameters of the need to a peace shift parameter b discrete processing, the original continuous translational expansion component transform: a=ajo, j as an integer, a > 1 scale step length for a fixed value, including translational component b = kboaoj , and bo > o and is associated with a form . K is an integer. Discrete wavelet can be defined as:

$$\psi_{j,k}(t) = \frac{1}{\sqrt{a_0^j}}\psi\left(\frac{t - kb_0a_0^m}{a_0^m}\right) = a_0^{-j/2}\psi\left(a_0^{-j}t - kb_0\right) \quad (9)$$

Corresponding discrete wavelet transform:

$$W_f(v,k) = a_0^{-v/2}\int_{-\infty}^{+\infty} f(t)\psi_{v,k}(t)dt \quad (10)$$

The wavelet transform Wf (a, b) can fully present the properties and transformation process of signal function f (t) in the case of a>o and b∈ (−∞, +∞), and the discrete wavelet can also describe the properties and change process of the function when selecting appropriate parameters $a_o$ and $b_o$.

### *2) Continuous Wavelet Transform*

The natural extension of the discrete wavelet transform is the continuous wavelet transform (CWT), which transforms a continuous function into a highly redundant function with two continuous variables (translation and scale). The resulting conversions are easy to interpret and valuable for time-frequency analysis.

A continuous squared integral function *f(x)* converts the continuous wavelet of the real-valued wavelet $\Psi(x)$ to

$$W_{\psi}(s,\tau)=\int_{-\infty}^{\infty} f(x)\psi_{s,\tau}(x)dx \quad (11)$$

where

$$\psi_{s,\tau}(x)=\frac{1}{\sqrt{s}}\psi\left(\frac{x-\tau}{s}\right) \quad (12),$$

$^{s}$and$^{\tau}$ are called scale and translation parameters respectively.

Given $W\psi(s,\tau)$, the inverse continuous wavelet transform can be obtained )

$$f(x)=\frac{1}{C_{\psi}}\int_{0}^{\infty}\int_{-\infty}^{\infty}W_{\psi}(s,\tau)\frac{\psi_{s,\tau}(x)}{s^{2}}d\tau ds \quad (13)$$

where

$$C_{\psi}=\int_{-\infty}^{\infty}\frac{|\Psi(\mu)|^{2}}{|\mu|}d\mu \quad (14)$$

$\Psi(\mu)$ is the Fourier transform of. $\Psi(x)$ Equations (11) to (14) define a reversible transformation as long as the so-called permissible conditions are met $C_{\psi}<\infty$ , (Grossman and Morlet [1984]). )

### C. Emergency Treatment System

The system consists of three parts: signal emergency plan, electricity emergency plan and power and signal emergency plan.

*1) Signal emergency plan*

The UAV is allowed to fly only when the transmitter and receiver are successfully connected via WiFi. When the UAV rotor is started, the system records the starting point position through GPS positioning and stores it in the database. In the process of UAV flight, if the UAV signal is insufficient or lost, the control system will make the UAV automatically switch from flight to hover state and try to connect again. The connection time is two minutes. If the connection time-out, the UAV will read the take-off position and plan the path to return to landing.

*2) Electricity emergency plan*

The UAV is allowed to fly when the power is higher than 40%. When the UAV rotor starts, the system records the starting point position through GPS positioning and stores it in the database. When the UAV battery power is less than 20%, the system will remind the operator to operate the aircraft immediately through the human-computer interaction interface. When the UAV power is less than 10%, no one has the opportunity to read the position of the starting point, and plan the path to force the return, so as to prevent the crash caused by insufficient power supply. When the power of the UAV is less than 5% and the UAV has not returned to the initial position, the UAV will make a forced landing nearby according to the ground area given by the GPS map, so as to avoid the forced landing in the dangerous areas such as rivers and roads. After the forced landing, the unmanned aerial vehicle will send the position to the operator and enter the sleep state after that, so that the operator can find the UAV according to the positioning.

*3) Power and signal emergency plan*

If the battery power of the UAV is less than 5% during the process of reconnection or during the process of returning after the connection timeout, the UAV will make a forced landing near the safe range of the map and send positioning by GPS.

## IV. SYSTEM SOFTWARE AND HARDWARE DESIGN

The system is divided into three parts: communication control, ultrasonic obstacle avoidance and image processing.

### A. Communication Control System

The communication control system of the UAV is mainly to connect to the Internet through WIFI, and then control the UAV to execute commands such as forward, back, left and right steering, takeoff and landing through the APP control interface of the ground control terminal [24]. Figure 3 is the flow chart of flight control system.

The system first initializes the port and the sensor, then detects and reads the remote control command data. The PID is adaptive adjusted through command data and attitude data. The adjusted PID parameters are input to the PID controller to calculate the speed of the corresponding motor. Finally, the PWM signal is adjusted to drive the motor.

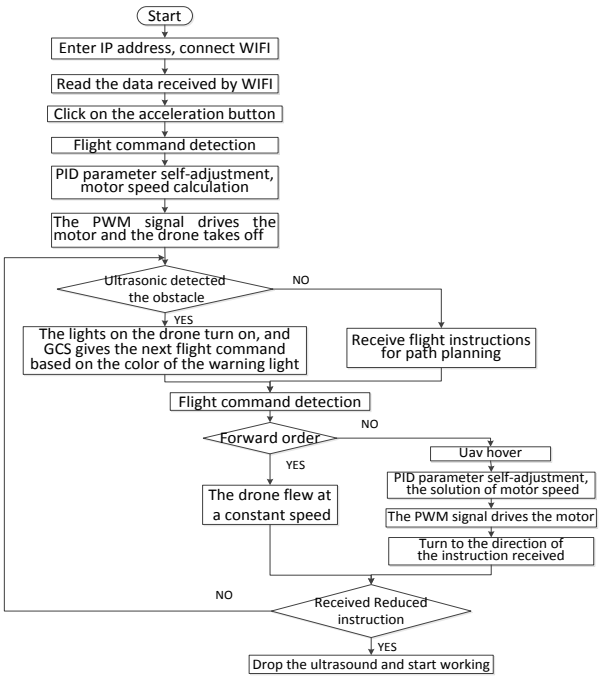


*Fig. 3:* Flow chart of flight control system

In the process of controlling the UAV flight, ultrasonic detects the surrounding obstacles by rotating the steering gear. If detected, the tri-color LED light on the UAV will be on, and the ground control station will judge the safe direction of the next flight according to the LED light color. If no obstacle is detected, the UAV will point to the next command until the landing command is received, and the ultrasonic wave below starts to work. The landing process is shown in Figure 4.

## B. UAV Landing Obstacle Avoidance System

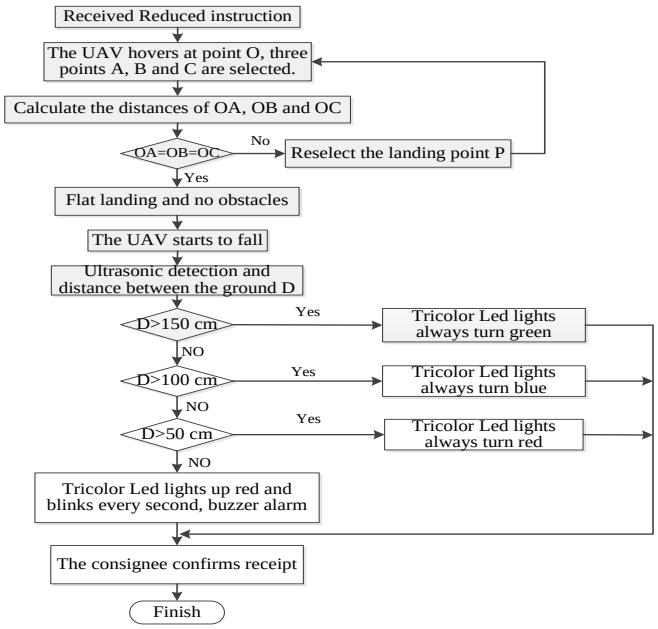


*Fig. 4:* Flow chart of descending ultrasonic obstacle avoidance system

When the UAV receives the descending command, it is assumed that point P is the pre-landing point on the ground, and point O is the position of the UAV hovering in the air, and OP is perpendicular to the landing surface. Choose A, B and C within the radius of 1m with P as the center of the circle. The height between these three points and the UAV can be determined by calculation. If it is the same, it means that the landing surface is flat, then it begins to fall. At the same time, ultrasonic measure the distance D from the ground to remind the operator to pay attention and ensure a safe landing. If not, then re-select the landing point. After the UAV lands, the receiver confirms receiving the goods, as shown in Figure 5.

## C. The Image Processing

First determine if the drone receives a descent command. If a down command is received, the drone arrives at the destination. The image taken by the camera is compared with the image of the pick-up person in the database to verify whether it is the pick-up of the item. Described as follows:

1. *Original image:* The original RGB image captured by the camera.
2. *Grayscale:* The raw RGB image taken is grayed out.
3. *Banalizations:* Binarize the grayscale image [25].
4. *Morphology:* The image after binarization is processed by erosion and expansion to restore the image.

The captured image is compared with the image information of the pick-up person in the database. If the information is the same, the verification is successful, and if the information is different, the verification fails.

After the verification is successful, the pick-up information and image are displayed. At this time, the drone drops and confirms the receipt; the verification fails, the image is displayed, and the information is not recognized.

The landing of the UAV: The process of landing is shown in Figure 4. Confirm receipt or fail to verify the UAV will return.

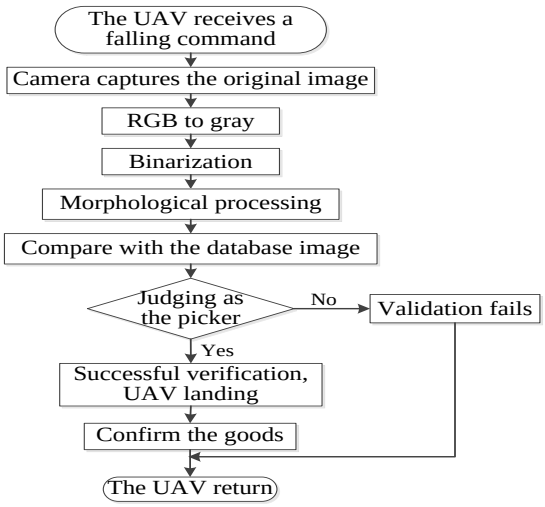


*Fig. 5:* Flow chart of picture processing

## V. SIMULATION COMPARATIVE AND ANALYSIS

The simulation, comparison and analysis are divided into two parts: improved PID and image processing algorithm.

### A. Improved PID Algorithm

Symbol description:

1. *y(k)* -- discrete value of system response output;
2. *u(k)* -- discrete value of digital PID control output;
3. *r(k)* -- the discrete value of the expected output (known), which in this case is a constant (i.e., step input);
4. e(k)--e(k)=r(k)-y(k), is expected value - actual value, is the error comparison signal with unit negative feedback.

*a) Compare and Analyze the Influence of PID Output Parameters*

In this paper, in order to study the influence of three PID parameters $Kp$, , and $Kd$ , we set up an array of PID, $Kp$, $Ki$ , and $Kd$ take a value of the array each time, and then set a loop function for simulation. Then, all PID effects are output to a graph for comparison, and the output subgraph matrix is shown in Figure 6 (a) ~ (f).

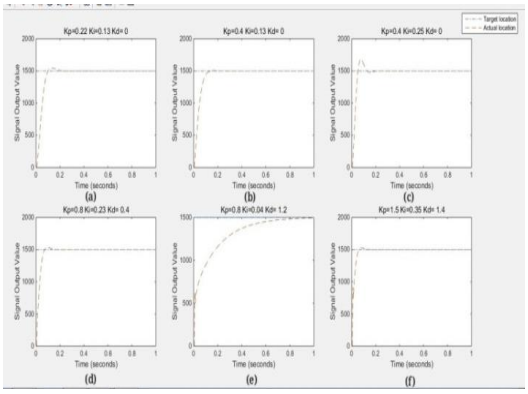

*Fig. 6:* Comparison diagram of PID parameter influence effect

According to Figure 6 (a) and (b), modification of $Kp$ will shorten the rise time, but may also bring about a large overshoot. Overshoot is not absolute. A small $K_p$ may cause a large overshoot, while a large $K_p$ will cause a small overshoot (for example, in Figure 6, the comparison between Figure (a) and (b)). However, the introduction of integral is also necessary, otherwise it will take a long time to reduce the error e(k) (such as the (e) diagram in Figure 6. The introduction of differential is equivalent to a leading correction, which will reduce overshoot, but the transitional differential is likely to cause tail oscillation, and the system will gradually become unstable. So there's a balance between the differential and the integral, and when that balance is met, the system has almost no oscillations, and the response is fast. It can be known from Figure 6 that (c) overshoot is caused by excessive integration in Figure (d) and (f) are ideal.

*b) Improve PID Algorithm*

When U(k) > $U_{max}$ , if e(k) > 0 means that the output value has not reached the specified value, or if U(k) < 0, if e(k) < 0 means that the output value exceeds the specified value, the integration will bring a lag, no more integration. $Umax = (k)$ is assumed in this simulation, and the comparison curve of the output of improved PID algorithm is shown in Figure 7.

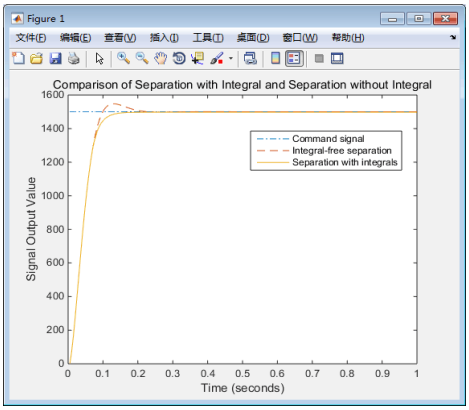


*Fig. 7:* Improved PID algorithm curve

According to Figure 7, the overshoot of the system is significantly reduced, and the adjustment time is also shortened. This paper proposes an improved PID method, which not only eliminates the steady-state error but also reduces the lag effect brought by the integral link.

Based on the above, the PID regulation can be summarized into the following two points:

*1)* When $K_p$ is small, the system is sensitive to the introduction of differential and integral links. Integral will cause overshoot, so should not be too large; Differentials can cause oscillations, and overshoot increases when oscillations are severe.
*2)* When $K_p$ increases, the overshoot of integral due to lag gradually decreases, but it should not be too small, otherwise the adjustment time will be too long. In this case, if you want to continue to reduce the overshoot, you can introduce the differential appropriately. The system may be unstable if $K_p$ is increased continuously. Therefore, when $K_p$ is increased and $Kd$ is introduced to reduce overshoot, good steady-state characteristics and dynamic performance can be achieved even when $K_p$ is not very large.

### *B. Image Processing*

In order to verify the denoising performance of the wavelet method used in this paper, we add the same mean and variance white Gaussian noise [26] on the basis of the original image. In this experiment, the wavelet decomposition level is set to N=2, and in the selection of wavelet bases, the db8 wavelet decomposition basis function is selected. The simulation results are shown in Figure 8.

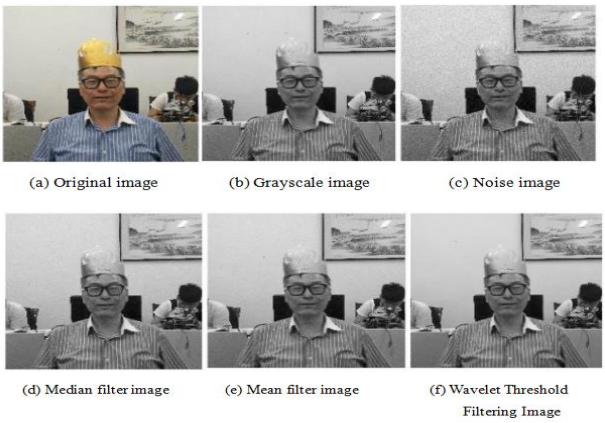


*Fig. 8:* Simulated image comparison results

In the simulation experiment, the denoising of the blurred image is simulated by using the traditional filtering function and the wavelet threshold method selected in this paper. The image denoising effect of different methods is judged by quantitative analysis of image contrast. In the quantitative evaluation index, besides the traditional MSE (mean square error) and PSNR (peak signal-to-noise ratio), the latest mean structure similarity (MSSIM) is introduced to evaluate the denoising effect of the filter function. The comparative analysis data are shown in Table 1.

*Table 1:* Simulated Image Denoising Comparison T Able (Unit Db)

| Evaluating indicator / hreshold function | MSE | PSNR | MSSIM |
|---|---|---|---|
| Raw noise image | 99.8095 | 28.1391 | 0.5087 |
| Median filtering | 28.0514 | 33.6513 | 0.8159 |
| Mean filtering | 25.8242 | 34.0105 | 0.8600 |
| Wavelet threshold filtering | 24.6278 | 34.2165 | 0.8849 |

In Table 1, the noise removal can be clearly obtained by comparing the indices. The wavelet threshold method used in this paper has a better changer than the original image in both the contrast of Figure 8 (d) ~ (f) and the detail clarity of the image. From the MSE, PSNR and MSSIM in the table, it can be seen that the wavelet threshold method used in this paper is superior to the traditional mean and median filtering for the denoising effect of the simulated image. The

results shown that the wavelet threshold denoising method is effective.

## VI. EXPERIMENTAL RESULT

The experimental results are divided into two parts: UAV flight test and image processing.

### A. UAV Flight Test Result

We flew the drone in a relatively empty playground for safety reasons. Figure 9 (a) ~ (h) refers to the whole process of logistics UAV from delivery to picking up by operators. Among them, figure (a) shows the operator putting a small cargo into the UAV cargo box; Then we connect the phone App to the drone successfully, click the "Faster" button, and the drone takes off. Figure (b) shows the UAV in the process of taking off; During the flight, the front steering engine continuously rotates ultrasonic wave to detect obstacles. If obstacles are not detected, the UAV will point to the next command. If obstacles are detected, as shown in figure (c), the UAV will hover in the air; Meanwhile, the mobile APP of the ground control terminal displayed "Warning: Suggest to turn left", as shown in figure (d). After receiving the obstacle alarm, the operator will send corresponding steering instructions according to the prompt, and the UAV will continue to fly, as shown in figure (e). Fly to the designated place, hover, and identify the cargo picker through webcam, as shown in figure (f), the specific identification process is as shown in part C (image processing); If the authentication is successful, the UAV will dock at an appropriate location, as shown in figure (g). Finally, the pick-up takes out the goods from the cargo box and completes the distribution task, as shown in figure (h); If the authentication fails, as shown in figure (i), the UAV will not dock and continue to fly, as shown in figure (j).

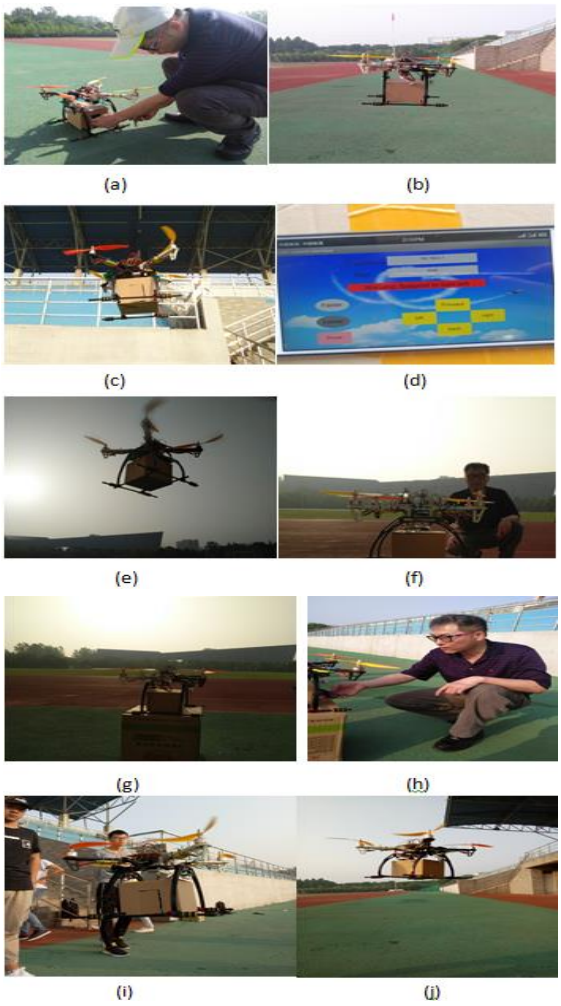


*Fig. 9:* The process of Logistics UAV Deliverying and Pick-up

### B. Image Processing

Face information collection should be the first step in face image detection and recognition. We collected 10 face information from 20 people and established a separate folder for each person to distinguish the information of different people, so we stored 200 face information in the face database. Information of partial face database is shown in Figure 10 (a), (b) and (c).

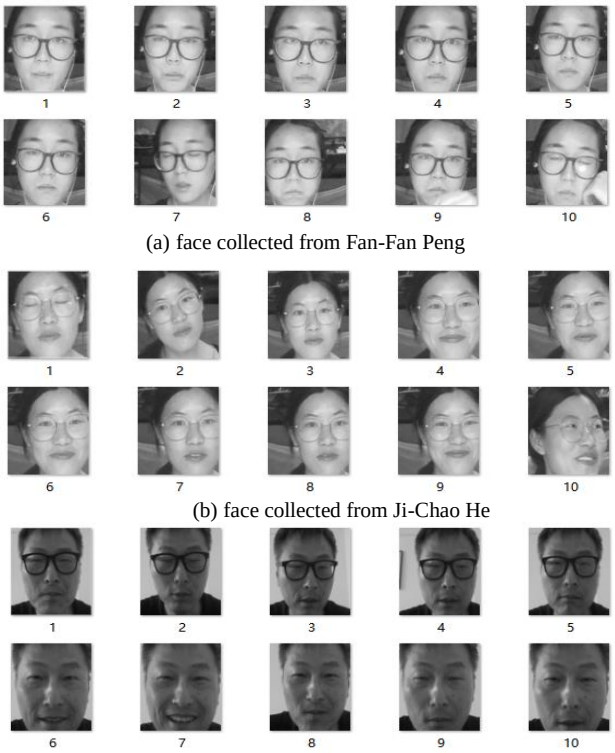


(a) face collected from Fan-Fan Peng

(b) face collected from Ji-Chao He

face collected from Hai-Wu Lee

*Fig. 10:* Partial Face Information Graph Collected from Face Database

After the preparation of face collection, face detection and recognition are carried out. The experimental results are divided into the following three situations:

In the first case, there is only one person in the image and that person is the consignee. Experimental results as shown in Figure 11 (a) to (i), as shown in Figure (a) as the original Figure, Figure (b) as the original Figure turned gray, Figure (c) to turn gray image binarization, Figure (d) show the grayscale histogram, Figure (e) for binary image morphology processing, make the face more clearly, Figure (f) for label, Figure divided label (g), Figure (h) as the garage face Figure, matching with the Figure (i), according to identify the identity of the information, and landing UAV as shown in Figure 9 (g).

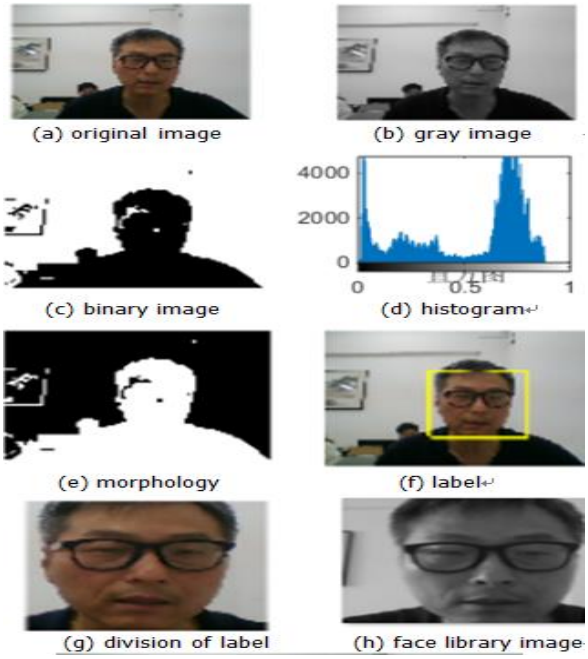


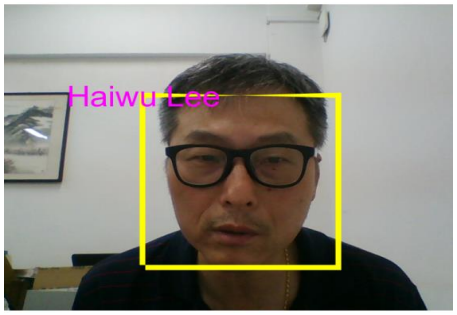


(i) face detection and recognition result image

*Fig. 11:* Image of Experimental Results in the First Case

In the second case, there are three people in the image at this time, two of them are in the face database, and the other one is not in the face database. Figure 12 (c) is the receiver after matching with Figure 12 (d) of the face database. The same is shown in Figure 11 (i).

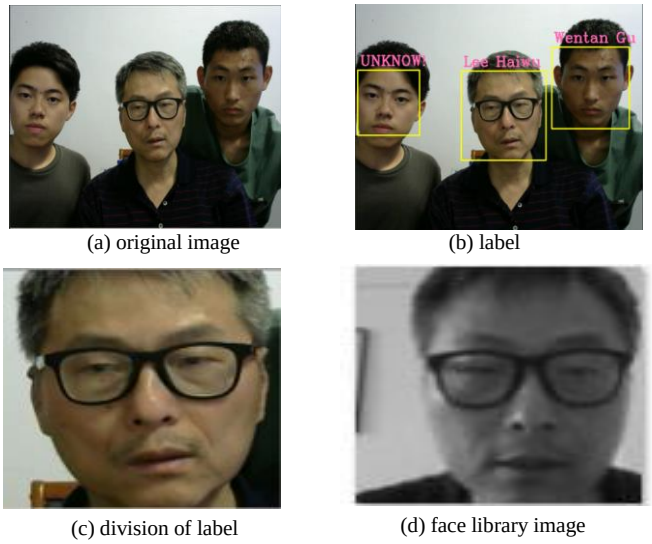


(a) original image (b) label

(c) division of label (d) face library image

*Fig. 12:* Image of Experimental Results in the Second Case

In the third case, three people in the experimental images are not pickers, and the information of three people is stored in the face database. Similarly, Figure 12(c) and Figure 12(d) are non-cargo pickers. The experimental results are shown in Figure 13, and the UAV directly returns without landing, as shown in Figure 9(j).

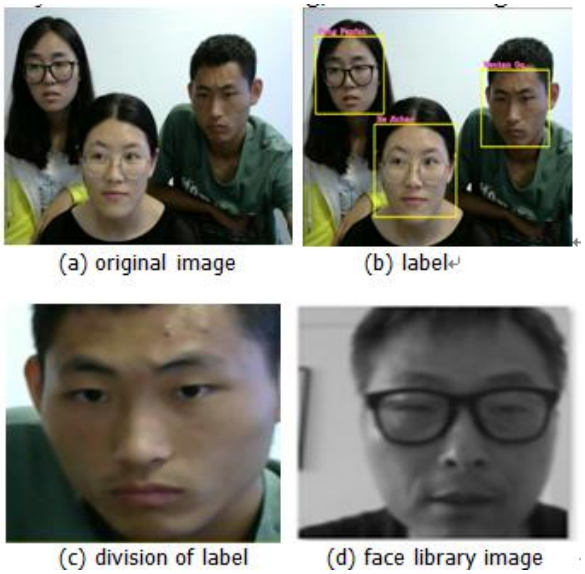

(a) original image (b) label

(c) division of label (d) face library image

*Fig. 13:* Image of Experimental Results in the Third Case

## VII. CONCLUSION

In this paper, an improved intelligent UAV flight control system is proposed for the environmental adaptability of four-rotor logistics UAV, and hardware design, attitude calculation, software simulation and test flight test are carried out for the system. The system delivers goods to the destination through GPS positioning system. At the same time, the wavelet algorithm is used to clear the fuzzy image taken by the UAV, so as to identify the identity of the consignee and ensure the safe and accurate delivery of the goods. Therefore, the advantages of this logistics UAV mainly lie in solving the distribution problem of small packages, improving work efficiency and reducing labor costs. The experimental results show that the system is feasible.

## REFERENCES

1. P. Castillo, A. Dzul and R. Lozano, "Real-time stabilization and tracking of a four-rotor mini rotorcraft," in IEEE Transactions on Control Systems Technology, vol. 12, no. 4, pp. 510-516, July 2004, doi: 10.1109/TCST. 2004. 825052.
2. N. K. Yang, K. T. San and Y. S. Chang, "A Novel Approach for Real Time Monitoring System to Manage UAV Delivery," 2016 5th IIAI International Congress on Advanced Applied Informatics (IIAI-AAI), Kumamoto, 2016, pp. 1054-1057, doi: 10.1109/IIAI-AAI.2016.195.
3. N. H. Motlagh, T. Taleb and O. Arouk, “Low-altitude unmanned aerial vehicles-based internet of things services: Comprehensive survey and future perspectives,” IEEE Internet Things J., vol. 3, no. 6, pp. 899–922, Dec. 2016.
4. I. Bisio, C. Garibotto, F. Lavagetto, A. Sciarrone and S. Zappatore, “Blind Detection: Advanced Techniques for WiFi-

Based Drone Surveillance," in IEEE Transactions on Vehicular Technology, vol. 68, no. 1, pp. 938-946, Jan. 2019.
5. Xu, X. Liao, J. Tan, H. Ye and H. Lu, "Recent Research Progress of Unmanned Aerial Vehicle Regulation Policies and Technologies in Urban Low Altitude," in IEEE Access, vol. 8, pp. 74175-74194, 2020, doi: 10.1109/ACCESS.2020.2987622.
6. N. H. Motlagh, M. Bagaa and T. Taleb, "Energy and Delay Aware Task Assignment Mechanism for UAV-Based IoT Platform," in IEEE Internet of Things Journal, vol. 6, no. 4, pp. 6523-6536, Aug. 2019, doi: 10.1109/JIOT. 2019.2907873.
7. S . Ahmed, M. Z. Chowdhury and Y. M. Jang, "Energy-Efficient UAV-to-User Scheduling to Maximize Throughput in Wireless Networks," in IEEE Access, vol. 8, pp. 21215-21225, 2020, doi: 10.1109/ ACCESS.2020.2969357.
8. K. Kuru, D. Ansell, W. Khan and H. Yetgin, "Analysis and Optimization of Unmanned Aerial Vehicle Swarms in Logistics: An Intelligent Delivery Platform," in IEEE Access, vol. 7, pp. 15804-15831, 2019, doi: 10.1109/ ACCESS. 2019.2892716.
9. Y. Chen, L. Liu, Z. Gong and P. Zhong, "Learning CNN to Pair UAV Video Image Patches," in IEEE Journal of Selected Topics in Applied Earth Observations and Remote Sensing, vol. 10, no. 12, pp. 5752-5768, Dec. 2017.
10. P. L. Shui, "Image denoising algorithm via doubly local Wiener filtering with directional windows in wavelet domain," in *IEEE Signal Processing Letters*, vol. 12, no. 10, pp. 681-684, Oct. 2005, doi: 10.1109/LSP.2005. 855555.
11. L. Meng, Z. Sun and O. Tejada Collado, "Efficient approach to de-identifying faces in videos," in IET Signal Processing, vol. 11, no. 9, pp. 1039-1045, 12. 2017.
12. G. Plonka, S. Tenorth and D. Rosca, "A New Hybrid Method for Image Approximation Using the Easy Path Wavelet Transform," in IEEE Transactions on Image Processing, vol. 20, no. 2, pp. 372-381, Feb. 2011.
13. S. Kim, W. Kang, E. Lee and J. Paik, "Vaguelette-wavelet decomposition for frequency adaptive image restoration using directional wavelet bases," in IEEE Transactions on Consumer Electronics, vol. 57, no. 1, pp. 218-223, February 2011.
14. Z. J. Xiang and P. J. Ramadge, "Edge-Preserving Image Regularization Based on Morphological Wavelets and Dyadic Trees," in IEEE Transactions on Image Processing, vol. 21, no. 4, pp. 1548-1560, April 2012.
15. N. Remenyi, O. Nicolis, G. Nason and B. Vidakovic, "Image Denoising with 2D Scale-Mixing Complex Wavelet Transforms," in IEEE Transactions on Image Processing, vol. 23, no. 12, pp. 5165-5174, Dec. 2014.
16. S. R. Dubey, S. K. Singh and R. K. Singh, "Local Wavelet Pattern: A New Feature Descriptor for Image Retrieval in Medical CT Databases," in IEEE Transactions on Image Processing, vol. 24, no. 12, pp. 5892-5903, Dec. 2015.
17. N. Ansari and A. Gupta, "Image Reconstruction Using Matched Wavelet Estimated from Data Sensed Compressively Using Partial Canonical Identity Matrix," in IEEE Transactions on Image Processing, vol. 26, no. 8, pp. 3680-3695, Aug. 2017.
18. M. Ayi, A. K. Ganti, M. Adimulam and B. Karthik, "Interfacing of MATLAB with Arduino for face detection and tracking algorithm using serial communication," 2017 International Conference on Inventive Computing and Informatics (ICICI), Coimbatore, 2017, pp. 944-948.

19. A. A. Shah, Z. A. Zaidi, B. S. Chowdhry and J. Daudpoto, “Real time face detection/ monitor using raspberry pi and MATLAB,” 2016 IEEE 10th International Conference on Application of Information and Communication Technologies (AICT), Baku, 2016, pp. 1-4.
20. Z. Chen, D. Yin, D. Chen, M. Pan and J. Lai, "WiFi-based UAV Communication and Monitoring System in Regional Inspection," 2018 International Computers, Signals and Systems Conference (ICOMSSC), Dalian, China, 2018, pp. 386-392, doi: 10.1109/ ICOMSSC45026. 2018.8941637.
21. M. Itani, A. Haroun and W. Fahs, "Obstacle Avoidance for Ultrasonic Unmanned Aerial Vehicle Monitoring Using Android Application," 2018 International Arab Conference on Information Technology (ACIT), Werdanye, Lebanon, 2018, pp. 1-4, doi: 10.1109/ACIT.2018.8672681.
22. Verma and P. K. Padhy, "Indirect IMC-PID controller design," in IET Control Theory & Applications, vol. 13, no. 2, pp. 297-305, 29 1 2019, doi: 10.1049/iet-cta.2018.5454.
23. Gonzalez. Woods. “Digital Image Processing.” Princeton: Pearson Education, 2008, 473~485.
24. H. W. Lee, Y. Zhu, X. Shi, F. F. Peng and W. J. Jin, “Research of Four-axis Aircraft Using WIFI and Rotary Anti-collision System,” 2018 IEEE International Conference on Applied System Invention (ICASI), Chiba, 2018, pp. 665-668.
25. U. Braga-Neto and J. Goutsias, "Grayscale level connectivity: theory and applications," in IEEE Transactions on Image Processing, vol. 13, no. 12, pp. 1567-1580, Dec. 2004, doi: 10.1109/TIP. 2004. 837514.
26. A. V. Balakrishnan and R. R. Mazumdar, "On Powers of Gaussian White Noise," in IEEE Transactions on Information Theory,vol. 57, no. 11, pp. 7629-7634, Nov.2011,doi:10.1109/TIT.2011.2 158 062.

HAI-WU LEE (Member, IEEE) received the degree from the Department of Electronic Engineering, Kun Shan University, in 2000, the master's degree from the Institute of Computers, Communications, and Control, National Taipei University of Technology, in 2003, and the Ph.D. degree from the Department of Electrical Engineering, National Taiwan University of Science and Technology, Taipei, Taiwan, in 2014. He is currently a Professor with the Department of School of Science and Engineering, Xiangsihu College of Guangxi University for Nationalities. His research interests include the design and application of optimal control systems for biped walking robots, image processing, and intelligence RFID. He is a Reviewer of journals, such as IEEE TRANSACTIONS ON EDUCATION and IEEE ACCESS etc...

# London Journal Press Membership

For Authors, subscribers, Boards and organizations

London Journals Press membership is an elite community of scholars, researchers, scientists, professionals and institutions associated with all the major disciplines. London Journals Press memberships are for individuals, research institutions, and universities. Authors, subscribers, Editorial Board members, Advisory Board members, and organizations are all part of member network.

Read more and apply for membership here:
*https://journalspress.com/journals/membership*

## For Authors

Author Membership provide access to scientific innovation, next generation tools, access to conferences/seminars /symposiums/webinars, networking opportunities, and privileged benefits.
Authors may submit research manuscript or paper without being an existing member of LJP. Once a non-member author submits a research paper he/she becomes a part of "Provisional Author Membership".

## For Institutions

Society flourish when two institutions come together." Organizations, research institutes, and universities can join LJP Subscription membership or privileged "Fellow Membership" membership facilitating researchers to publish their work with us, become peer reviewers and join us on Advisory Board.

## For Subscribers

Subscribe to distinguished STM (scientific, technical, and medical) publisher. Subscription membership is available for individuals universities and institutions (print & online). Subscribers can access journals from our libraries, published in different formats like Printed Hardcopy, Interactive PDFs, EPUBs, eBooks, indexable documents and the author managed dynamic live web page articles, LaTeX, PDFs etc.

GO GREEN AND HELP
SAVE THE ENVIRONMENT

## JOURNAL AVAILABLE IN

PRINTED VERSION, INTERACTIVE PDFS, EPUBS, EBOOKS, INDEXABLE DOCUMENTS AND THE AUTHOR MANAGED DYNAMIC LIVE WEB PAGE ARTICLES, LATEX, PDFS, RESTRUCTURED TEXT, TEXTILE, HTML, DOCBOOK, MEDIAWIKI MARKUP, TWIKI MARKUP, OPML, EMACS ORG-MODE & OTHER

SCAN TO KNOW MORE

support@journalspress.com
www.journalspress.com

*THIS JOURNAL SUPPORT AUGMENTED REALITY APPS AND SOFTWARES